AD-A058 958 TEXAS UNIV AT AUSTIN APPLIED RESEARCH LABS F/G 8/11
ACOUSTICS OF IN SITU AND LABORATORY SEDIMENTS.(U)
AUG 78 D J SHIRLEY, D W BELL N00014-76-C-0117
UNCLASSIFIED ARL-TR-78-36 NL

1 OF 1
ADA
058958

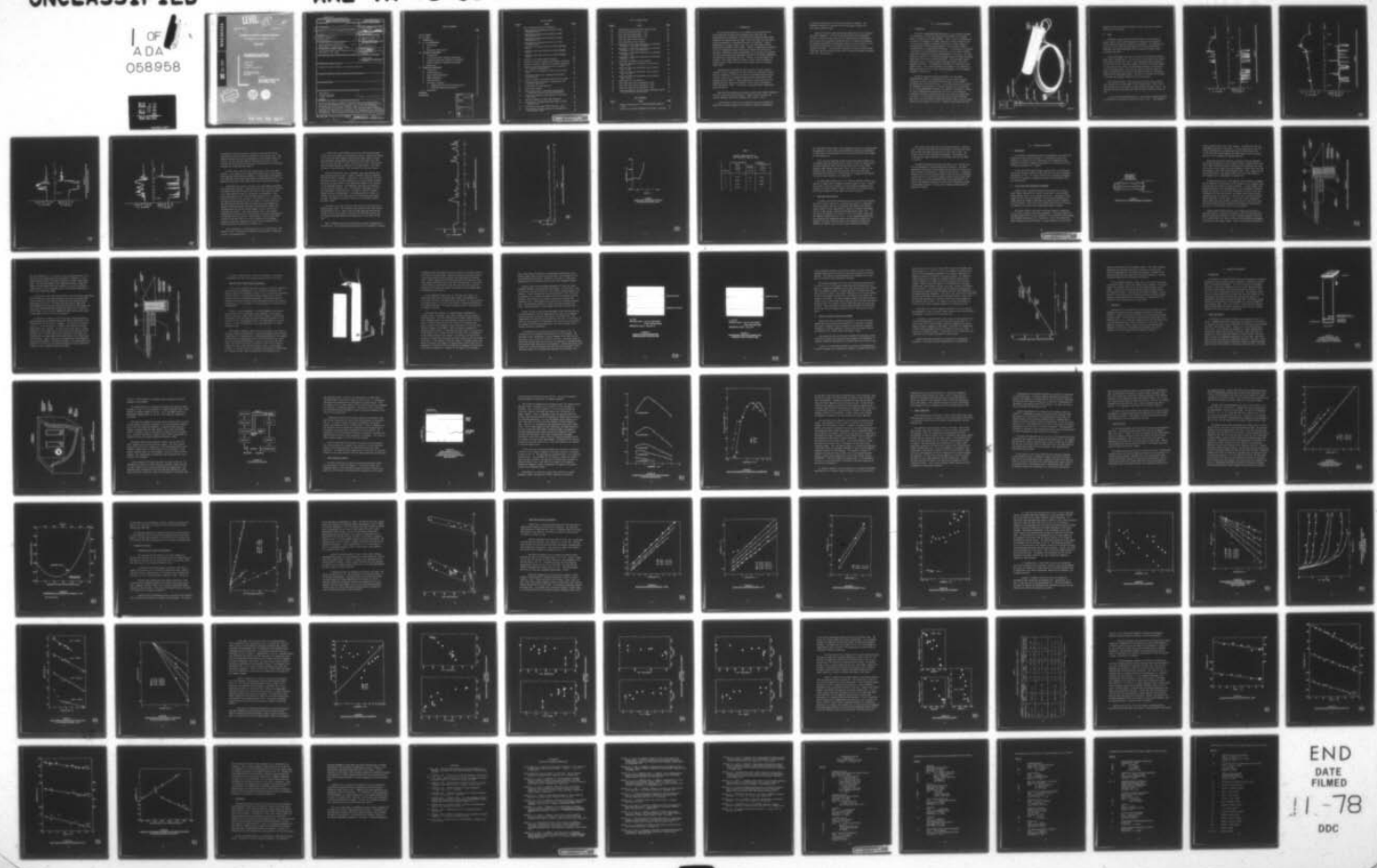

END
DATE FILMED
11-78
DDC

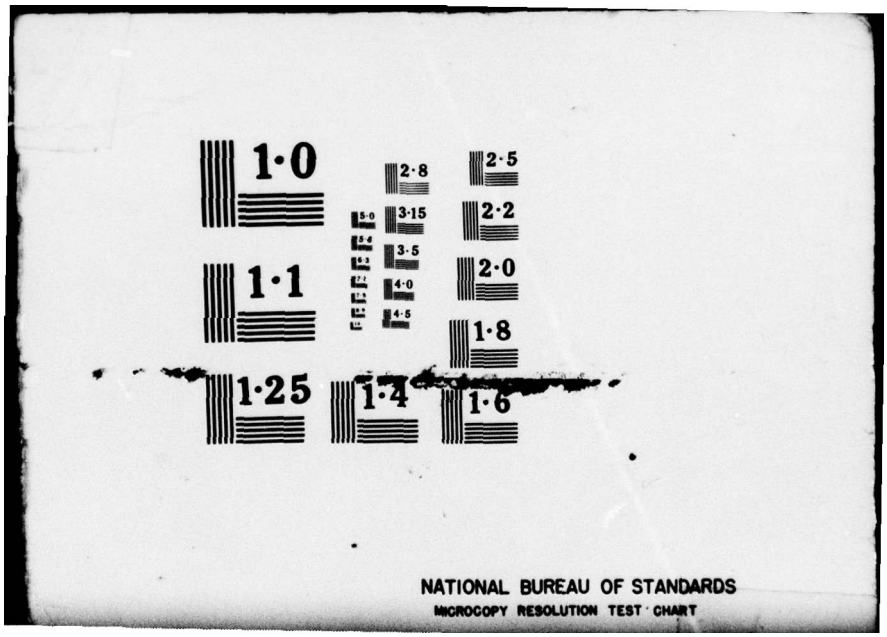
1·0
1·1
1·25
2·8
3·15
3·5
4·0
4·5
1·4
2·5
2·2
2·0
1·8
1·6
NATIONAL BUREAU OF STANDARDS
MICROCOPY RESOLUTION TEST CHART

LEVEL II (10)

ARL-TR-78-36

Copy No. _____

ACOUSTICS OF IN SITU AND LABORATORY SEDIMENTS

Annual Report under Contract N00014-76-C-0117

Donald J. Shirley
David W. Bell

APPLIED RESEARCH LABORATORIES
THE UNIVERSITY OF TEXAS AT AUSTIN
POST OFFICE BOX 8029, AUSTIN, TEXAS 78712

14 August 1978

Annual Report

1 January - 31 December 1977

Prepared for:

NAVAL OCEAN RESEARCH AND
DEVELOPMENT ACTIVITY
NSTL STATION, MS 39529

UNCLASSIFIED

SECURITY CLASSIFICATION OF THIS PAGE (When Data Entered)

REPORT DOCUMENTATION PAGE

READ INSTRUCTIONS BEFORE COMPLETING FORM

1. REPORT NUMBER	2. GOVT ACCESSION NO.
3. RECIPIENT'S CATALOG NUMBER	
4. TITLE (and Subtitle)	5. TYPE OF REPORT & PERIOD COVERED
ACOUSTICS OF IN SITU AND LABORATORY SEDIMENTS	Annual Report 1 Jan[illegible] - 31 Dec[illegible]77,
	6. PERFORMING ORG. REPORT NUMBER ARL-TR-78-36
7. AUTHOR(s)	8. CONTRACT OR GRANT NUMBER(s)
Donald J. Shirley David W. Bell	N00014-76-C-0117
9. PERFORMING ORGANIZATION NAME AND ADDRESS	10. PROGRAM ELEMENT, PROJECT, TASK AREA & WORK UNIT NUMBERS
Applied Research Laboratories The University of Texas at Austin PO Box 8029, Austin, Texas 78712	98 p.
11. CONTROLLING OFFICE NAME AND ADDRESS	12. REPORT DATE 14 Aug[illegible]978
Naval Ocean Research and Development Activity NSTL Station, MS 39529	13. NUMBER OF PAGES 93 pages
14. MONITORING AGENCY NAME & ADDRESS (if different from Controlling Office)	15. SECURITY CLASS. (of this report) UNCLASSIFIED
	15a. DECLASSIFICATION/DOWNGRADING SCHEDULE

16. DISTRIBUTION STATEMENT (of this Report)

Approved for public release; distribution unlimited.

17. DISTRIBUTION STATEMENT (of the abstract entered in Block 20, if different from Report)

18. SUPPLEMENTARY NOTES

19. KEY WORDS (Continue on reverse side if necessary and identify by block number)

Shear Waves
Compressional Waves
Acoustic Impedance
In situ
Sediment

Work reported here

20. ABSTRACT (Continue on reverse side if necessary and identify by block number)

(U) During the period 1 January to 31 December 1977, work under Contract N00014-76-C-0117 consisted of three parts: (1) in situ determination of compressional wave speed in ocean sediments using the ARL:UT profilometer; (2) development of transducers to measure shear wave and acoustic impedance parameters of sediments both in situ and in the laboratory; and (3) laboratory measurement of shear wave and compressional wave parameters of real and artificial sediments. Data obtained for the three parts of the program are reported.

DD FORM 1 JAN 73 1473 EDITION OF 1 NOV 65 IS OBSOLETE

78 08 20 008

UNCLASSIFIED

SECURITY CLASSIFICATION OF THIS PAGE (When Data Entered)

404 434

TABLE OF CONTENTS

LIST OF FIGURES

LIST OF FIGURES CONT'D

List of Tables

I. INTRODUCTION

The viscoelastic properties of a sediment can be characterized by the determination of three elastic parameters plus shear wave and compressional wave attenuation. The three elastic parameters most readily determined are compressional wave speed, shear wave speed, and bulk density. A major consideration in obtaining these data is reliability. Acoustic measurements are normally made on cores that have been removed from the ocean bottom and brought to the surface. Changes in temperature and pressure as well as disturbances during coring tend to reduce the reliability of such data. Appropriate acoustic measurements in situ increase the reliability of the data because the measurements are made at the ambient temperature and pressures on undisturbed sediments. Further, if the measurements can be made at little added expense and effort, during a routine geophysical operation such as coring, the cost of such acoustic data can be reduced significantly.

Applied Research Laboratories, The University of Texas at Austin (ARL:UT), has had a program for the past several years sponsored by ONR to develop a capability to make in situ acoustic measurements during coring. To date, a system that is capable of making routine measurements of the compressional wave speed in a deep ocean sediment during coring has been designed and built (Shirley and Anderson, 1975a; Shirley and Anderson, 1975b; and Shirley, 1977a). The system is called the ARL:UT compressional wave profilometer.

Work under the program has also been to develop small rugged transducers that can be used with the profilometer to measure shear wave speed and acoustic impedance (Shirley and Anderson, 1975; Shirley, 1977a).

A major fallout of the in situ program has been the development of shear wave transducers capable of very sensitive laboratory measurements

of speed and attenuation in both real and artificial sediments. This measurement capability can provide data not previously available on a wide range of sediment types.

During 1977 the work under ONR Contract N00014-76-C-0117 was organized into three categories. (1) The existing compressional wave profilometer was used on one field trip to make in situ compressional wave measurements and to field test a preliminary design for an in situ shear wave transducer. (2) Extensive development and laboratory testing was done on several in situ and laboratory type shear wave transducers and on an in situ acoustic impedance transducer. (3) Laboratory measurements of shear wave and compressional wave speed and attenuation were made on laboratory sediments including sand, silt, and clay types.

II. IN SITU MEASUREMENTS

A. Introduction

The ARL:UT compressional wave profilometer is an instrument designed and constructed to attach to existing coring equipment with a minimum amount of modification to that equipment. Figure 1 shows the equipment and the method of attachment to a corer. Electronic circuits, batteries, and a cassette tape recorder are housed in an aluminum cylinder capable of withstanding 6.9×10^4 kPa ambient pressure. The electronic package is attached to the top, weighted end of the corer. Two transducers are attached to the cutter at the bottom end of the corer such that a pulse of 200 kHz sound can be propagated across the inside diameter of the corer. The transducers are connected to the electronic package through two armored electrical cables taped to the outside of the core barrel. The measurement taken is the travel time of the acoustic pulse across the diameter of the corer through the sediment. A measurement is also made of the amplitude of the received pulse. The electronic package also includes an accelerometer to measure deceleration of the corer, and this measurement can be integrated to produce a depth record.

The ARL:UT compressional wave profilometer was used aboard USNS DESTEIGUER (AGOR-12) in conjunction with piston coring activities carried out by Naval Ocean Research and Development Activity (NORDA) personnel during cruise 13X3-77, leg 2. The primary objectives of ARL:UT's participation in the cruise were to obtain compressional wave speed data, to test a new profilometer instrument which had been constructed to replace one lost in previous coring operations, and to test a new transducer configuration designed to measure both shear wave speed and compressional wave speed. Five cores were attempted with the profilometer attached, four cores were taken, and four sound speed profiles made; the first attempt failed due to pretrigger of the corer. Laboratory sound speed data were

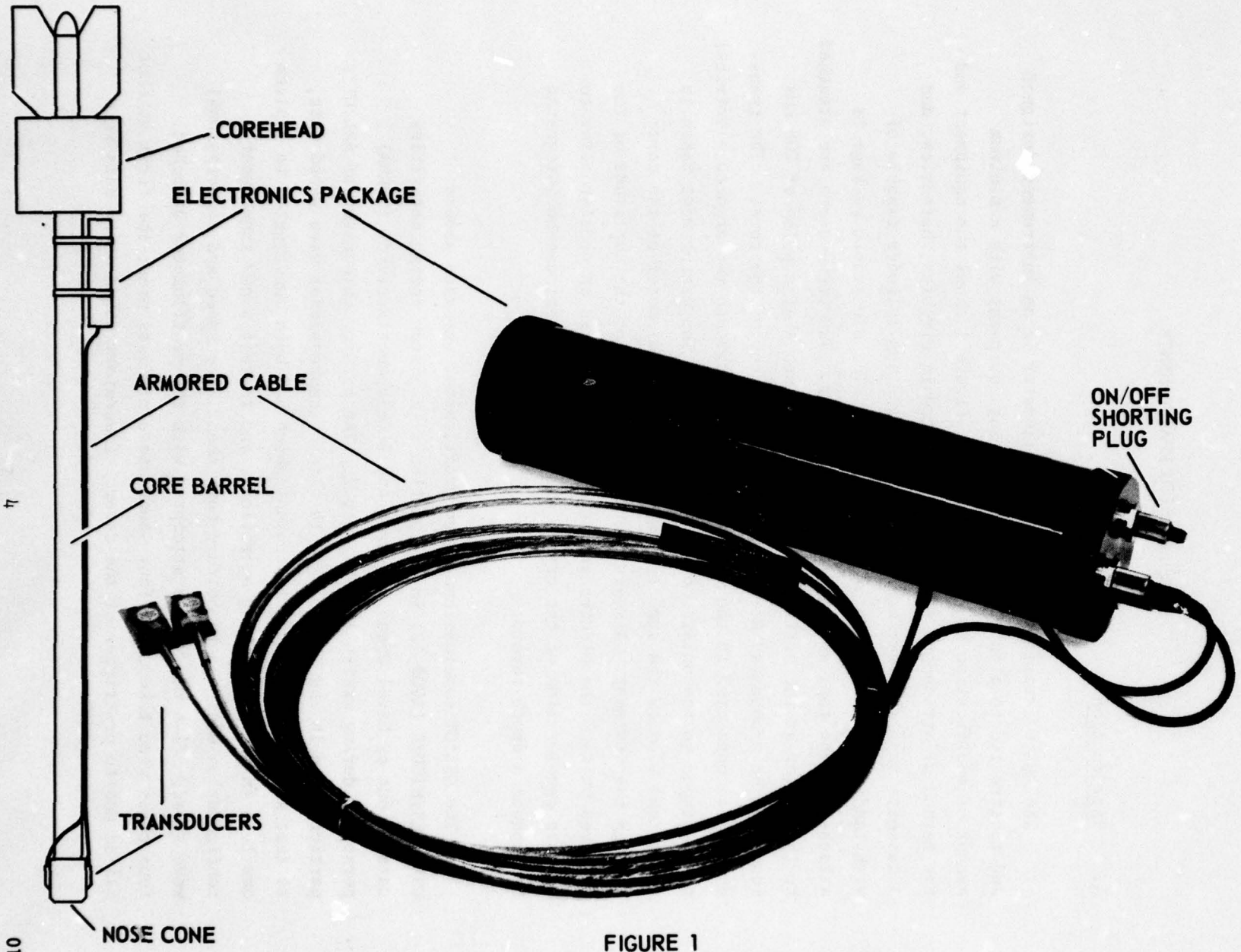

FIGURE 1

ARL : UT COMPRESSIONAL WAVE PROFILOMETER

8-1(1)9610

measured on three of the cores through the plastic liner after retrieval of the cores on board ship.

B. Data

The primary purpose of using the profilometer on the corer was to provide acoustic data to NORDA personnel for comparison and correlation to core lithology and physical properties measurements. To accomplish this task, both in situ sound speed measurements with the profilometer and laboratory sound speed measurements with an Underwater Systems sediment velocimeter were made.

Figures 2 through 5 show the in situ profiles for the four retreived cores (Core 3 through Core 6). The top trace in each figure is the deceleration profile and the bottom trace is the compressional wave sound speed. In each of the figures, the water-sediment interface is at the point marked A. To the left of this point, the sound speed indicated on the record is that of the bottom water. Depth into the sediment increases toward the right as indicated by the nonlinear scale marked between the deceleration profile and the sound speed profile. The depth at each point on the record is calculated by a double integration of the deceleration.

The records for Cores 3 and 4 were made in the same area in fairly soft sediments with a large number of thin turbidite beds. Cores 5 and 6 were also made near each other but at some distance from Cores 3 and 4. The sediment for the last two cores was almost pure sand overlaid by a layer of mud.

In each of the sound speed profiles, a large number of sudden decreases in sound speed are indicated, especially in Cores 5 and 6. These apparent

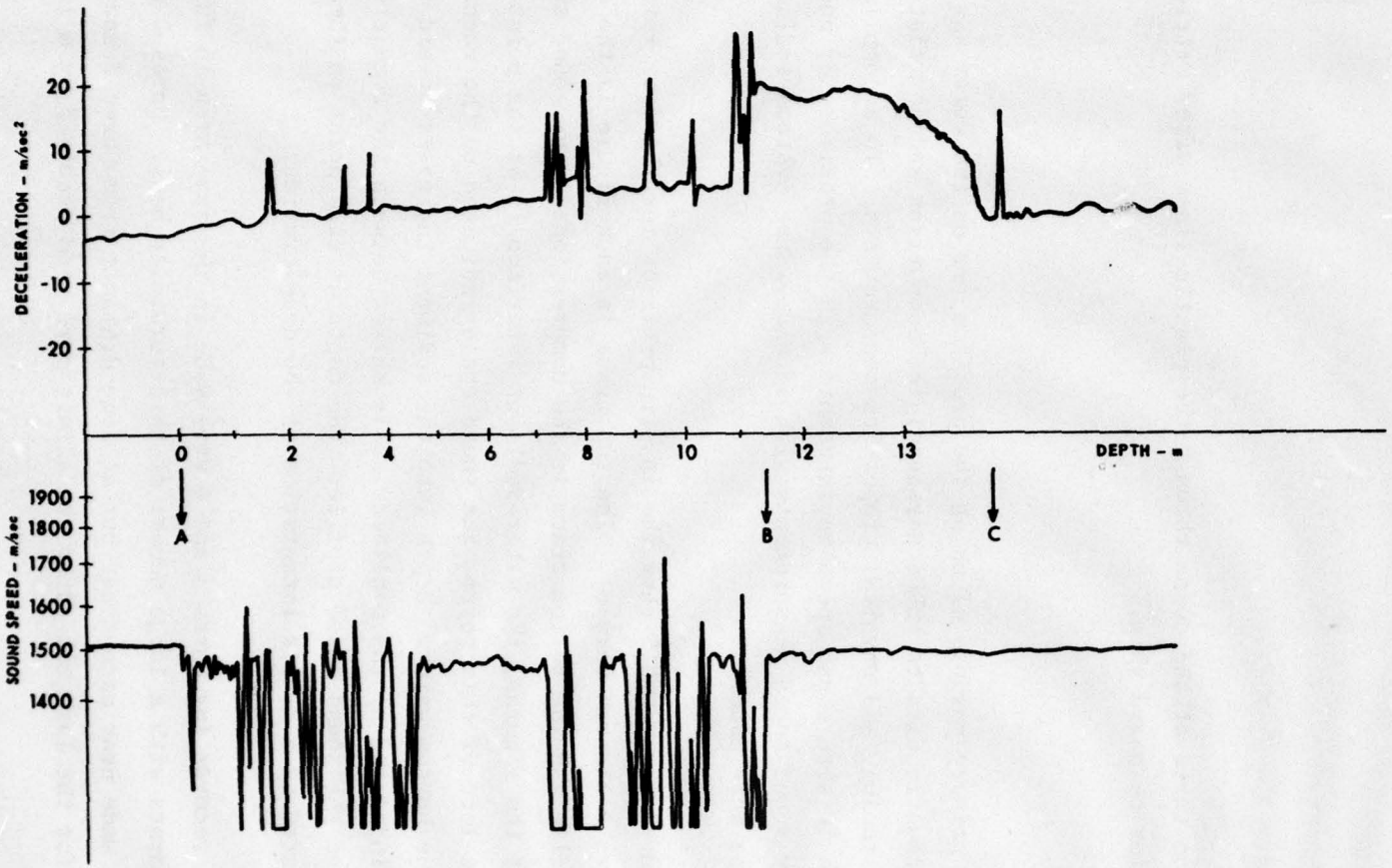

FIGURE 2
SOUND SPEED AND DECELERATION PROFILES FOR USNS DESTEIGUER CORE 3

ARL:UT
BS-78-1212
DJS-GA
7-12-78

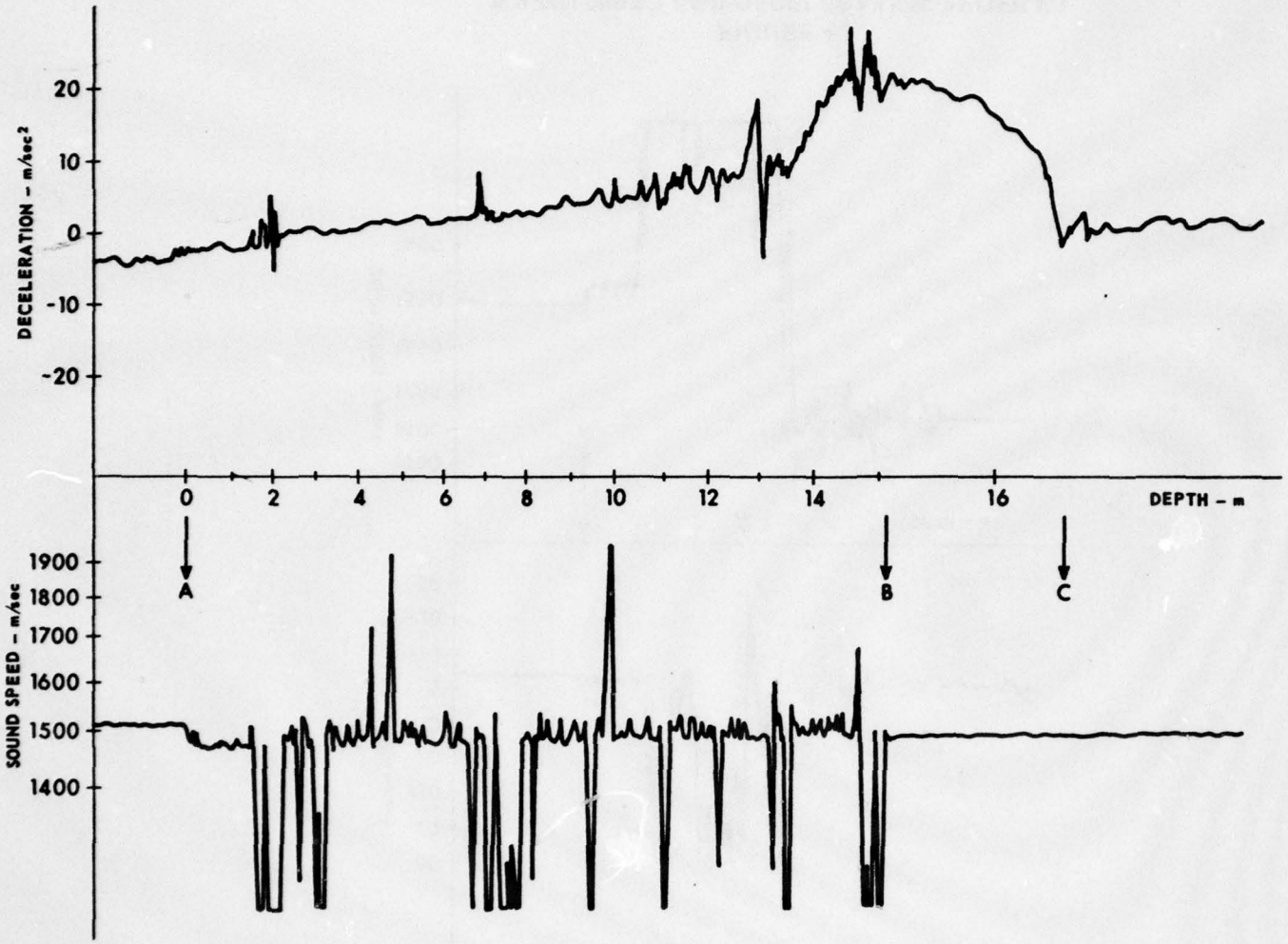

FIGURE 3
SOUND SPEED AND DECELERATION PROFILES FOR USNS DESTEIGUER CORE 4

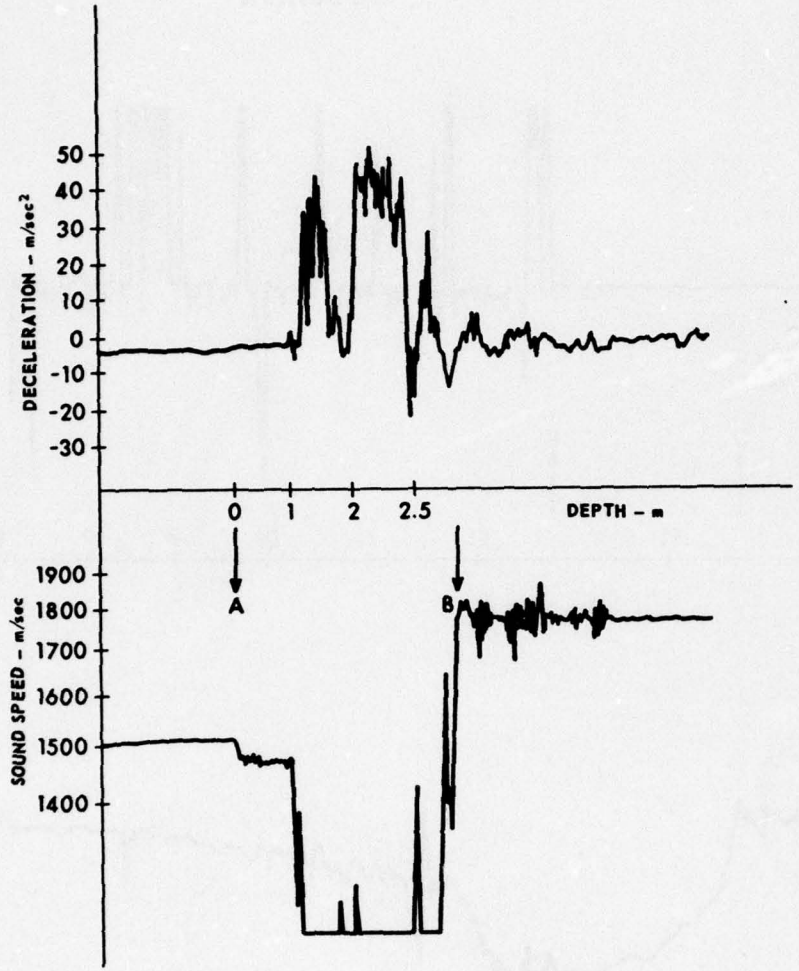

FIGURE 4
SOUND SPEED AND DECELERATION PROFILES
FOR USNS DESTEIGUER CORE 5

ARL:UT
BS-78-1214
DJS-GA
7-12-78

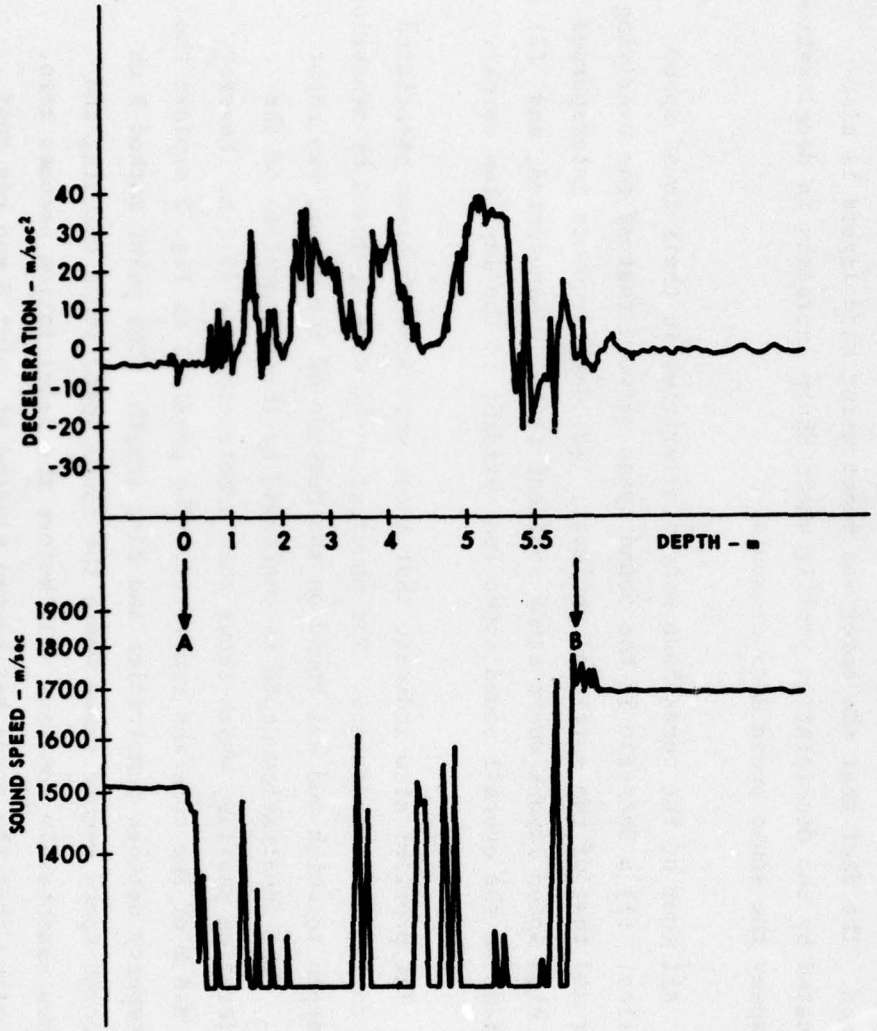

FIGURE 5
SOUND SPEED AND DECELERATION PROFILES
FOR USNS DESTEIGUER CORE 5

low speeds are artifacts caused by a decrease in the amplitude of the received pulse below the detection threshold of the receiver system. The amplitude decrease occurs during penetration of hard sediment layers such as sand. The fact that the corer was penetrating hard layers is also indicated by the deceleration profile where sharp increases in deceleration accompany the sound speed data dropouts.

All four of the cores have many similarities in their sound speed profiles: (1) a decrease in the sound speed between that of the overlying water and that of the surficial sediment, (2) data dropouts interspersed with high speed layers where sandy sediment is being penetrated, and (3) a gradient in the overall sound speed (not evident in the last two cores).

The profiles also indicate that there were some problems associated with coring these sediments. The penetration of Core 3, found by measuring the depth to which mud was found on the outside of the corer, was about 13 m. This penetration depth is confirmed by the integration of the deceleration profile, which shows that penetration was 13.2 m. However, only 8.8 m of the core was recovered. The profiles in Fig. 2 explain the discrepancy between penetration and core length. The point marked B on the sound speed record shows where the sound speed stops changing and becomes essentially constant well before the deceleration becomes zero, indicating that the corer has become plugged at point B and has quit accepting more sediment. This would cause the corer to have greater penetration resistance and in turn would cause an increase in deceleration, as indicated in the top profile. Although point B would indicate there should have been more than 11 m of core, probably the corer plugged gradually so that less sediment was retained than was indicated, thus greatly distorting the depth axis of the profile.

Core 4 measured 16.2 m penetration and 9.8 m of retained core. The profiles in Fig. 3 indicate that essentially the same process occurred as in Core 3, the preceding core.

In Cores 5 and 6, this problem did not occur since the sound speed record is the same length as the deceleration record. However, the penetration of the very sandy sediment caused excessive data dropouts and kept the profilometer from accurately measuring the sound speed in the sand until the corer had come to a stop. The mud layer on top of the sand does show the normal decrease in speed due to its high porosity. This layer was about 1 m thick for Core 5, but only about 0.3 m thick for Core 6.

After retrieval of the cores, laboratory sound speed profiles were made through the plastic liner. Figures 6 through 8 show the laboratory profiles for Cores 3 through 5, respectively. Sound speeds for the cores have been corrected to in situ conditions at the water-sediment interface. No account was made for any in situ temperature gradient in the sediment or for overburden pressure. The laboratory sound speeds were measured at 8 cm intervals along the core. The laboratory measurements on Core 3 were made about 4 h after retrieval. For Core 4, three days elapsed between retrieval and measurement. The flattened profile of Core 4 is probably the result of this long delay, which allowed the sandy layers to drain. No gradient is evident in either of the laboratory profiles for Cores 3 and 4.

Only about 1 m of Core 5 could be removed from the core pipe due to bending during coring. The laboratory sound speeds for this short section are displayed in Fig. 8. Most of the low sound speed mud layer that was evident in the in situ profile is missing in the laboratory profile and was probably destroyed during the hard penetration of the corer into the sand.

Table I summarizes the in situ and laboratory acoustic parameters for the four cores. The tabulated sound speed ratios were calculated by dividing

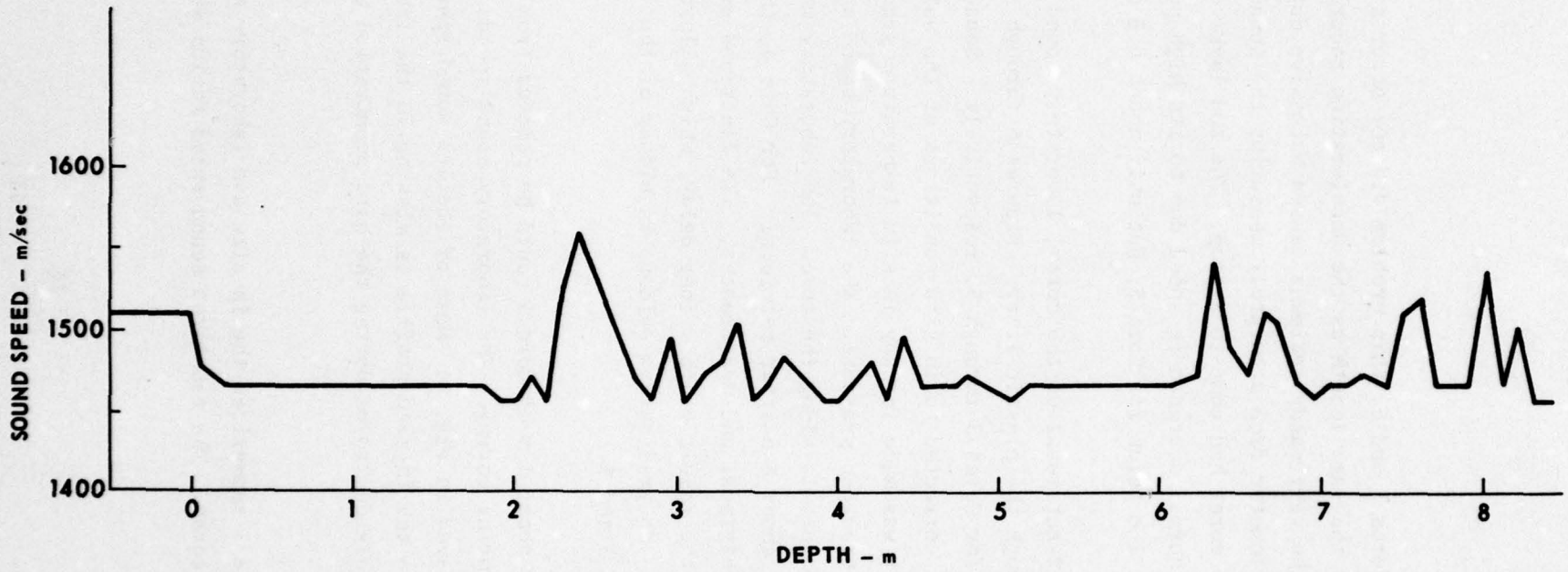

FIGURE 6
LABORATORY SOUND SPEED PROFILE FOR USNS DESTEIGUER CORE 3

ARL-UT
AS-78-1218
DJS-GA
7-14-78

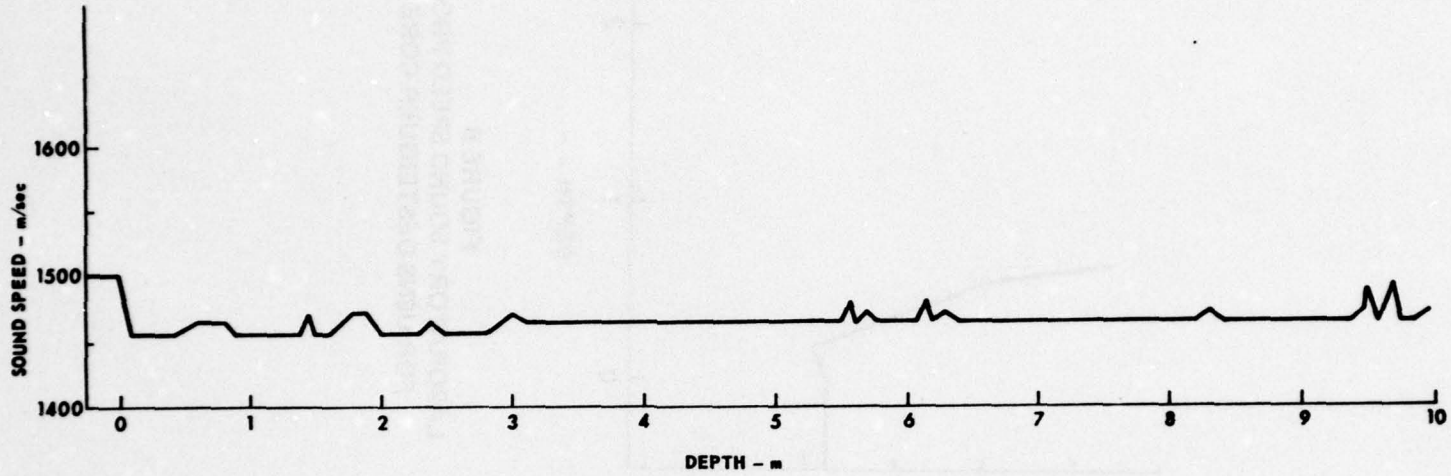

FIGURE 7
LABORATORY SOUND SPEED PROFILE FOR USNS DESTEIGUER CORE 4

ARL:UT
AS-78-1219
DJS-GA
7-14-78

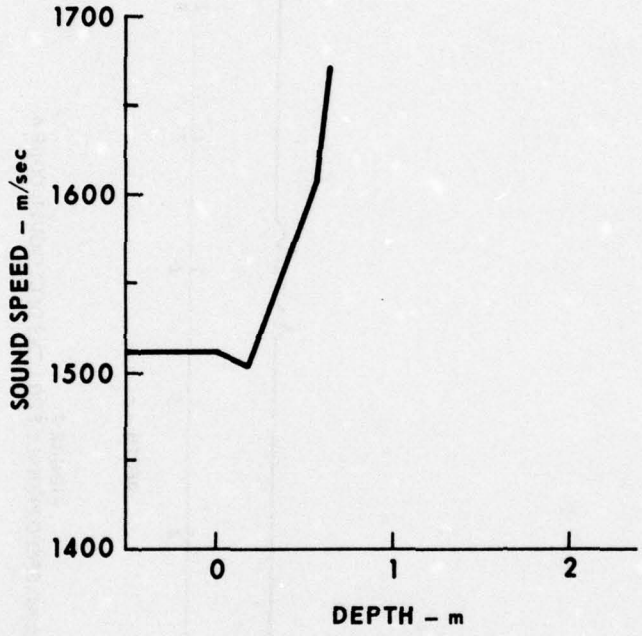

FIGURE 8
LABORATORY SOUND SPEED PROFILE
FOR USNS DESTEIGUER CORE 5

ARL:UT
AS-78-1220
DJS-GA
7-14-78

TABLE I

ACOUSTIC CHARACTERISTICS OF
USNS DESTEIGURE (AGOR-12) CORES

Core No.	In Situ Interface Ratio $\left(\frac{c_s}{c_w}\right)$	In Situ Gradient (sec^{-1})	Laboratory Interface Ratio $\left(\frac{c_s}{c_w}\right)$
3	0.976	1.6	0.970
4	0.976	1.6	0.969
5	0.976	---	0.993
6	0.977	---	---

the sound speed at the surface of the sediment by that of the overlying water. The gradients for Cores 3 and 4 were calculated by dividing the difference in sound speed at the beginning and end of the profile by the actual length of the retained core.

The in situ and laboratory values for the sound speed interface ratio are somewhat lower than reported values (0.985 to 1.061) for abyssal plain turbidites (Hamilton, 1970), but are well above lowest values (0.950) found for other sediment types (Akal, 1972). The in situ values for the interface ratio are more consistent than the laboratory values again indicating that disturbance is a prime factor in accepting values measured in situ over those measured in the laboratory.

The sound speed gradient of 1.6 sec^{-1} that was measured on the in situ profiles is higher than the commonly accepted average of 1 sec^{-1}. However most values of sound speed gradient are from sonobouy measurements which average over several hundreds of meters of sediment and so cannot be used for a direct comparison to data taken over only a few meters.

C. Discussion and Conclusion

In summary, the ARL:UT profilometer was used on one field trip during this year to obtain four new in situ sound speed profiles in deep water. Two of the profiles were made in relatively soft material and exhibit a typical profile for this type material, showing an interface sound speed ratio less than one and a sound speed gradient greater than 1 sec^{-1}. In the case of the gradient, the value of 1.6 sec^{-1} is somewhat larger than the commonly accepted value of 1 sec^{-1}. In the laboratory profiles which are uncorrected for temperature gradient and overburden pressure, the gradient is missing, indicating that all the mechanisms creating the gradient are released once the core becomes isothermal and isobaric.

The last two cores were made in stiff sand overlaid by a thin mud layer. Accurate sound speeds were only obtained in the mud layer except for the high sound speed observed once the corer came to rest. The accuracy of this latter sound speed measurement is questionable due to the expected large disturbance to the sediment from the hard impact in the sand.

The ARL:UT profilometer has again been shown to be a valuable tool for the measurement of ocean bottom acoustic parameters. The above measurements were made at little expense and not much extra effort since they were made as an adjunct to a routine coring exercise. A comparison between the in situ and laboratory profiles shows the value of obtaining acoustic data in situ since the laboratory profile rapidly changes with time and does not retain information about sound speed gradient. Of course, the laboratory data could be corrected for temperature gradient and overburden pressure, but these data in themselves must either be measured or assumed.

III. TRANSDUCER DEVELOPMENT

A. Introduction

In its present configuration the ARL:UT profilometer can measure only compressional wave acoustic parameters. A measurement of shear wave parameters in conjunction with a measurement of the compressional wave parameters and acoustic impedance would enable the calculation of all the viscoelastic parameters of a sediment.

As part of the ONR funded sediments program ARL:UT is continuing to develop the technology required to make shear wave and acoustic impedance measurements in situ. As a result of the in situ transducer development, more sensitive laboratory transducers for shear wave measurements have also been produced.

B. In situ Shear Wave Transducer Development

Figure 9 shows a schematic drawing of the operation of a ceramic bender element composed of two layers of piezoelectric ceramic rigidly bonded together and driven out of phase so that one layer expands in the length mode while the other contracts. The resulting differential size change causes the element to bend along its length in direct response to a driving voltage. Shear waves can be coupled from either end or both if the element is in contact with a medium which exhibits rigidity.

The ceramic bender is the heart of the ARL:UT effort to develop an in situ device to measure shear wave propagation. The bender exhibits two desirable properties for in situ transducers (1) the bender has low frequency, wide bandwidth characteristics in a small size, and (2) the bender has a higher compliance than other ceramic or crystal elements so it has better

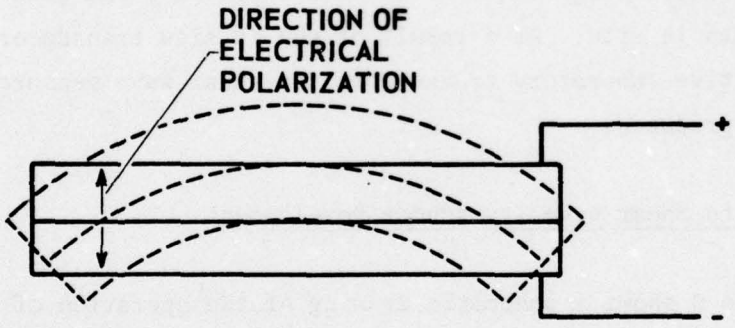

FIGURE 9
OPERATION OF A CERAMIC BENDER TRANSDUCER

ARL:UT
AS-77-1413-P
DJS - RFG
12 - 7 - 77

coupling characteristics with a soft sediment. The bender does have two requirements which must be satisfied: (1) each element must be left free to move independently for maximum compliance and maximum output, and (2) the most useful bender elements are rather fragile since the element must be as thin as possible for maximum compliance.

Preliminary designs for shear wave transducers used for laboratory testing had incorporated an array of bender elements arranged side by side with a layer of compliant material separating each element and also covering the entire array except for the end intended to couple shear waves into the propagation media (Shirley and Anderson, 1975). Such a transducer was rugged and produced a good signal-to-noise ratio (S/N) when working in soft sediments over a pathlength up to about 10 cm.

For high ambient pressure, the compliant spacers between the elements and the compliant covering around all the elements must be eliminated since high pressure would crush the compliant material. A single element could be potted directly in the encapsulant and, if the encapsulant is flexible enough, the element could still bend and generate or detect a shear wave. Transducers have been constructed in this manner using various flexible encapsulants such as Scotchcast 221, PRC 1527 (both are flexible urethane potting compounds), and RTV rubber. In the best of these transducers, signal levels across an equivalent sediment path were reduced 30 dB from the levels obtained with the laboratory type transducer described above; this level is not sufficient for work in clays and muds.

Another possible method for holding the element and protecting it from water would be to enclose the element in a metal housing filled with pressure compensated transducer oil with a flexible membrane to keep the oil in and the water out. The oil would not introduce appreciable damping on the motion of the bender element. Figure 10 illustrates the design of

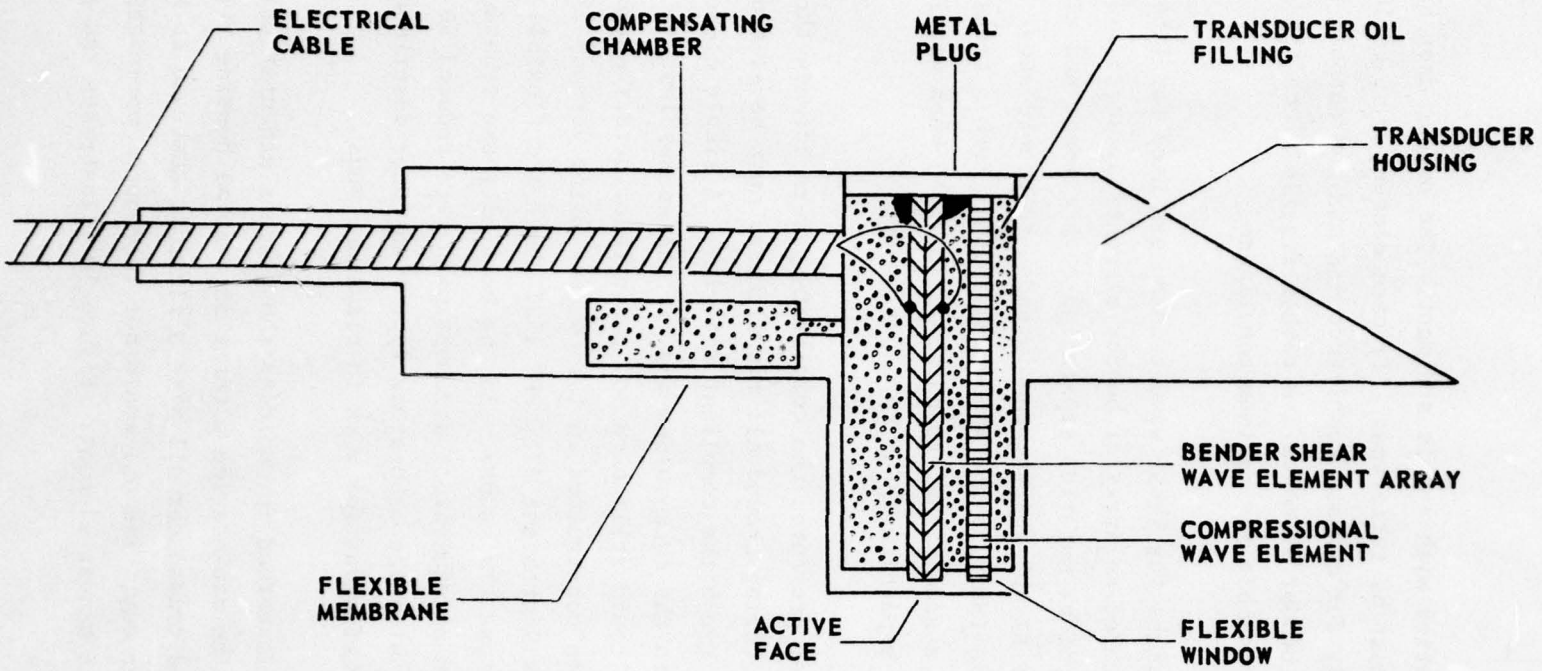

FIGURE 10
SCHEMATIC DRAWING OF COMPOSITE PROFILOMETER TRANSDUCER

ARL - UT
AS-77-787
DJS - RFG
7 - 22 - 77

this type transducer as it is fitted in a metal housing identical to the one used for the compressional wave profilometer transducers. A long length expander element is included to generate and detect compressional waves. The flexible membrane on the compensating chamber is made much thinner than the window across the transducer so that all the change in volume of the oil due to increased pressure and decreased temperature is made by the compensating chamber.

In situ tests of the above design indicate that the pressure compensation works but that the single element design of the shear wave element does not have sufficient sensitivity to overcome the noise generated during penetration of the corer. The single test that could be made on the USNS DESTEIGUER field trip was not conclusive because a sandy sediment was cored, which characteristically generates more noise than a softer one. The hard impact in the sand also damaged the window material and allowed a small amount of water to enter the transducer.

To overcome the weaknesses found in the above transducer design, a modified design was incorporated which would increase sensitivity of the transducer and also increase the ruggedness. The design is illustrated in Fig. 11. In the new design, a 5-element array replaces the single element shear wave transducer. The active end of this array is rigidly cemented to a small compressional wave transducer which operates in the thickness mode. Thus the shearing mode vibrations of the benders are transferred to the compressional wave element which in turn couples them to the sediment. Again, a thin flexible window protects the transducer from water contamination. Cementing the benders to the compressional wave element and to the rear of the chamber maintains the spacing between the elements so that no compliant spacers are needed.

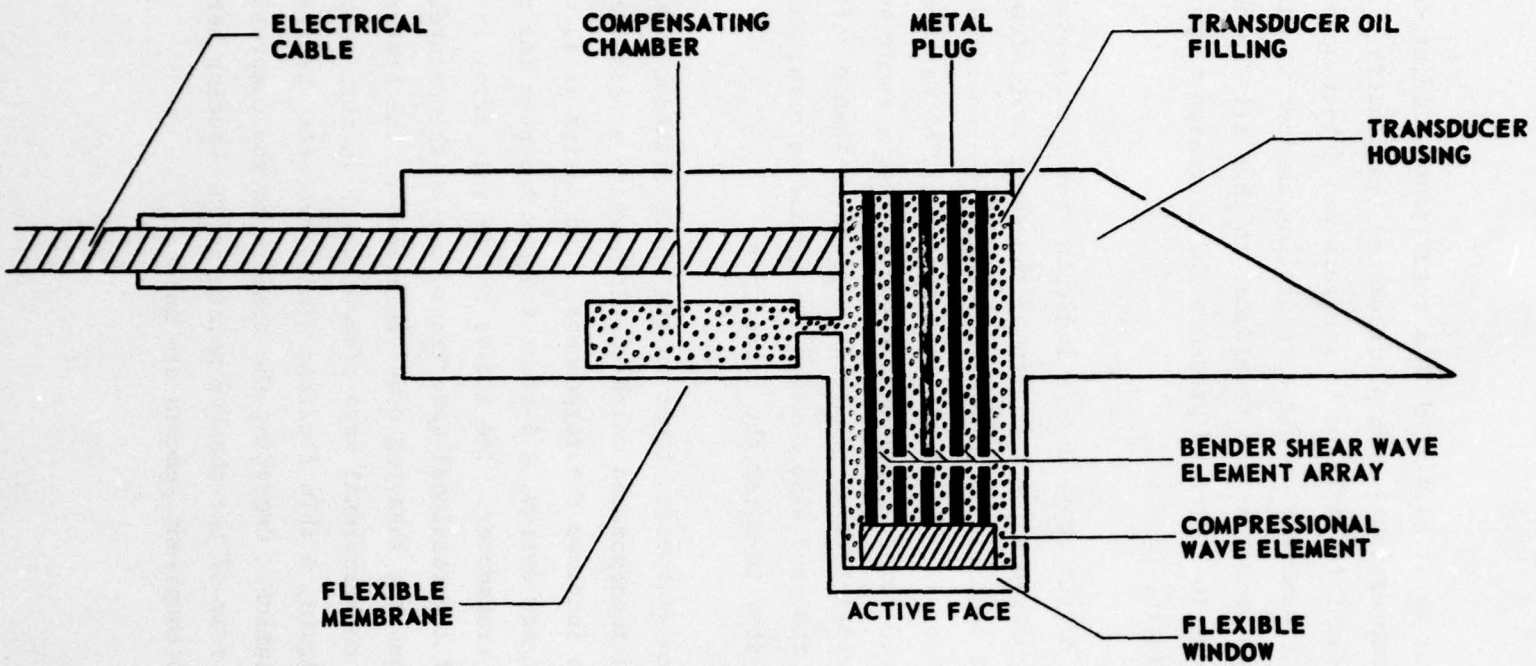

FIGURE 11
SCHEMATIC DRAWING OF COMPOSITE PROFILOMETER TRANSDUCER

ARL:UT
AS-78-1294
DJS - GA
8 - 2 - 78

The above transducer shows significant improvement in sensitivity in laboratory tests and is now awaiting further testing in the field.

C. Laboratory Shear Wave Transducer Development

In the initial stages of the present program to develop the capability to make shear wave measurements in situ, laboratory measurements were generally made to test preliminary designs of in situ shear wave transducers. As work progressed, it became evident that valuable new data could be obtained with the new shear wave transducers. It was also found that laboratory transducers could be designed for greater sensitivity and wider bandwidth but were not suitable for in situ use due to limitations on size and ruggedness.

Figure 12 shows a photograph of a typical transducer configuration using a bender element for the shear wave transducer. The transducer design incorporates a small compressional wave element to facilitate the measurement of both shear wave and compressional wave parameters of the sediment over the same propagation path. The compressional wave element consists of a thin piezoelectric ceramic plate operated in the length extensional mode.

The transducer holder is composed of a thin stainless steel blade to which the elements are attached by a semiflexible urethane potting compound (Scotchcast No. 8) that also acts as a water proof coating for the elements. Neither element is mechanically attached to the metal blade but, rather, the potting compound holds each one in place in the plane of the metal blade. This method of attaching the elements to the holder allows the elements to freely vibrate in their respective modes, and yet enough stiffness is retained to protect the elements from damage and to hold them at a constant spacing. Small insulated wires are connected to the

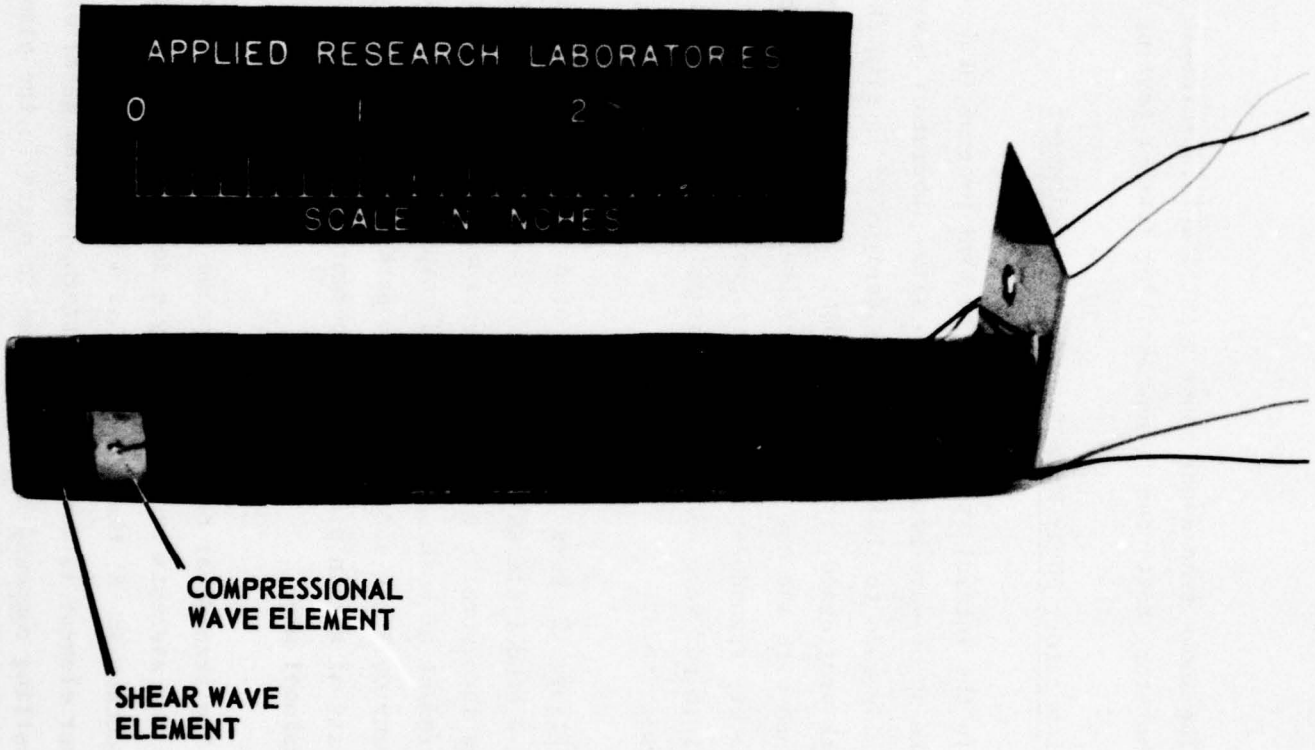

FIGURE 12
COMPOSITE SHEAR WAVE/COMPRESSIONAL WAVE TRANSDUCER
FOR LABORATORY MEASUREMENTS

transducer element electrodes and are also encased in the potting material the length of the metal blade. Transducers have also been made in which a long narrow printed circuit board has been substituted for the metal blade. Printed conductors on the board attached to the respective transducer element electrodes replaces the small insulated wires. The printed circuit method of construction reduces the cross-sectional area of the transducer and minimizes the amount of disturbance to the sediment when the transducers are inserted.

In the transducer shown in Fig. 12, the shear wave element is a Gulton type R102S series connected bender element with dimensions of 2.54 x 0.64 x 0.05 cm. The compressional wave element is a thin piezoelectric ceramic plate 1.27 x 0.64 x 0.16 cm which is polarized and driven in its thinnest dimension. The length extensional mode for this element has a resonance of 150 kHz.

Since the bender element is a long thin plate incorporating a leverage effect, it exhibits a much lower stiffness than an equivalent sized shear plate. The lower stiffness of the bender element provides a closer impedance match to an unconsolidated sediment than does the shear plate. By totally immersing the bender element in the medium, more acoustic energy can be propagated because the medium can be driven along the entire length of the element. When the element is embedded in a medium, mechanical motion is transferred from the element to the particles in the medium in such a manner that particle motion will be perpendicular to the length dimension of the element. The motion at the ends of the element is in phase while the middle will have a phase of 180° with respect to the ends. If the medium in which the element is embedded exhibits some amount of rigidity, the sideways or shearing motion of the medium will be propagated as a shear wave with the direction of propagation perpendicular to the particle motion (i.e., parallel to the length of the elements).

Only a small amount of energy will be propagated perpendicular to the element length, since the particle motions cancel in the farfield in all four perpendicular directions. Therefore, the result is a shear wave propagating in both directions from the ends of the transducer element.

Figure 13 shows an oscilloscope photograph of a shear wave pulse propagated through a water saturated sand sediment. The top trace is the received pulse and the bottom trace is the driving waveform applied to the projector. Center frequency for the driving pulse was 4 kHz. There was a separation of 5 cm between the edges of the receive transducer and the projector, and each was set up with the long axes of the shear wave elements in line. Both projector and receiver were of identical construction. The propagating medium was a quartz beach sand saturated with water. Shear wave speed for this sediment was found to be 95.2 m/sec.

Figure 14 shows an oscilloscope photograph of the received pulse and driving waveform for a 150 kHz compressional wave which was propagated over the same path through the same sediment as the shear wave. The compressional wave speed for the sediment was 1736 m/sec. In both Figs. 13 and 14 the small pulse at the beginning of the receive trace is an electrical feedover of the driving voltage due to the close proximity of the transmit and receive transducers.

The waveform of the received shear wave pulse shown in Fig. 13 illustrates the wide bandwidth characteristics of the transducer. The measuring circuit incorporates a variable bandpass filter which for the data shown in Fig. 13 was set at 350 Hz to 12.0 kHz. The filter tends to distort the received pulse, but the filter is necessary to eliminate acoustic and electrical noise picked up by the transducers. Without the filter in the system, the received pulse almost duplicates the driving waveform. Since shear wave speeds can be determined by measuring the time delay to an

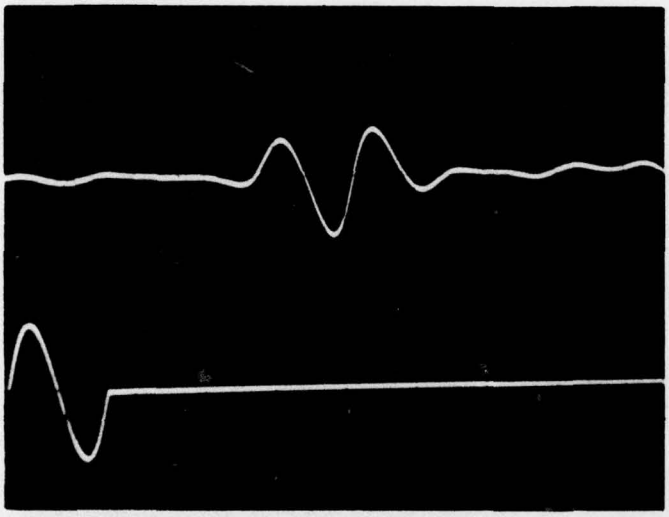

RECEIVED PULSE

TRANSMITTED PULSE

f_0 = 4 kHz
VERTICAL SCALE: 0.05 V/div TOP TRACE
20 V/div BOTTOM TRACE
HORIZONTAL SCALE: 200 μsec/div

FIGURE 13
SHEAR WAVE PULSE PROPAGATED THROUGH WATER SATURATED SAND

ARL - UT
AS-77-1044-P
DJS - DR
9 - 15 - 77

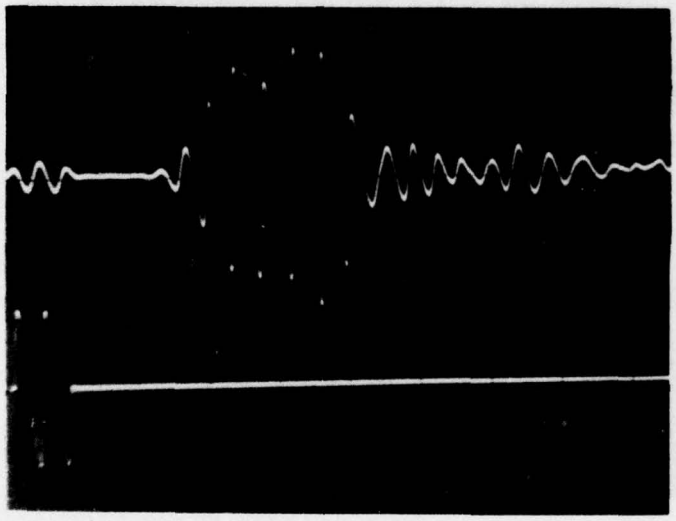

f_0 = 150 kHz
VERTICAL SCALE: 0.05 V/div TOP TRACE
20 V/div BOTTOM TRACE
HORIZONTAL SCALE: 20 μsec/div

FIGURE 14
COMPRESSIONAL WAVE PULSE PROPAGATED THROUGH WATER SATURATED SAND

ARL - UT
AS-77-1045-P
DJS - DR
9 - 15 - 77

easily recognized feature of the received waveform at several different transducer spacings, the distortion of the received pulse does not cause problems. This method of speed measurement also eliminates the requirement of finding the exact beginning of the pulse.

The resonance frequency of the shear wave transducer described above is 8 kHz in air, but the frequency range over which measurements can be made in a sediment are dependent upon the shear wave speed in that sediment. Since the transducer element is totally immersed in the medium and both ends are free to vibrate, its greatest sensitivity will be at the frequency at which a wavelength of a shear wave in the medium is the same as the length of the element. The usable frequency range for the above transducer extends as low as 300 Hz when used in muds and clays with shear wave speeds around 10 m/sec to as high as 7 kHz for sands with shear wave speeds near 100 m/sec. Shear wave speed and attenuation measurements have been made on one sand over the frequency range of 2 kHz to 7 kHz using this transducer.

D. Acoustic Impedance Transducer Development

Another part of the transducer development in the ARL:UT sediments program has been the design and fabrication of a transducer to measure the acoustic impedance of marine sediments by detecting the electrical parameters of a driven transducer in contact with the sediment (Shirley and Anderson, 1975; Shirley, 1977a; and Shirley, 1977b).

Work during the past year has been concerned with developing an easy calibration procedure for testing various transducers and examination of different transducer configurations to find one that could be used in situ.

To date, the calibration procedure has consisted of determining the electrical impedance of a transducer at resonance in contact with various

media such as air ($\rho c \simeq 0$), water ($\rho c \tilde{=} 1.5 \times 10^5$), and various sediments from clay to sand ($\rho c = 2 \times 10^5$ to 4×10^5). The drawback to the above procedure is that an independent measurement of the acoustic impedance of a sediment is difficult to make and is not very accurate. If a number of liquids could be used instead, the procedure would be easier and the acoustic impedance of a liquid is more readily measured and not easily changed. Figure 15 shows the results of a calibration of a transducer using various liquid mixtures of water, salt water, alcohol, and ethylene glycol antifreeze. Acoustic impedance of the liquids was determined by measuring their densities with a picnometer and their sound speeds with a set of compressional wave transducers. The data in Fig. 15 show less scatter than previous data obtained using laboratory sediments (Shirley, 1977a), and the data were measured over a relatively short time (1 day) compared to the sediment data (12 days). The increase in accuracy and decrease in time will allow various transducer designs to be tested more easily.

The design of an acoustic impedance transducer for in situ work has been hampered by a lack of suitable ceramic materials and by the difficulty in designing a transducer for high pressure work.

Piezoelectric ceramic materials that are best for high pressure work, such as lead metaniobate, are also the ones that have the lowest Q. A lower Q results in a smaller change in electrical impedance for a given change in acoustic impedance in the medium. Conversely, the formulations of lead zirconate titanate that have the highest Q also show a large sensitivity to ambient pressure. A great many tests are necessary to find a material with the proper performance at high pressure.

Another difficulty encountered in the design of an appropriate transducer is the amount of cable (approximately 15 m) between the

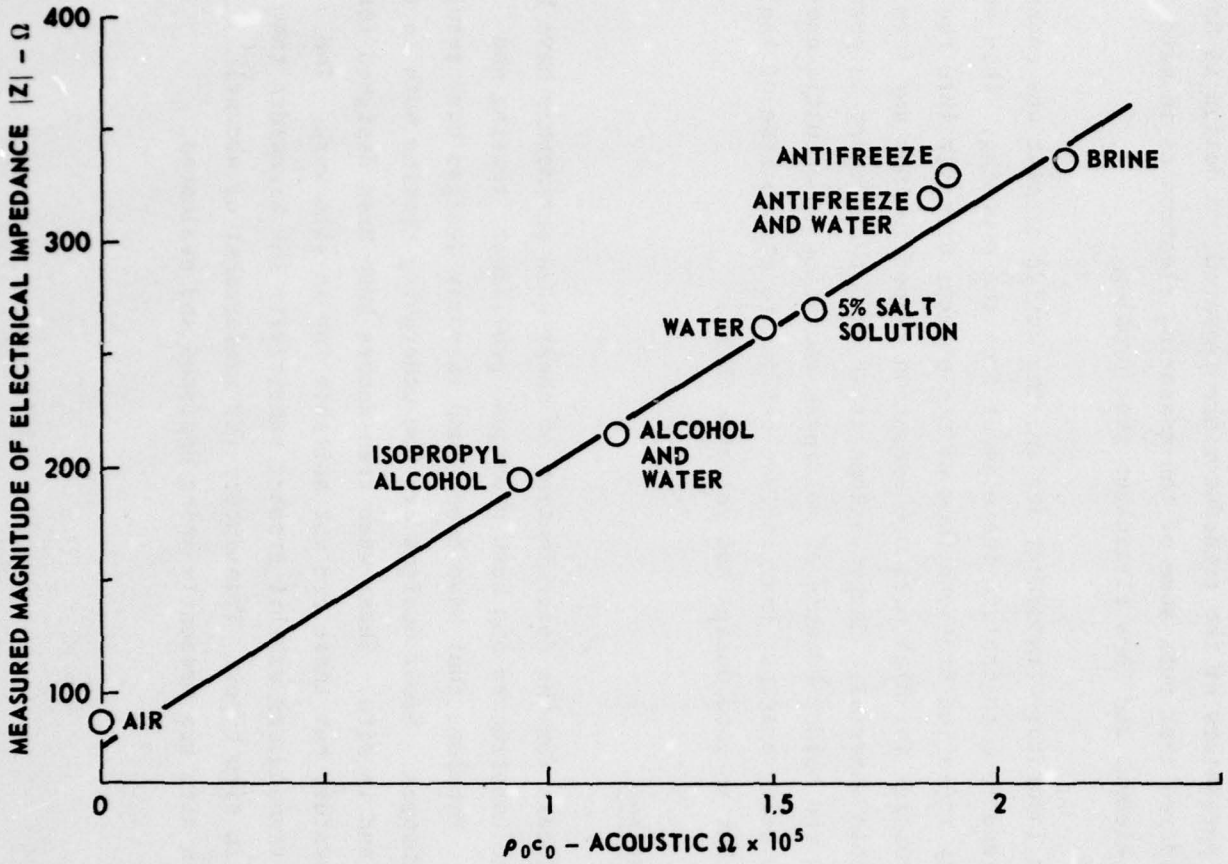

FIGURE 15
ACOUSTIC IMPEDANCE TRANSDUCER CALIBRATION IN LIQUIDS

ARL:UT
AS-78-1293
DJS-GA
7-31-78

measuring electronics and the transducer element. This cable introduces capacitance and inductance that must be tuned out so that only the electrical parameters of the transducer are measured. A design is now being considered that puts some of the measuring electronics in with the transducer element and thus eliminates that problem.

In the laboratory transducer design, the active element was encased in polystyrene foam to isolate the element from the mounting. This design allowed only radiation from one face of the element directly into the medium. A design for high pressure operation cannot include any form of collapsible material. Complications arise when the element is potted directly in the holder because of multipath radiation of acoustic energy. Designs are being examined that include baffles to absorb some of the multipath, but no good design has yet been found.

E. Conclusions

Transducers for the determination of shear wave parameters have been designed and constructed and have undergone preliminary testing and evaluation. Problems that have been found in early designs have resulted in design changes. Newer designs are now undergoing testing both in the laboratory and in situ. Shear wave transducers have been designed for use in the laboratory but these are not suitable for in situ work. The laboratory transducers exhibit greater sensitivity and bandwidth than comparable in situ types. Transducers for measurement of acoustic impedance in situ are presently being designed and evaluated.

IV. LABORATORY MEASUREMENTS

A. Introduction

The capability of making accurate shear wave measurements in laboratory sediments has evolved as the result of a program to include such measurements in the ARL:UT profilometer. Not only are laboratory measurements necessary to refine the transducers for in situ work; these measurements are useful in the general characterization of marine sediments in that there is a lack of comprehensive shear wave data. The parameters needed for such a characterization are the shear wave speed and attenuation, the compressional wave speed and attenuation, and the bulk density or, equivalently, the porosity and mineral composition. The present program includes the determination of these parameters for specific examples of three sediment types: sand, silt, and clay. Similar work for different sands performed under the present contract has been previously reported (Shirley, 1977) and will not be repeated here.

B. System Description

The sediment to be studied is placed in an aluminum tank (16 x 20 x 30 cm). Suspended vertically in the center of the tank are two thin sheets of stainless steel which serve as mounts for the transducers used to generate and receive the acoustic signals. Figure 16 is a full scale drawing of such a mount. The transducers are imbedded in a casting compound which provides both support and electrical insulation. One of the mounts is attached to a rigid crossbar and remains in a fixed location. The other mount is fixed to a threaded rod located on top of the tank. Rotation of this rod moves the second set of transducers relative to the first. Small sheets of cork prevent acoustic transmission through the support mechanism. Figure 17 gives the orientation of the mounts within the tank. Also shown

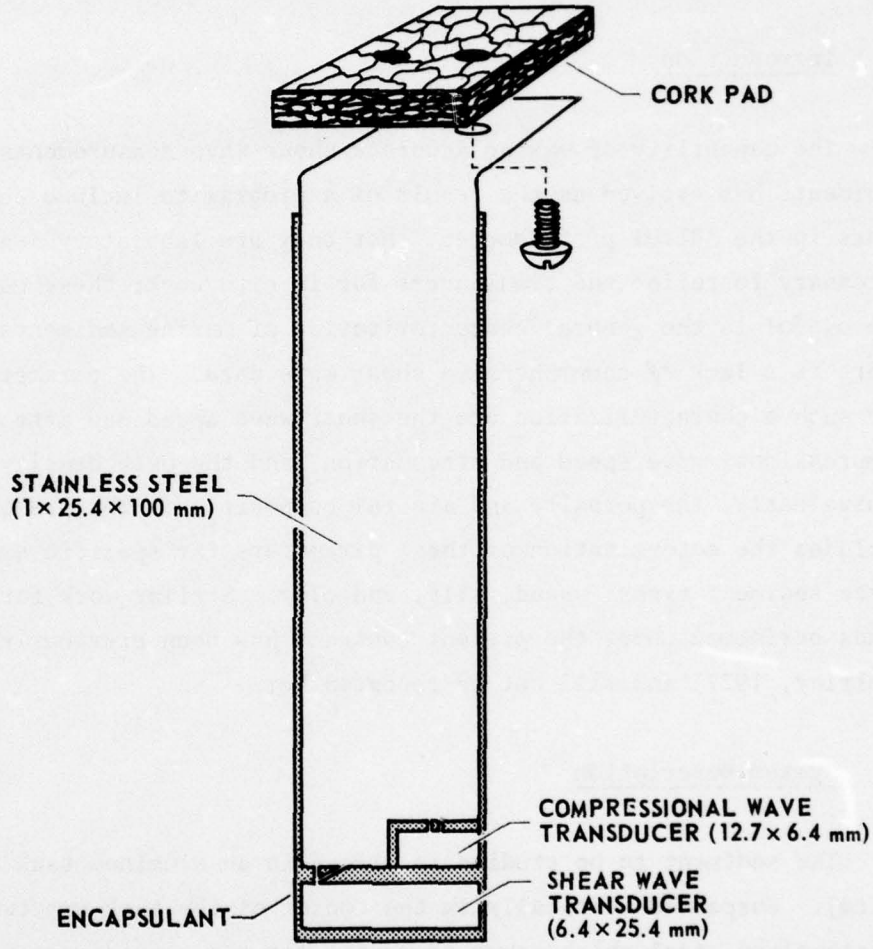

FIGURE 16
TRANSDUCER MOUNT FOR SHEARWAVE/COMPRESSIONAL WAVE LABORATORY TRANSDUCER

ARL:UT
AS-78-182
DWB-GA
1-23-78

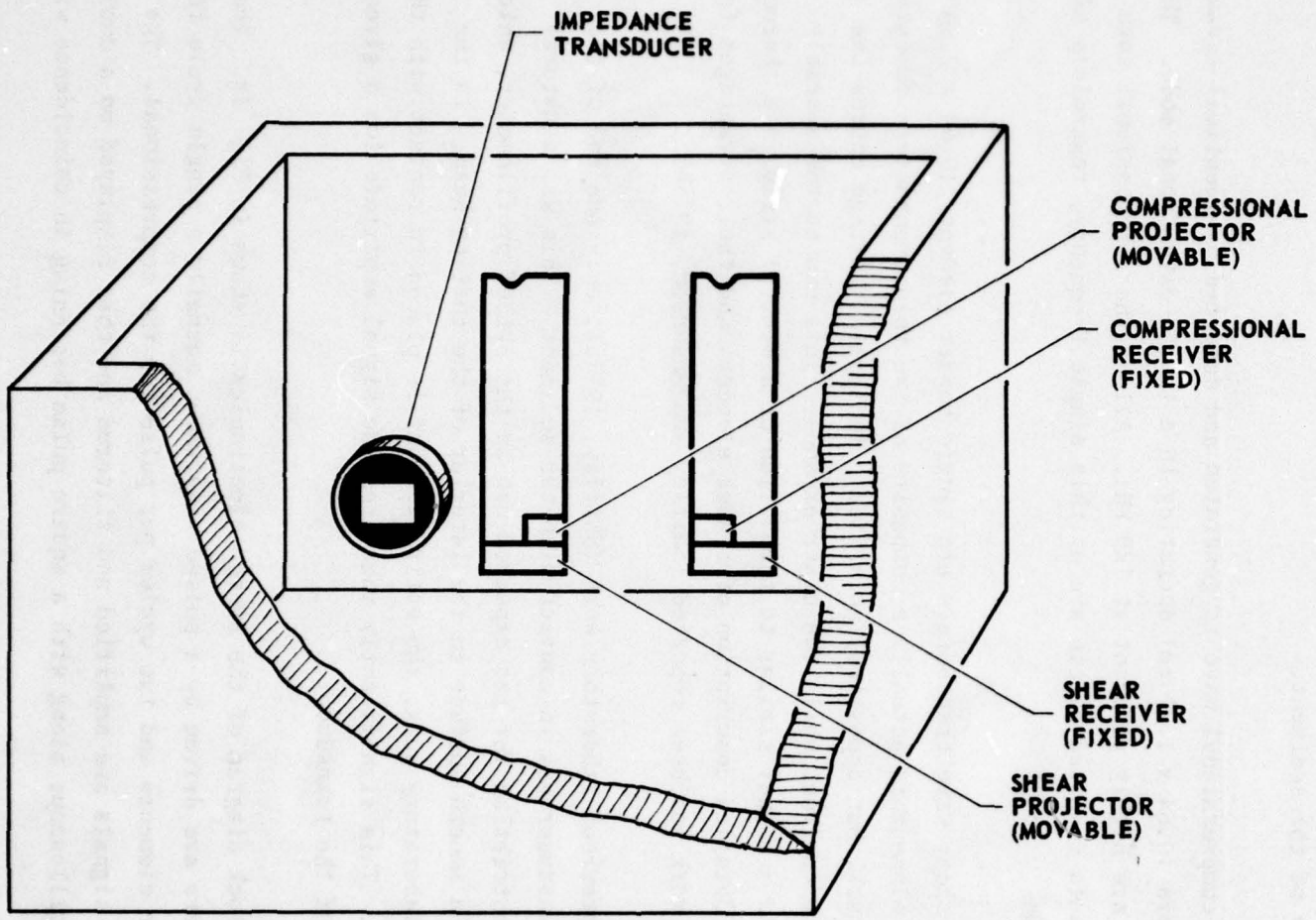

FIGURE 17
PROJECTOR-RECEIVER CONFIGURATION

ARL:UT
AS-78-183
DWB-GA
1-23-78

in Fig. 17 is the location of a transducer used to measure the acoustic impedance of the sediment.

The compressional wave is generated and detected by identical ceramic transducers (0.64 x 1.27 cm) operating in a length extensional mode. These elements are highly resonant at 120 kHz. All of the compressional wave measurements reported herein are at this single frequency, regardless of the medium.

The shear wave transducers are single bender elements (0.64 x 2.54 cm). A bender element is actually a composite of two thin transducers cemented back to back, but oppositely polarized. An applied voltage causes one element to contract while the other expands. This causes the assembly to bend in a manner similar to the action of a bimetal strip in a thermostat. A detailed description of bender elements and their advantages for sediment work has been reported (Shirley and Anderson, 1975b).

In previous laboratory work (Shirley, 1977a), only one end of the shear transducer was in contact with the sediment. This was a natural design restriction for its expected use in the ARL:UT profilometer, which requires a smooth surface in the interior of the cutting head. In the present laboratory work, the entire element is placed in contact with the sediment. This significantly increases the signal amplitude for a given flexion of the transducer.

A block diagram of the system electronics is shown in Fig. 18. The transducers are driven by a pulsed sine wave, normally a single cycle for the shear elements and two cycles per pulse for the compressional. The received signals are amplified and filtered and then displayed on a dual trace oscilloscope along with a square pulse beginning in coincidence with

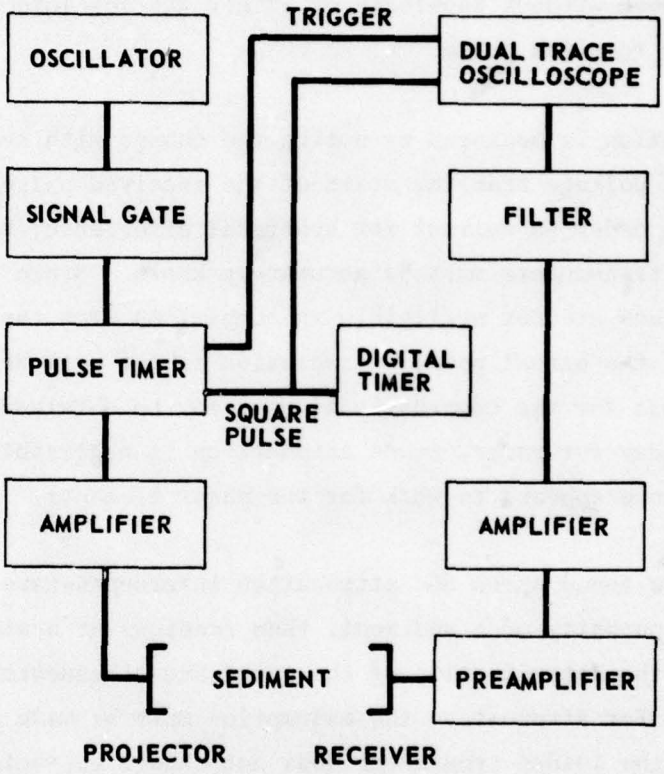

FIGURE 18
SYSTEM BLOCK DIAGRAM

ARL:UT
AS-78-184
DWB-GA
1-23-78

the transmitted pulse. The end of the square pulse is aligned with a particular peak of the received signal, as shown in Fig. 19. Concurrently, the period of the square pulse is displayed on a digital counter. Thus, the transit time of a chosen feature of the received pulse may be determined as a function of transducer separation. The slope of such a curve gives the sound speed without knowledge of either the absolute separation or the start of the received pulse.

Attenuation is measured by noting the change with separation of the peak to peak voltage near the start of the received pulse, as indicated in Fig. 19. In order to correct for spherical divergence, the distance between the transducers must be accurately known. Since the dimensions of the transducers are not negligible in comparison with the separations or wavelengths, the actual point of radiation is not well defined. The spreading loss for the compressional wave may be obtained by measuring the amplitude decay for water, whose attenuation is negligible. The center to center distance appears to work for the shear elements.

Once the sound speed and attenuation intercepts have been obtained for a given porosity of a sediment, then readings at a single separation suffice for the determination of the speed and attenuation at other porosities. For attenuation the assumption must be made that the amplitude response of the loaded transducer does not change appreciably with porosity.

C. Shear Transducer Response

The shear transducers are capable of generating measurable signals over approximately a decade of frequency. In practice, however, the frequency range set by the transducer response is further limited at the upper end by the increase of attenuation with frequency and at the lower

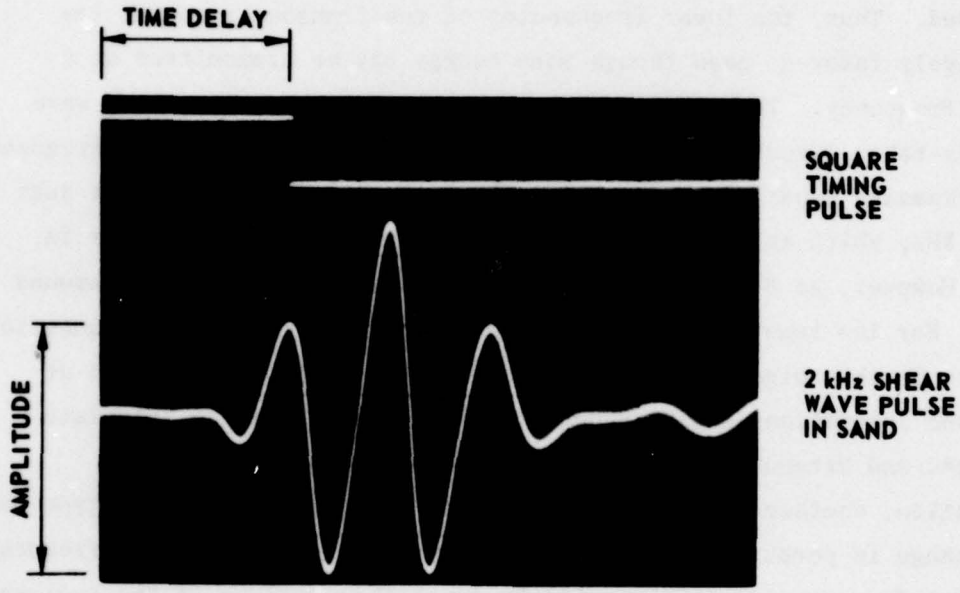

FIGURE 19
OSCILLOSCOPE TRACE OF SHEAR WAVE RECEIVED PULSE ILLUSTRATING TIME AND AMPLITUDE MEASUREMENTS

ARL:UT
AS-78-185
DWB-GA
1-23-78

end by the pulsed nature of the measured wave. The actual frequencies involved change with differences in sediment impedance.

The increase of attenuation with frequency shifts the maximum received amplitude lower in frequency as the separation of the transducers is increased. Thus, the lower frequencies of the transducer output are selectively favored, even though more energy may be transmitted at a higher frequency. This is illustrated in Fig. 20 where the shear wave voltages taken directly from the oscilloscope are plotted versus frequency for increasing separation. At 1 cm, the maximum voltage occurs at just over 4 kHz, which is close to the true resonance of the transducer in sand. However, at 8 cm separation, the maximum amplitude occurs around 3 kHz. For low input signals or high attenuations, the upper frequencies are lost in the noise level before a sufficient number of readings at increased separations can be made with which to confidently calculate the speed and attenuation. This effect increases with increasing attenuation, whether the increase is due to a different sediment type or to a change in porosity of the same sediment. Consequently, the frequency selection for porosity studies will be lower than optimum if the sediment is initially highly porous.

If the losses due to spherical spreading and attenuation are removed from Fig. 20, the frequency response of the shear transducer is obtained, as shown in Fig. 21. The amplitudes are expressed relative to an arbitrary reference level. The dependence of the transducer response on sediment load is clearly indicated. The frequency of maximum output decreases in going from sand to clay. Data taken at the edges of the transducer response are ambiguous because of frequencies introduced by the pulsed nature of the transmitted signal.

Measurements on a pulsed wave cannot refer strictly to a single frequency; rather, they apply to a band of frequencies controlled

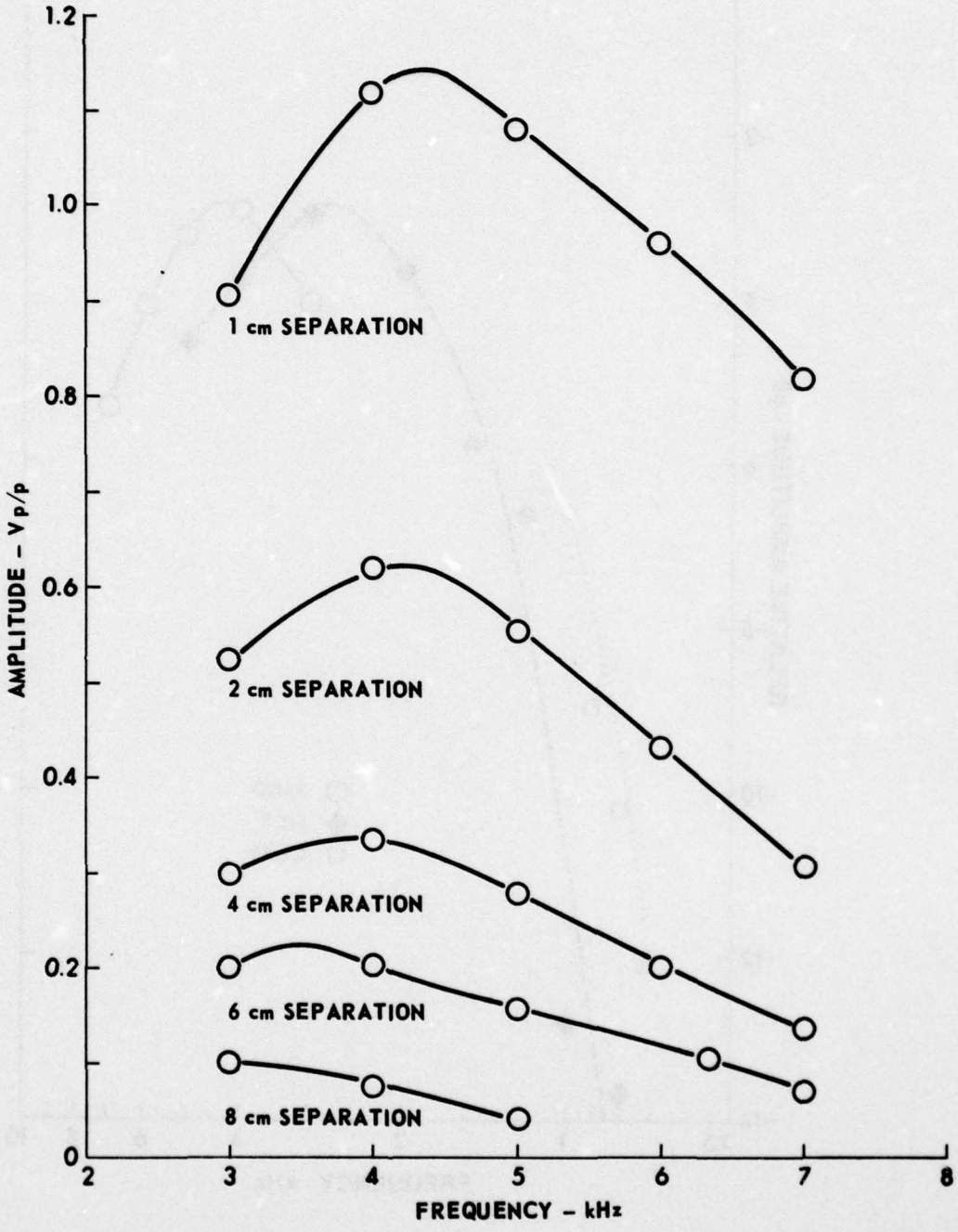

FIGURE 20
VARIATION OF AMPLITUDE WITH SEPARATION OF RECEIVED SHEAR WAVES

ARL:UT
AS-78-186
DWB - GA
1 - 23 - 78

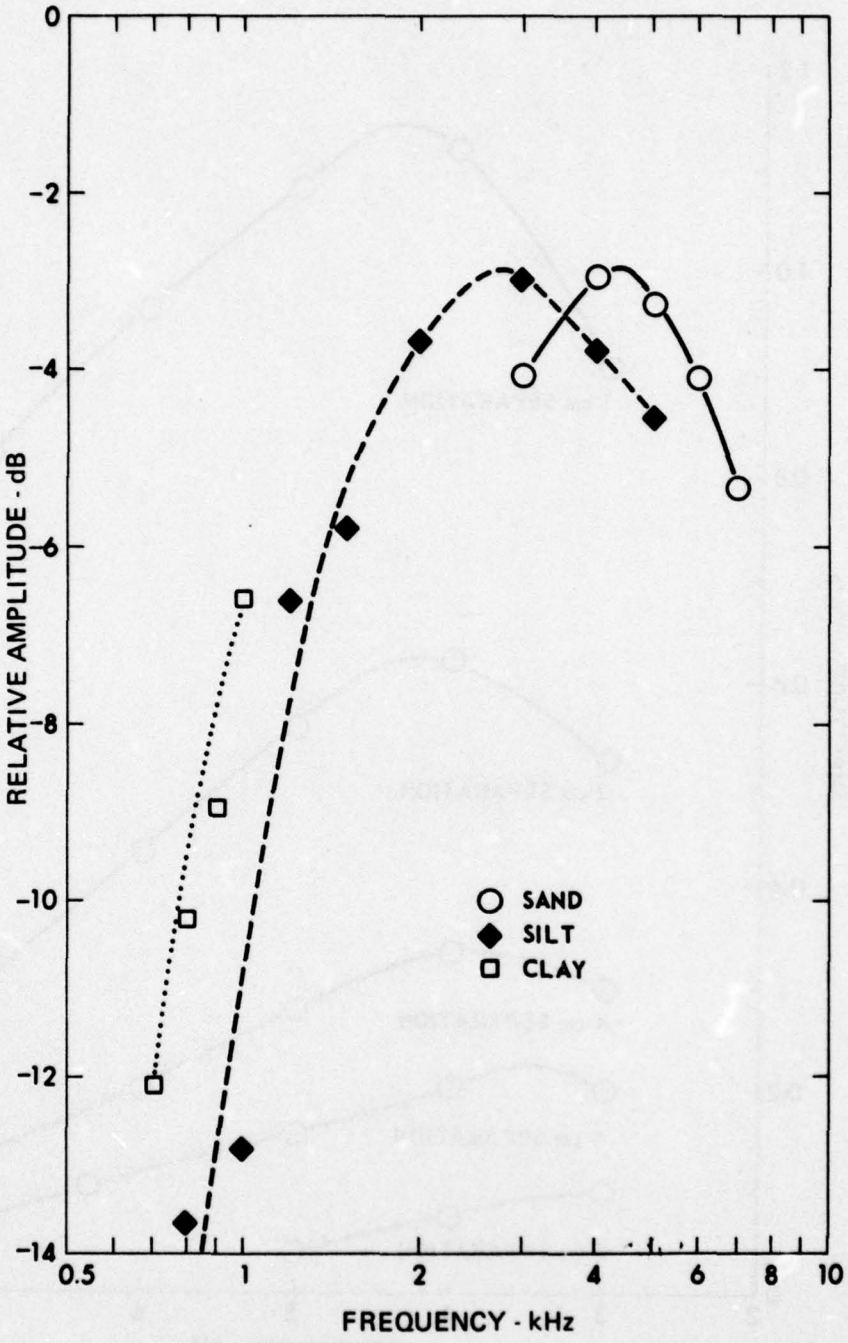

FIGURE 21
AMPLITUDE RESPONSE OF SHEAR WAVE TRANSDUCER

ARL:UT
AS-78-187
DWB-GA
1-23-78

by the width of the pulse and the characteristics of the filtering. With the use of a single cycle driving pulse, the width of the time gate will vary with frequency. Therefore, to maintain the same received signal shape, the filter applied to the pulse must also vary. If the only non-constant filter applied to the system is that purposely imposed on the electronic signal, then the pulse shape will remain the same if the filter is adjusted for constant Q. In this case Q is defined as the central frequency divided by the bandwidth. A larger Q gives a more reliable determination of frequency, but also decreases the signal amplitude.

The electronic filter, however, is not the only one applied to the signal. The transducer acts as a filter, as shown in Fig. 21, and the sediment itself constitutes a filter. In effect, the purpose of this project is to define the sediment filter and, to do this, filtering due to the transducers must be taken into account. While a measurable signal can be obtained, for example, at 500 Hz for the sand, such a signal may be dominated by the higher frequencies in the passband since the response of the transducer at this point is sharply decreasing. This is in fact observable on the oscilloscope trace. At the lower frequency settings, the period of the pulsed cycle is noticeably less than that of the continuous signal. Thus, one must be careful in assessing the sensitivity at the lower end of the transducer frequency to ensure that the frequency reported is actually the one measured. The frequency can better be determined by using more than a single cycle as the transmitted pulse. However, several cycles transmitted in a small tank creates too much interference. Even for a single cycle driven pulse, at low frequencies, the tail of the received wavelet is deformed at increased separation by the arrival of reflections.

As currently employed, the shear transducers are capable of reliable measurements over a frequency range of slightly less than a decade with

reasonable limits on sensitivity and noise. Two easily implemented modifications should increase this range. First, a larger tank will reduce the interfering reflections and allow a longer driving pulse. Second, the response of the transducers may be altered by changing the size of the elements. The individual readings of an array of different sized elements may then be combined to give an extended frequency range.

D. Sample Preparation

Three sediments have been studied: a mature, medium white quartz sand from Panama City, Florida; a calcareous silt of various mineral constituents, $\rho = 2.72$ g/cm^3, derived from a river gravel washing operation; and pure kaolinite clay.

The sand may be added directly to water in the tank. The silt and clay, however, must first be blended in a mixer to ensure total wetting of the grains. After the sediment has been introduced in the tank, the entrained air must be removed; this is accomplished with varying degrees of difficulty by vibrating the tank under vacuum. If the bubbles are not removed, the compressional wave is very highly attenuated and its speed is lowered. The compressional wave transducers have a second, width extensional resonance at 400 kHz which is normally about 20 dB below the primary resonance amplitude. Due to the difference in wavelength, this second mode is affected only slightly by the size of the bubbles. Hence, the ratio of the magnitudes at the two frequencies may be used if bubbles are suspected. It takes very little entrapped air to cause the second resonance to have a larger amplitude than the primary pulse. However, the shear wave does not appear to be affected by entrapped air at the frequencies studied. This is an area needing further research since gas is generated in some natural sediments.

The porosity of the individual sediments is controlled by variations in the grain packing. To measure speed and attenuation with changes in porosity, the sediment is initially made as loose as possible, by washing the sand with water and by stirring the silt and clay. Measurements are then made as the sediment settles due to gravity. For sand, the process may be accelerated by vibrating the tank.

Reliable measurements of the porosity as the sediment settles are difficult. A measurable decrease in the height of the sand would allow the porosity to be calculated if the minimum porosity were known. The minimum porosity can be accurately determined from a separate sample. However, the maximum change in height is approximately 1 cm for an initial depth of 15 cm. Fine graduations in the porosity thus require the accurate measurement of the sand level to at least a millimeter. This measurement is difficult, especially since vibrating the tank to ensure minimum porosity can cause fluctuations in sand level across the surface.

Porosities are determined for the silt and clay by measuring the weight change when small samples are removed from the tank and dried. The samples are obtained by a piston corer made from a plastic syringe 8 mm in diameter. For the clay, care must be taken to insert the probe to the same depth for each sample since compaction varies with depth. The repeatibility of these measurements is poor.

At this point, it may be noted that any minor physical disturbance of the sediment can cause a significant change in the arrival time and amplitude of the received shear pulse. Tapping the sides of the tank will cause an increase in the travel time, which normally will slowly return to its previous value. Vibrating the tank or inserting the corer, even at the opposite end from the transducers, will cause similar time shifts.

Thus, because the transducer spacing has been changed while vibrating the tank, the system must be allowed to stabilize before a reading is made. For a well sorted sand, 15 min may be enough, especially if the vibration amplitude is slowly decreased rather than abruptly stopped. For the silt, this stabilizing period may be longer than an hour. The clay is so greatly disturbed by the operation that only a single reading per day may be possible. The compressional wave pulse is not so easily affected.

The above observation reinforces the contention that reliable acoustic measurements in natural sediments must be obtained in situ with as little disturbance as possible. This appears to be even more crucial for shear wave measurements than for compressional wave data.

E. Data Acquisition

All of the measurements discussed below were made at room temperature, about 25°C. The slight variations about this figure do not appear to affect the results. Indeed, the time discrimination for the compressional wave is not sensitive enough to record the expected variation of sound speed with temperature. The sensitivity of the shear wave speed to temperature is not known and is an area worthy of future study. However, such variations must be well below the scatter in the present data introduced by coupling and porosity changes.

The compressional wave projector was driven at 30 Vp-p. The amplitudes recorded for the received pulse depend on the choice of a particular cycle within the pulse envelope. Maximum values of the center peak to peak voltage were typically around 10 V with 40 dB of gain applied. The tail of the received pulse will change shape with increasing separation as reflections begin to interfere; however, this presented no problems with

the separations used. Analyses made using values recorded for different parts of the beginning waveform were the same within experimental error. A 100 to 140 kHz bandpass filter about the center frequency of 120 kHz was applied to the received pulse. The cycle periods were essentially the same for the continuous oscillator output as for the pulsed signal.

Reliable shear wave measurements were made in the sand for 3, 4, 5, 6, and 7 kHz with a filter Q of 1. Maximum value of the received pulse was approximately 1 Vp-p with 60 dB of gain. For the silt, frequencies of 0.8, 1, 1.2, 1.5, 3, 4, and 5 kHz were used. Results for 0.7, 0.8, 0.9, and 1 kHz are reported for the clay. A filter Q of 2 was used for both of these sediments. Measurements were attempted at lower frequencies for the clay, but were hampered by the pickup of audible acoustic noise.

The number of data points per sediment type shown in Figs. 22 and 23 reflect the ease with which consistent readings were made. For the sand, readings were taken approximately every hour. After the time delays and amplitudes were recorded for both wave types, an electromechanical vibrator attached to the side of the tank was used to loosen the sand sufficiently to allow changes in spacing without compacting the sediment ahead of the transducer. Vibration was continued for approximately 15 min while the amplitude was slowly decreased to ensure return to lowest porosity. Sufficient time was then allowed for all readings to stabilize. Measurements were relatively easy to repeat. The same procedure was used for the silt with both the vibration and stabilization times increased. Consistent readings were harder to obtain due to the difficulty of returning exactly to the previous porosity. If, as occasionally occurred, the time delays were obviously off, and/or the wave shape was distorted, the vibration and settling process was repeated. The clay was even less tractable than the silt. Measurements were made a day after the spacing was changed. Those readings that were widely divergent from the mean were discarded.

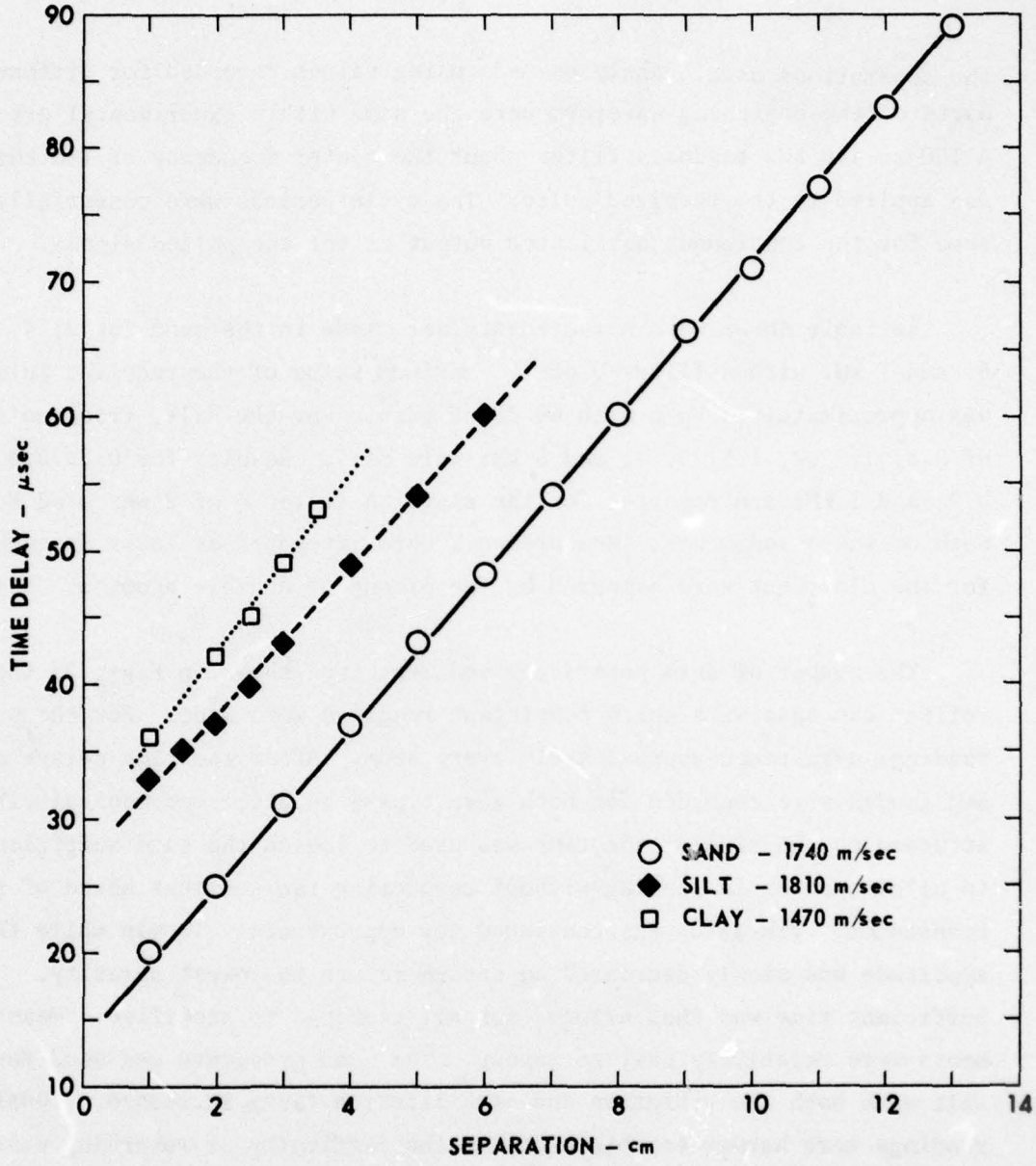

FIGURE 22
DETERMINATION OF
COMPRESSIONAL WAVE SPEED IN
THREE SEDIMENT TYPES

ARL:UT
AS-78-188
DWB - GA
1 - 23 - 78

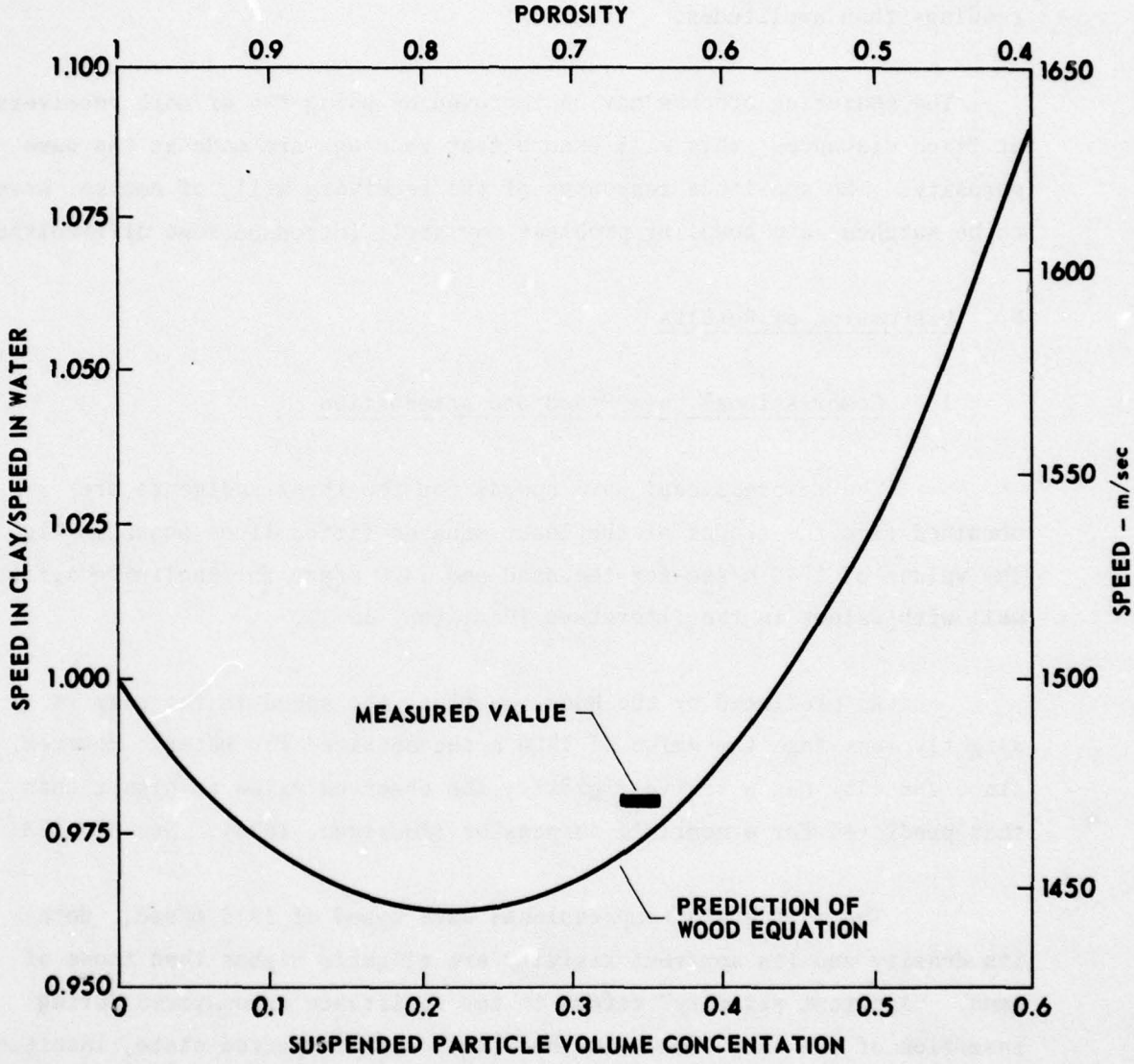

FIGURE 23
COMPRESSIONAL WAVE SPEED versus POROSITY - CLAY

(After Anderson 1974)

ARL:UT
AS-78-189
DWB - GA
1 - 23 - 78

The uncertainty in the measurements obviously increases when going from sand to clay. Note that it is easier to obtain consistent time delay readings than amplitudes.

The measuring process may be improved by using two or more receivers at fixed distances; this will ensure that readings are made at the same porosity. The amplitude responses of the receivers will, of course, have to be matched, and coupling problems may still introduce some difficulties.

F. Discussion of Results

1. Compressional Wave Speed and Attenuation

The compressional wave speeds for the three sediments are obtained from the slopes of the least squares fitted lines shown in Fig. 22. The values of 1740 m/sec for the sand and 1470 m/sec for kaolinite agree well with values in the literature (Hamilton, 1971).

As predicted by the Wood equation, the speed in the clay is slightly less than the value of 1500 m/sec obtained for water. However, since the clay has a finite rigidity, the observed value is higher than that predicted for a nonrigid suspension (Anderson, 1974). See Fig. 23.

The silt has a compressional wave speed of 1810 m/sec. Both its density and its apparent rigidity are slightly higher than those of sand. "Apparent rigidity" refers to the resistance encountered during insertion of the core tube. In the silt's most compacted state, insertion of a rod the size of a finger is difficult.

Figure 24 gives the observed decrease in amplitude with separation after a correction for spherical divergence has been applied. The scatter

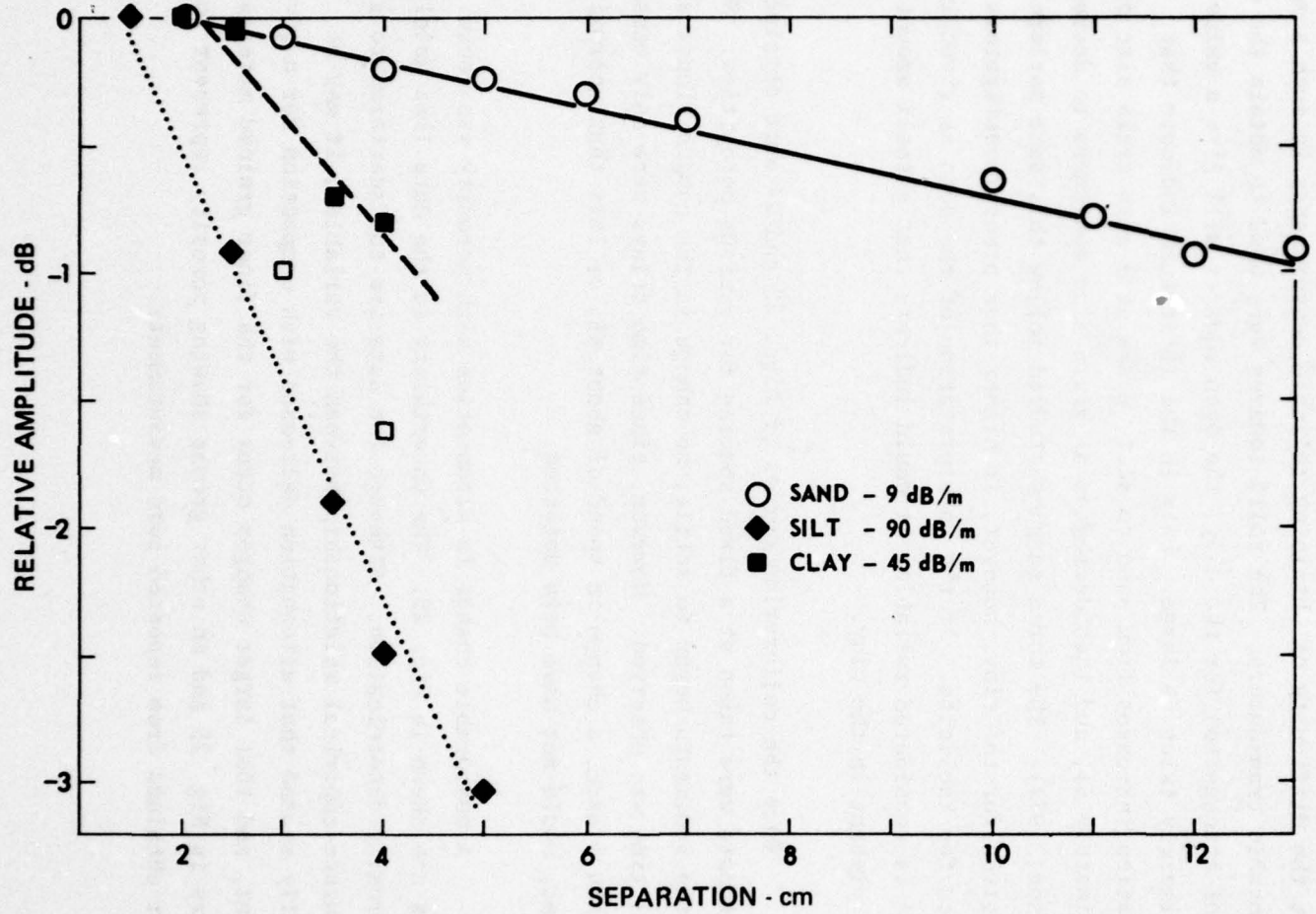

FIGURE 24
DETERMINATION OF COMPRESSIONAL WAVE ATTENUATION IN THREE SEDIMENT TYPES

ARL:UT
AS-78-190
DWB-GA
1-23-78

of the sand and silt measurements is small. The data for the clay, however, reflect the difficulty of obtaining reliable measurements in such a medium with movable transducers. The solid squares were used to obtain the quoted value of attenuation for the clay; the open squares will give a value approximately twice as large. Data in the literature indicate that attenuation increases from sand to silt, peaks at a mean grain size of approximately 5ϕ, and then decreases as grain size continues to decrease (Anderson, 1974). The three samples studied follow this same pattern. The value given for the clay, however, is higher than other investigators have reported for kaolinite. If the interpretation of the data as given in Fig. 24 is considered reliable, it would indicate that a small amount of air is present in the clay.

Once the calibration curves of Figs. 22 and 24 were obtained, measurements were taken at a fixed spacing for various porosities. Shortly after the sediments began to settle, no change in the compressional wave arrival time was observed. However, since time delays were only measured to within 1 μsec, a change in speed of about 4%, or less than approximately 60 m/sec, would not have been detected.

A measurable change in attenuation with porosity was found. The results are shown in Fig. 25. The uncertainty in the data lies mainly in the porosity determination. Although the data are too scattered to give an accurate empirical relationship between the variables, it may be generally stated that attenuation decreases with compaction for a given sediment, and that larger changes occur for the finer grained materials. The bars in Fig. 25 and on other graphs showing porosity represent the scatter obtained from repeated core measurements.

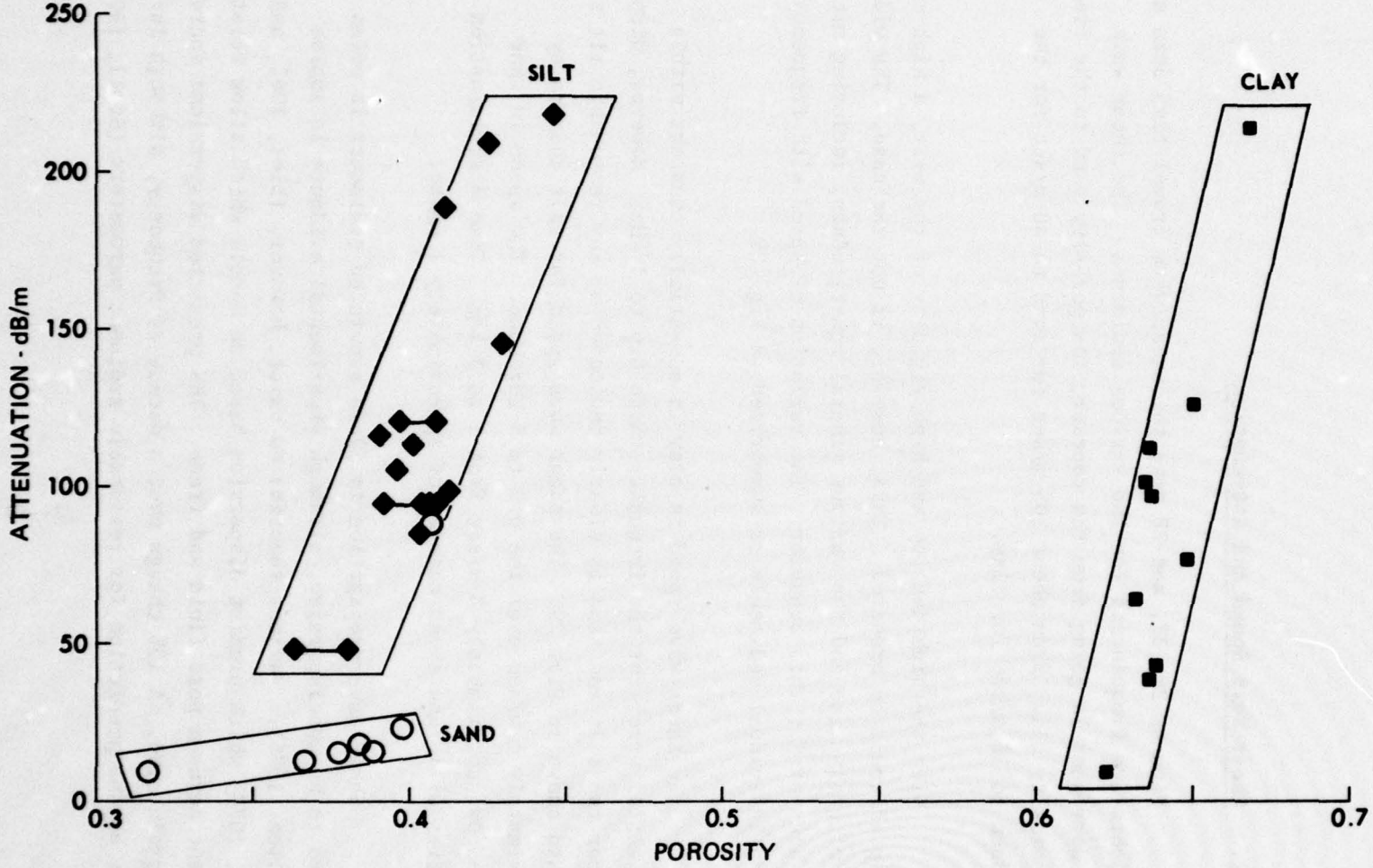

FIGURE 25
COMPRESSIONAL WAVE ATTENUATION versus POROSITY

ARL:UT
AS-78-191
DWB - GA
1 - 23 - 78

2. Shear Wave Speed and Attenuation

Figures 26, 27, and 28 give the shear wave travel time data at representative frequencies for the various sediments. The shear wave speed decreases in going from the coarser, low porosity sand to the finer, high porosity clay, from about 105 m/sec for sand to 40 m/sec for the silt down to 15 m/sec for clay.

With the high density and high rigidity of the silt, a high shear wave speed would be expected. This, however, is not the case. The wide range of grain size and the various mineral constituents, including mica, could account for this behavior. The variation of speed with frequency for the individual sediments is summarized in Fig. 29.

The shear wave speed in clay is essentially constant within experimental error for the frequency range 0.6 to 1 kHz. However, dispersion for the silt and sand is clearly indicated by any reasonable fit to the data shown in Fig. 29. The shear wave speed for silt changes by approximately 6 m/sec over the 0.9 to 5 kHz band. The speed in sand changes by approximately 8 m/sec from 3 to 7 kHz. Time discrimination abilities will show speed changes of approximately 1 m/sec.

Shear wave propagation in fluid saturated sediments is often assumed to be nondispersive, although experimental evidence is sparse (Hamilton, 1976). Various theories do exist, however, (Biot, 1962, and Stoll, 1977) which predict dispersion based on models which allow relative movement between pore fluid and frame. The predicted dispersions increase with grain size. A 10% change over a decade of frequency, although large, is not beyond prediction for reasonable sediment parameters (Stoll, 1977).

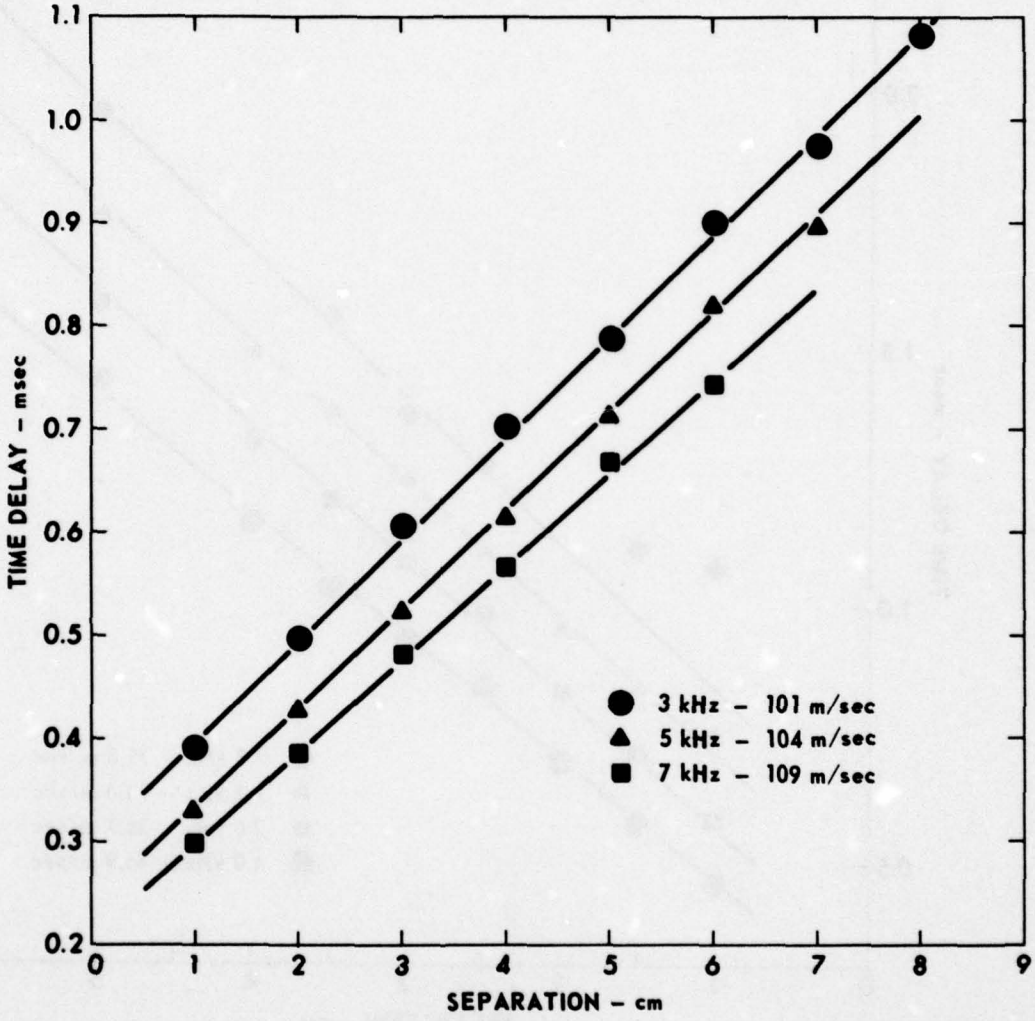

FIGURE 26
SHEAR WAVE SPEED MEASUREMENT - SAND

ARL:UT
AS-78-192
DWB-GA
1-23-78

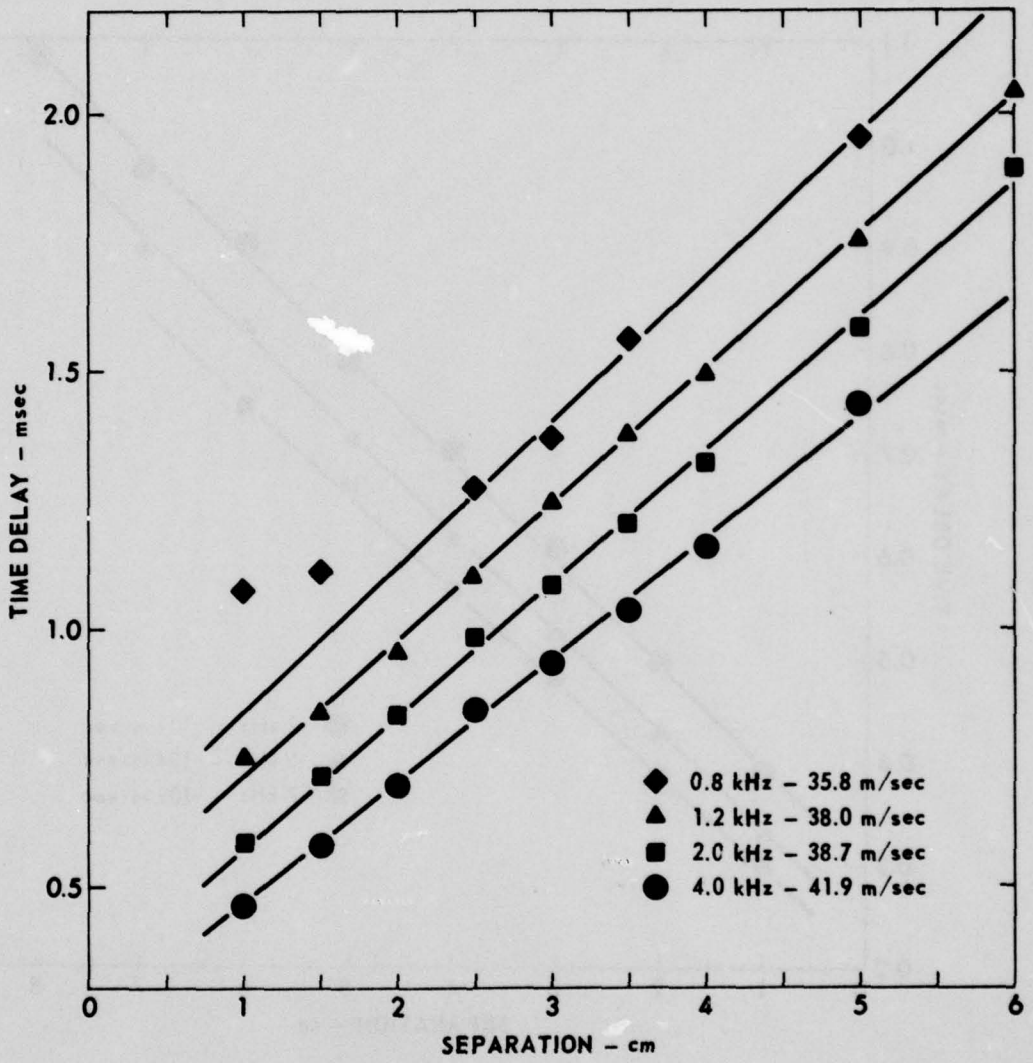

FIGURE 27
SHEAR WAVE SPEED MEASUREMENT - SILT

ARL:UT
AS-78-193
DWB-GA
1-23-78

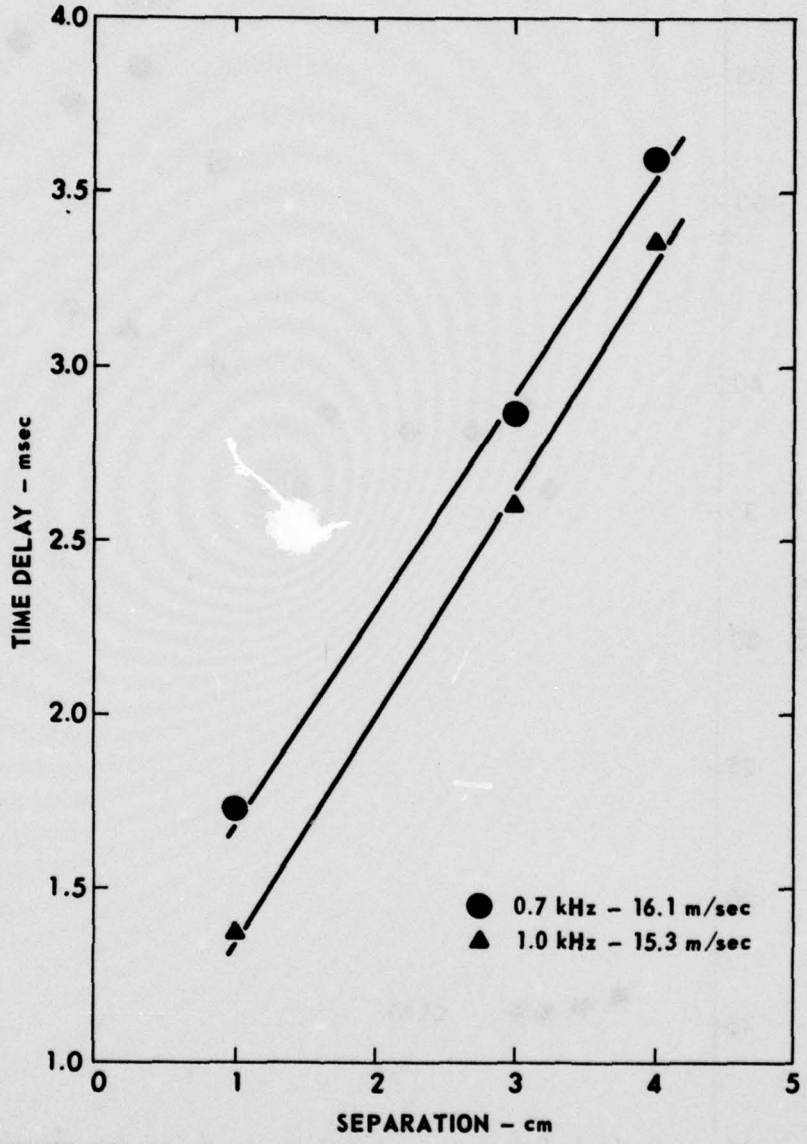

FIGURE 28
SHEAR WAVE SPEED MEASUREMENT - CLAY

ARL:UT
AS-78-194
DWB-GA
1-23-78

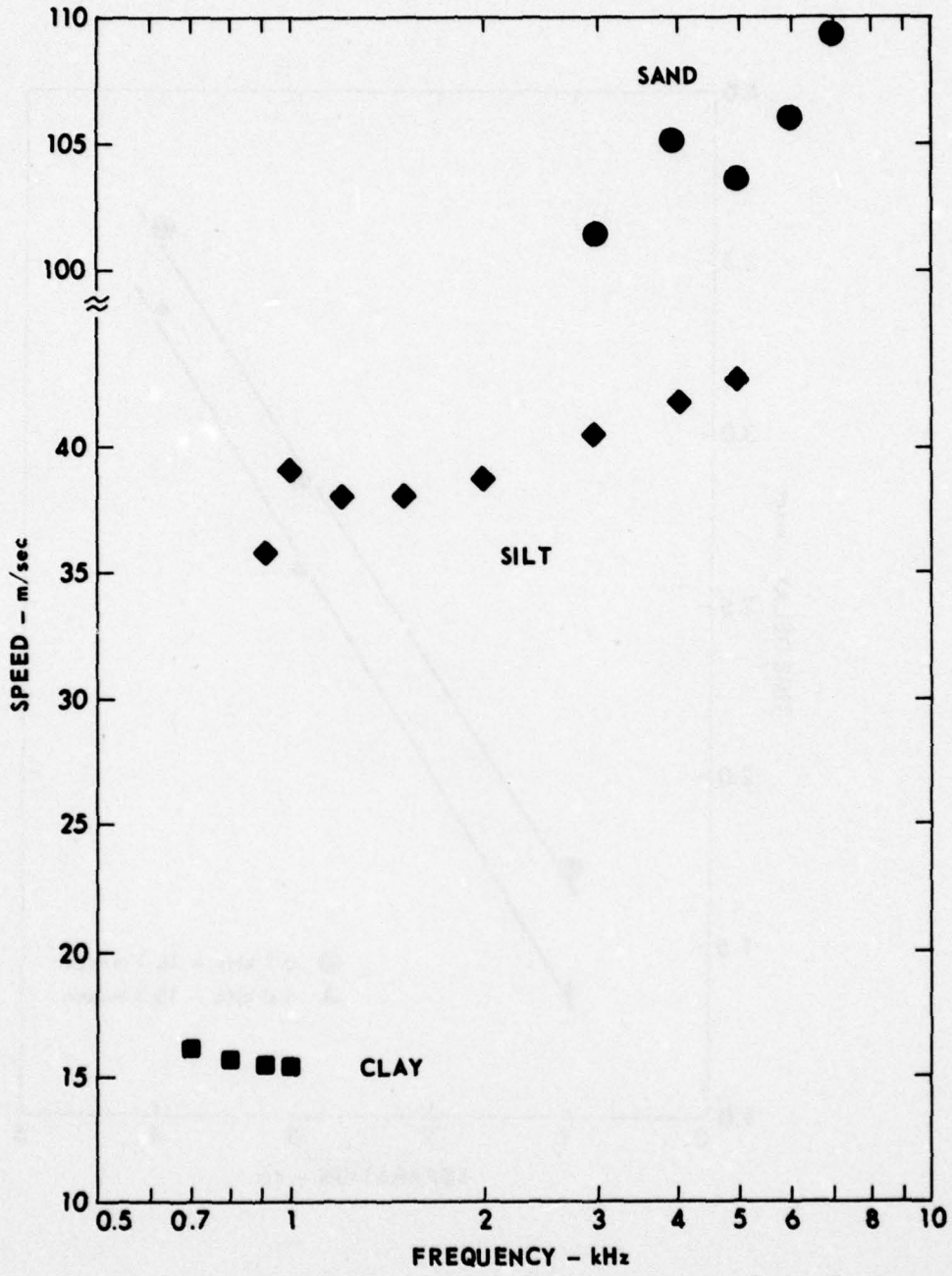

FIGURE 29
SHEAR WAVE SPEED versus FREQUENCY

ARL:UT
AS-78-195
DWB - GA
1 - 23 - 78

It is not felt that the data shown in Fig. 29 are of sufficient quality to validate shear wave dispersion. On the other hand, the data are too consistent to be lightly dismissed without explanation. In particular, most mechanisms that could be invoked to give a false dispersion would also cause the travel time curves of Fig. 26 to be nonlinear. Examples of such mechanisms would be nearfield encounters and pulse broadening due to greater attenuation at the higher frequencies of the narrow passband. One possible explanation is the interference of the direct arrival and the wave reflected from the tank wall behind the fixed transducer. If the wavelength of the transmitted pulse is large compared to the dimensions of the tank, then the various arrivals may no longer be discernible as separate events. The wavelengths appropriate to the speeds and frequencies in use are shown in Fig. 30. The maximum wavelength of 4.5 cm is less than half of the distance traveled by the earliest arriving reflected energy and greater than the mean separation. Ideally, this would allow discrimination of the pulses. Later arrivals are indeed evident on the oscilloscope trace. Furthermore, the wavelengths for the clay are essentially the same as those of the sand, although the dispersion indicated is much different.

It is perhaps best to leave open the question of dispersion until more conclusive data are obtained, especially since the measurements are soon to be repeated in a larger tank over an extended frequency band. If nothing more, the current measurements demonstrate the feasibility of obtaining such data.

Figures 31 through 34 display the shear wave amplitude measurements after correction for spreading loss. Open points, as in Fig. 31, were not used in the least squares fit. They are included in the figure to indicate the difficulties of returning to exactly the same sediment state after the transducers are moved.

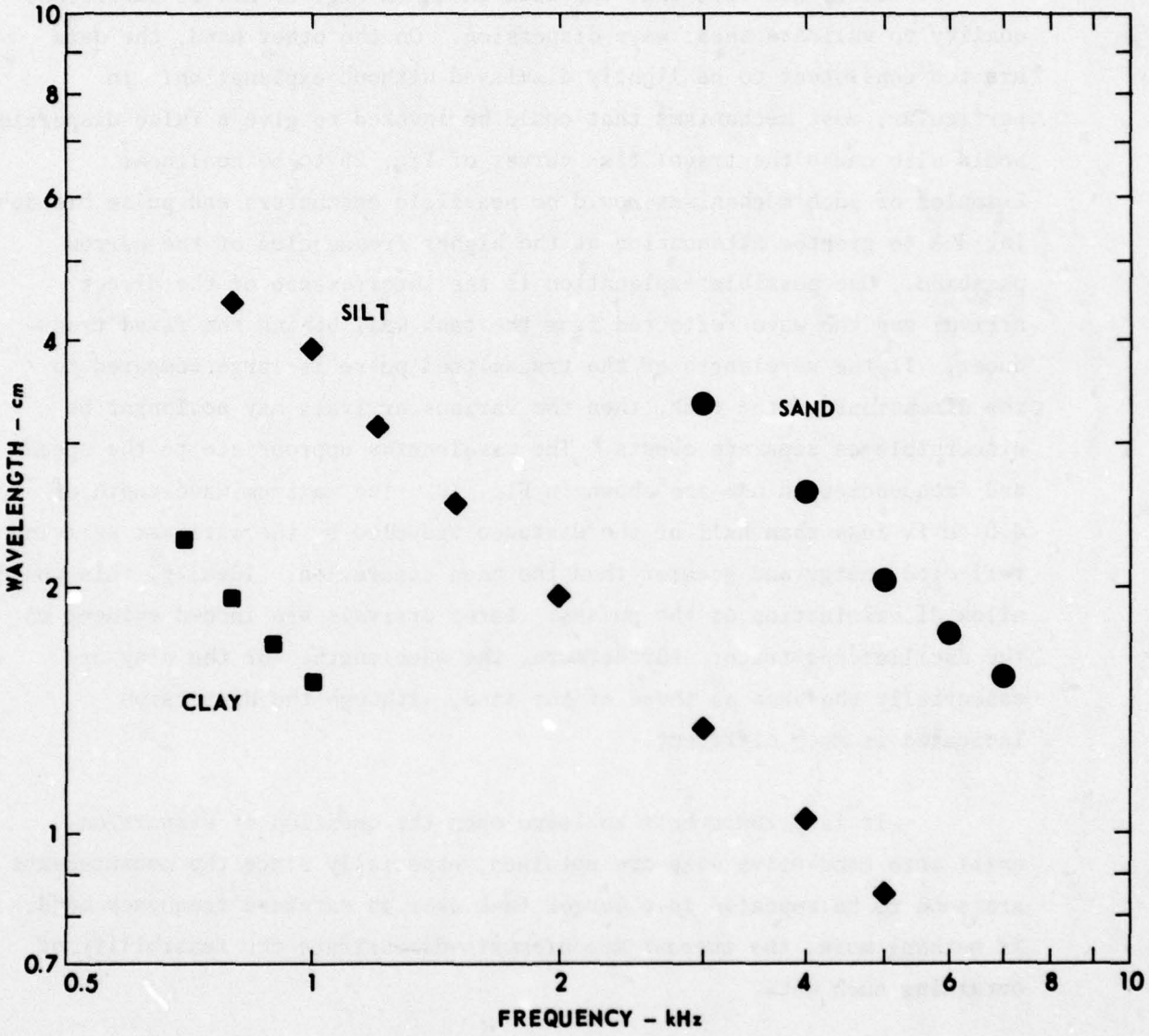

FIGURE 30
SHEAR WAVELENGTH versus FREQUENCY

ARL:UT
AS-78-196
DWB-GA
1-23-78

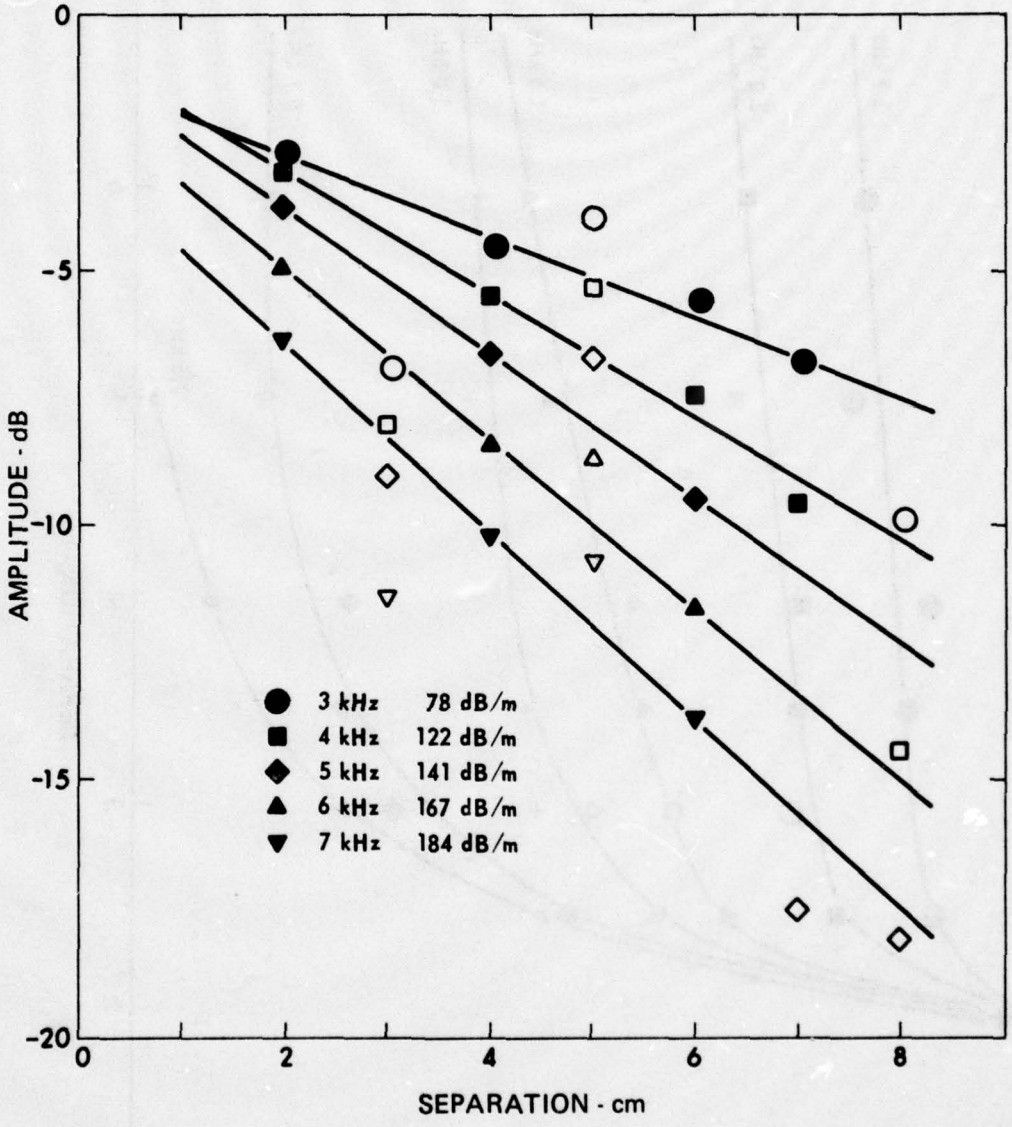

FIGURE 31
MEASUREMENT OF SHEAR WAVE ATTENUATION AT DIFFERING FREQUENCY - SAND HIGH FREQUENCIES

ARL:UT
AS-78-197
DWB - GA
1 - 23 - 78

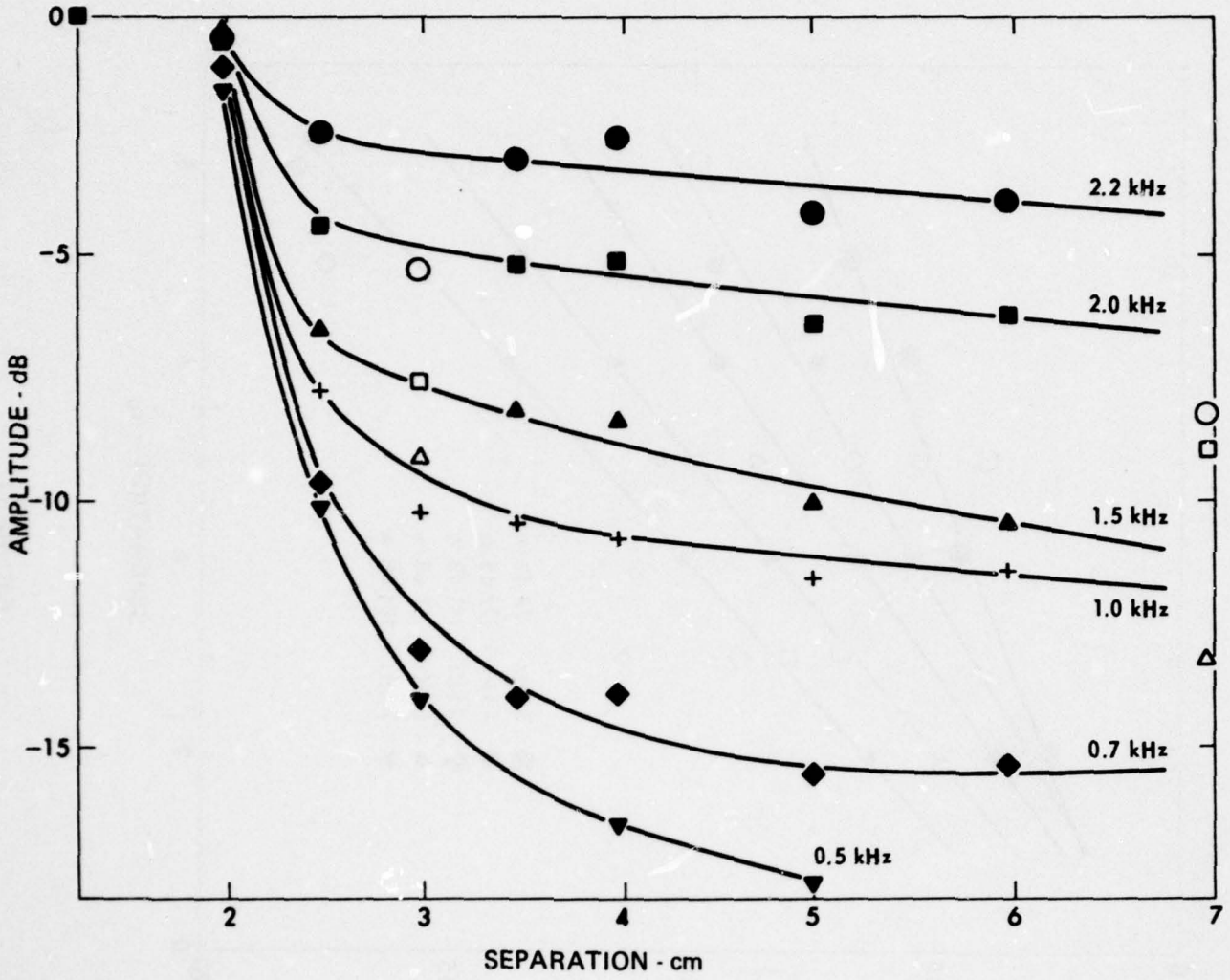

FIGURE 32
MEASUREMENT OF SHEAR WAVE ATTENUATION AT DIFFERING FREQUENCY - SAND LOW FREQUENCIES

ARL:UT
AS-78-198
DWB-GA
1-23-78

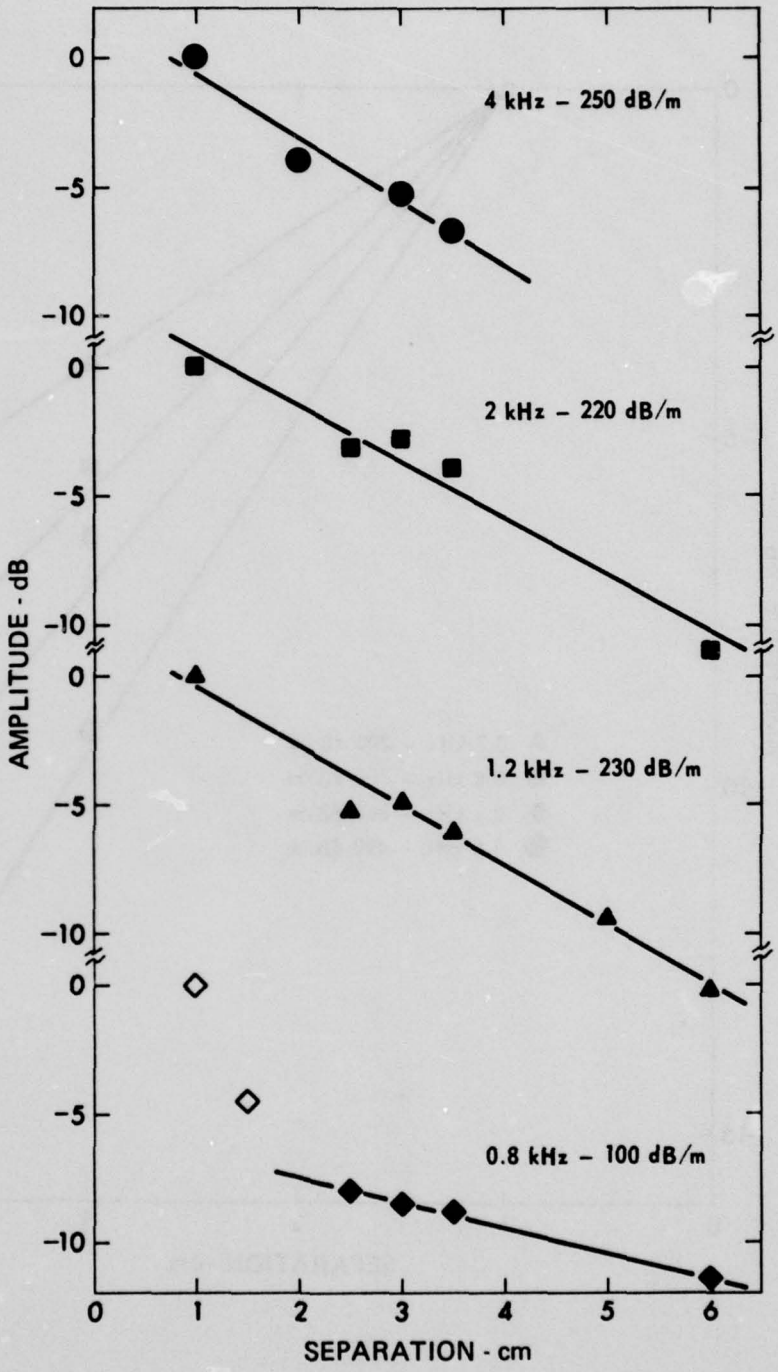

FIGURE 33
MEASUREMENT OF SHEAR WAVE ATTENUATION AT DIFFERING FREQUENCY - SILT

ARL:UT
AS-78-199
DWB - GA
1-23-78

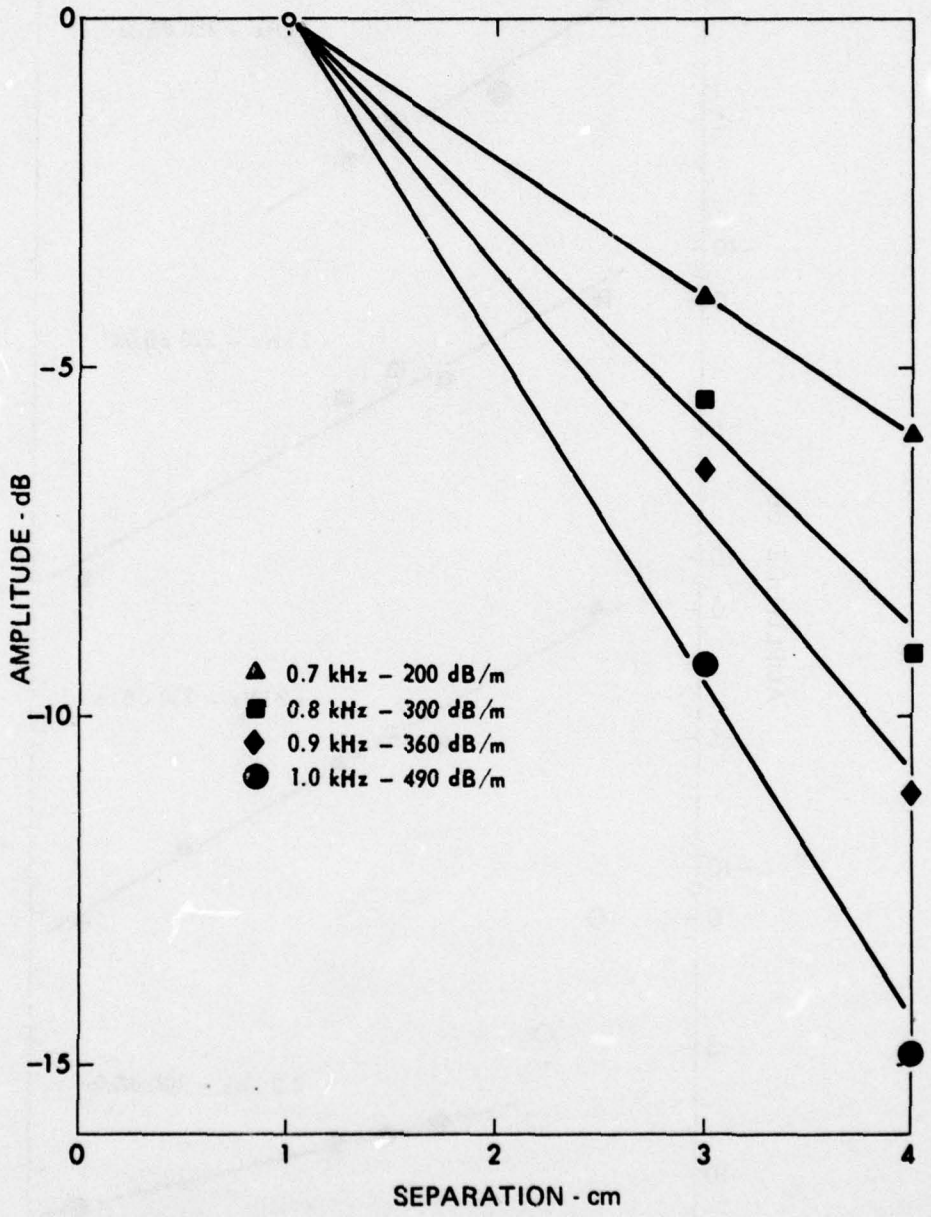

FIGURE 34
MEASUREMENT OF SHEAR WAVE ATTENUATION AT DIFFERING FREQUENCY - CLAY

ARL:UT
AS-78-200
DWB - GA
1 - 23 - 78

In the ideal case of a point source in an infinite medium, a plot of amplitude versus separation will give a straight line. That the curves of Fig. 32 are decidedly not straight reintroduces the problems associated with wavelengths that are comparable to the dimensions of the transducers and their separation. The wavelengths associated with the frequencies in Fig. 32 range from approximately 5 to 20 cm. Although problems with reflections are expected for such wavelengths, the progressive curvature of the amplitude versus separation lines suggests that the assumption of spherical spreading is not valid. The curves become linear at greater and greater separations as the wavelengths increase. Such behavior is not surprising since, at 2.5 cm, the transducers themselves are larger than the smaller separations. Figure 32 is included to better define the properties of the transducers; its data are not incorporated in the analysis of the sediment response.

Figure 35 summarizes the shear wave attenuation measurements. At a given frequency, the attenuation increases with decreasing grain size; i.e., the clay has a higher attenuation than the sand. The f^1 reference line favored by some investigators (Hamilton, 1976) is not a particularly good fit to the overall data. However, the measurements, expecially for the silt, are felt to be too uncertain to justify reporting regression equations for the various sediments. The same theories that predict dispersion of the shear wave velocities also predict nonlinearity of attenuation with frequency (Stoll, 1977). An increase in frequency range over that in Fig. 35 will be necessary to affirm or refute such behavior.

Once values of speed and attenuation for a particular frequency have been established, then variations with porosity may be studied. Figures 36 through 39 show these results. Again, although some of the plots, especially for the clay, are approximately linear, the uncertainty

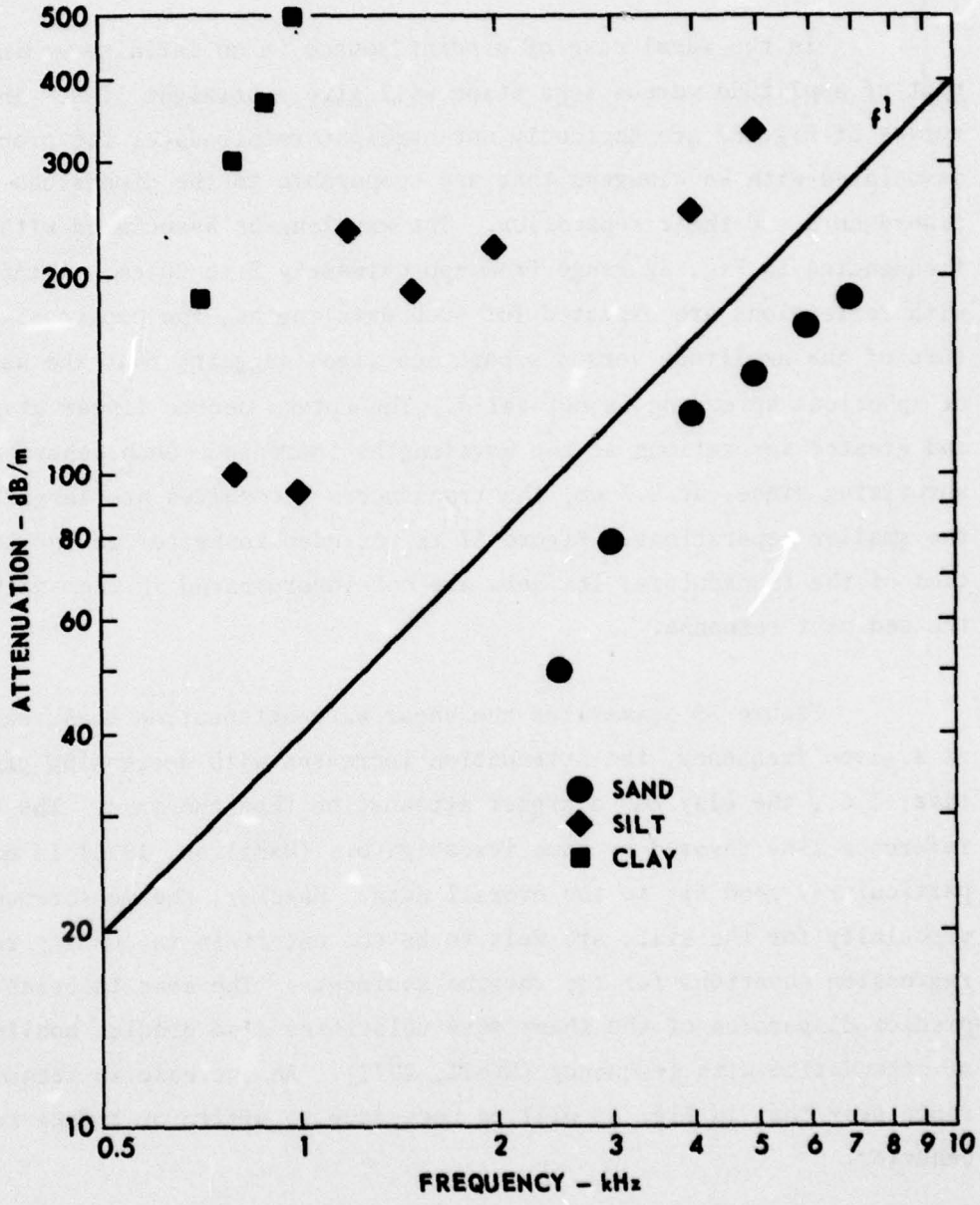

FIGURE 35
SHEAR WAVE ATTENUATION versus FREQUENCY

ARL:UT
AS-78-201
DWB-GA
1-23-78

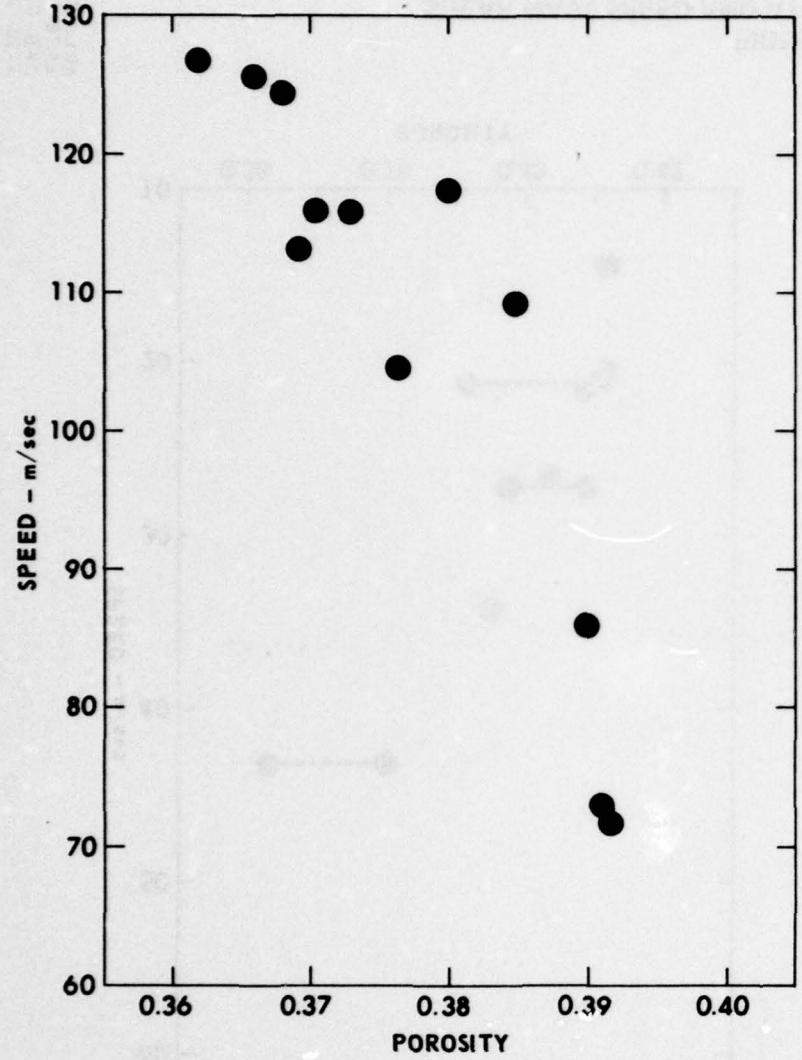

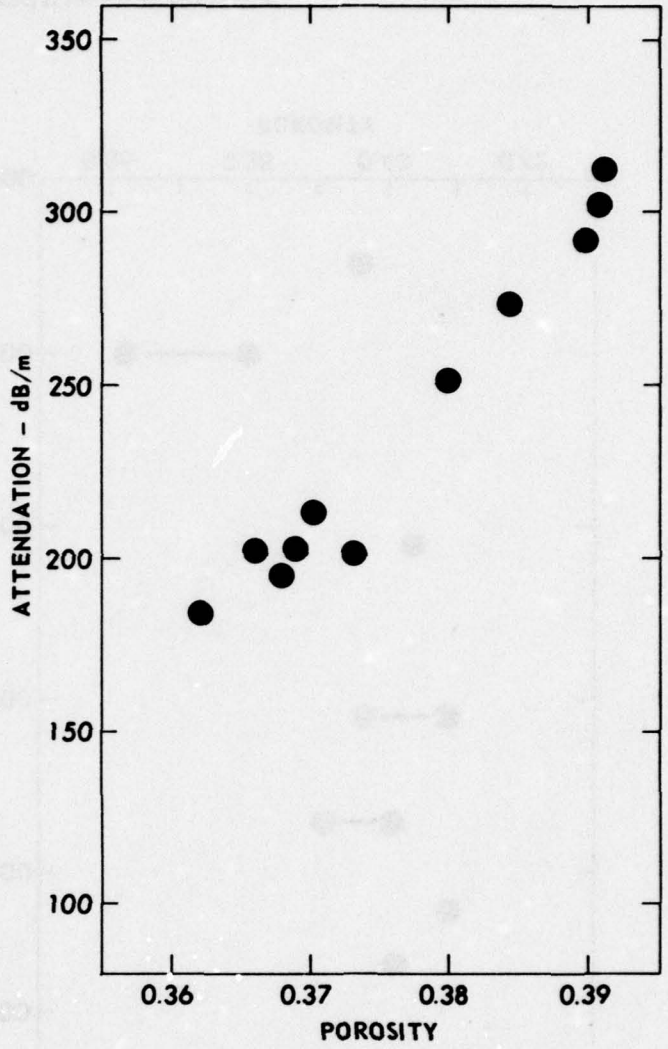

ARL:UT
AS-78-202
DWB-GA
1-23-78

FIGURE 36
SHEAR WAVE SPEED AND ATTENUATION versus POROSITY
SAND - 4 kHz

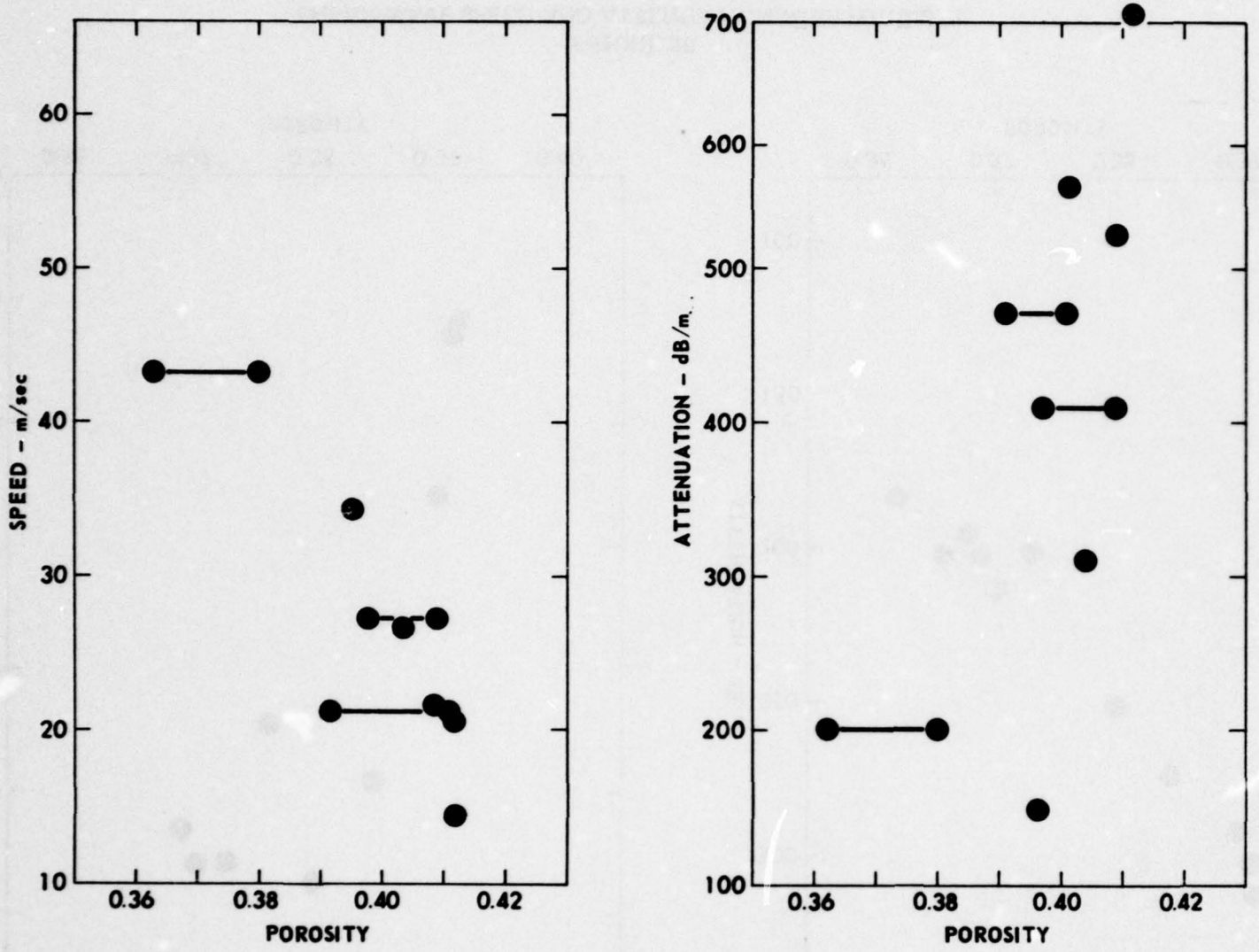

ARL:UT
AS-78-203
DWB - GA
1-23-78

FIGURE 37
SHEAR WAVE SPEED AND ATTENUATION versus POROSITY
SILT - 2 kHz

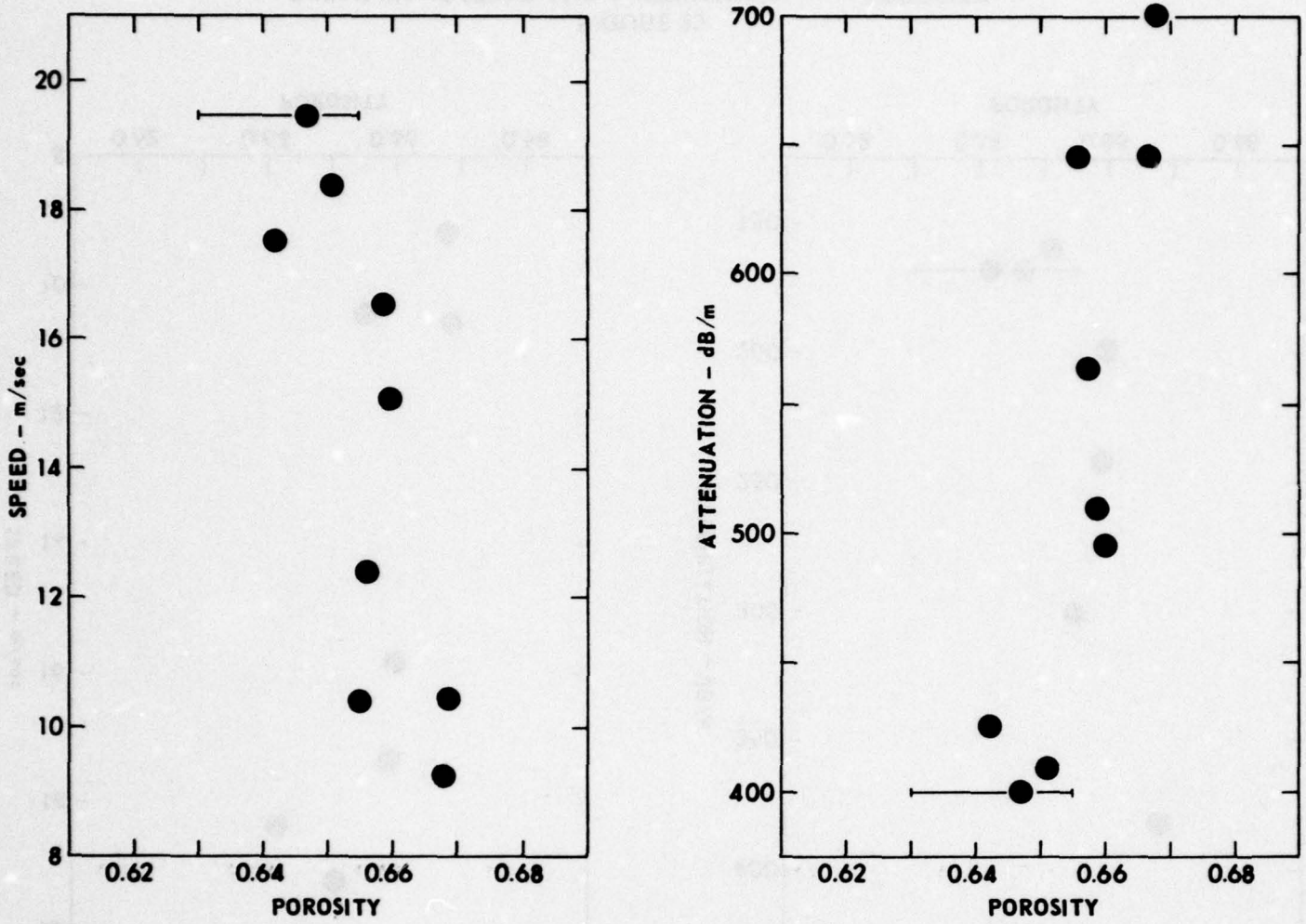

ARL:UT
AS-78-204
DWB - GA
1-23-78

FIGURE 38
SHEAR WAVE SPEED AND ATTENUATION versus POROSITY
CLAY - 1.0 kHz

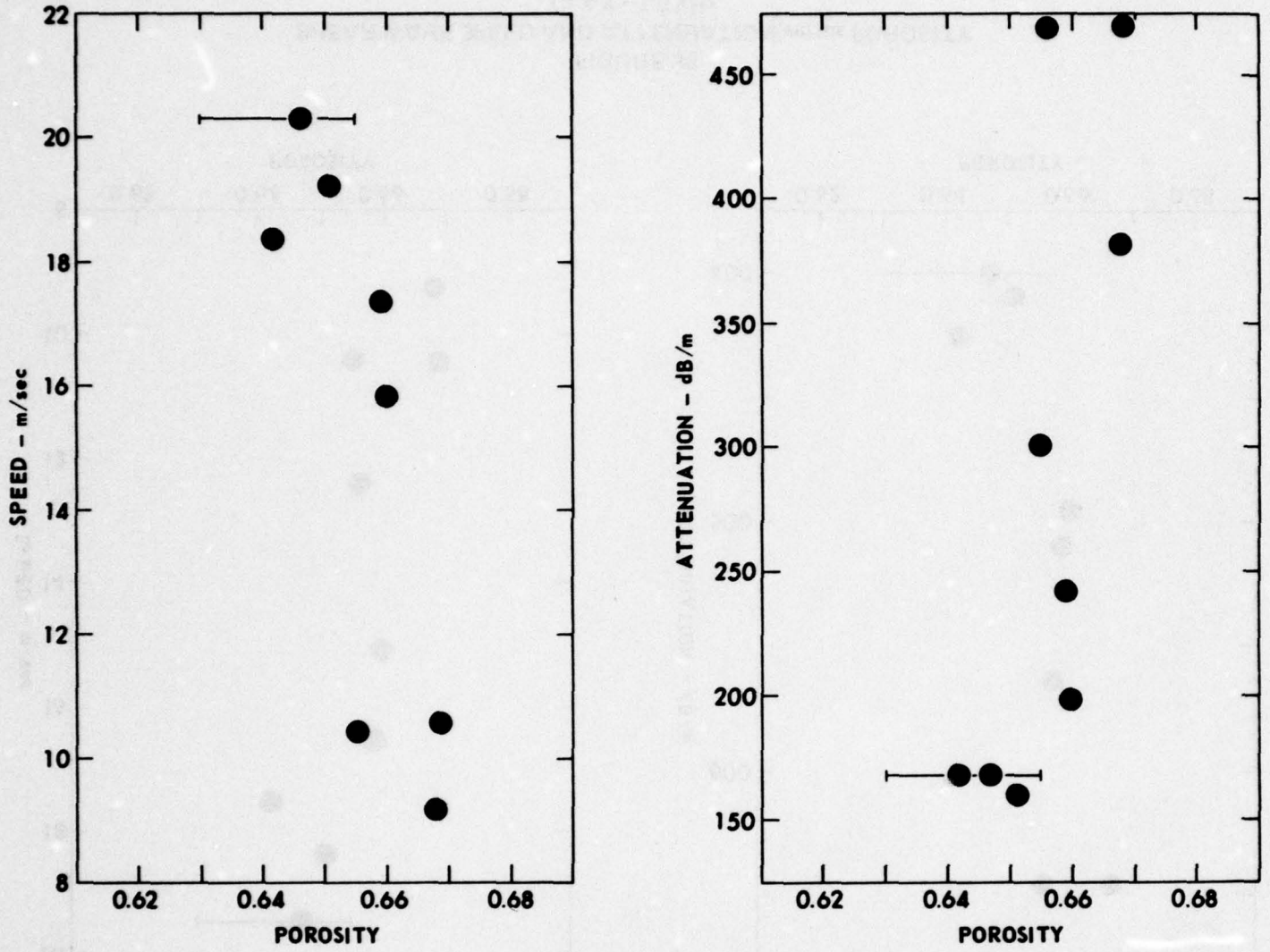

FIGURE 39
SHEAR WAVE SPEED AND ATTENUATION versus POROSITY
CLAY - 700 Hz

ARL:UT
AS-78-205
DWB-GA
1-23-78

in the porosity measurements makes curve fitting of dubious value. The results do, however, agree with intuitive expectations. As the sediment becomes more compacted, the shear wave speeds increase and the damping decreases. The speeds vary only slightly, if at all, with frequency, as demonstrated by Figs. 38 and 39. The attenuation, of course, exhibits considerable change with frequency.

The shear moduli may be computed from the speed and porosity data. The moduli increase with increasing compaction as shown in Fig. 40. The rigidity also apparently increases with increasing grain size, as seen from the plots for sand and silt whose porosities overlap. The mineral density, which is slightly higher for the silt, would tend to negate such an effect. From previous work (Shirley and Anderson, 1975), the shear transducers have been shown to generate measurable signals for shear moduli smaller by a factor of 100 than those shown in the figure.

Table II summarizes the maximum changes in the various parameters with the approximate spread in porosities. The significance of Table II lies not in the generality of the actual numbers. Three laboratory samples can hardly be said to characterize the multitude of marine sediments, regardless of any uncertainties involved in the data. However, the relative change in the numbers with porosity has definite implications. If only a small change in porosity can double the values of the shear wave parameters, then only order of magnitude estimates may be obtained from measurements in a sediment which has been disturbed. If one is interested only in corrections to compressional wave predictions due to a small, but finite, rigidity, then an order of magnitude estimate will probably be sufficient. If, however, the interest lies in actual shear wave propagation in unconsolidated materials, the values for the parameters used to characterize the sediment should be chosen carefully. Preference should be

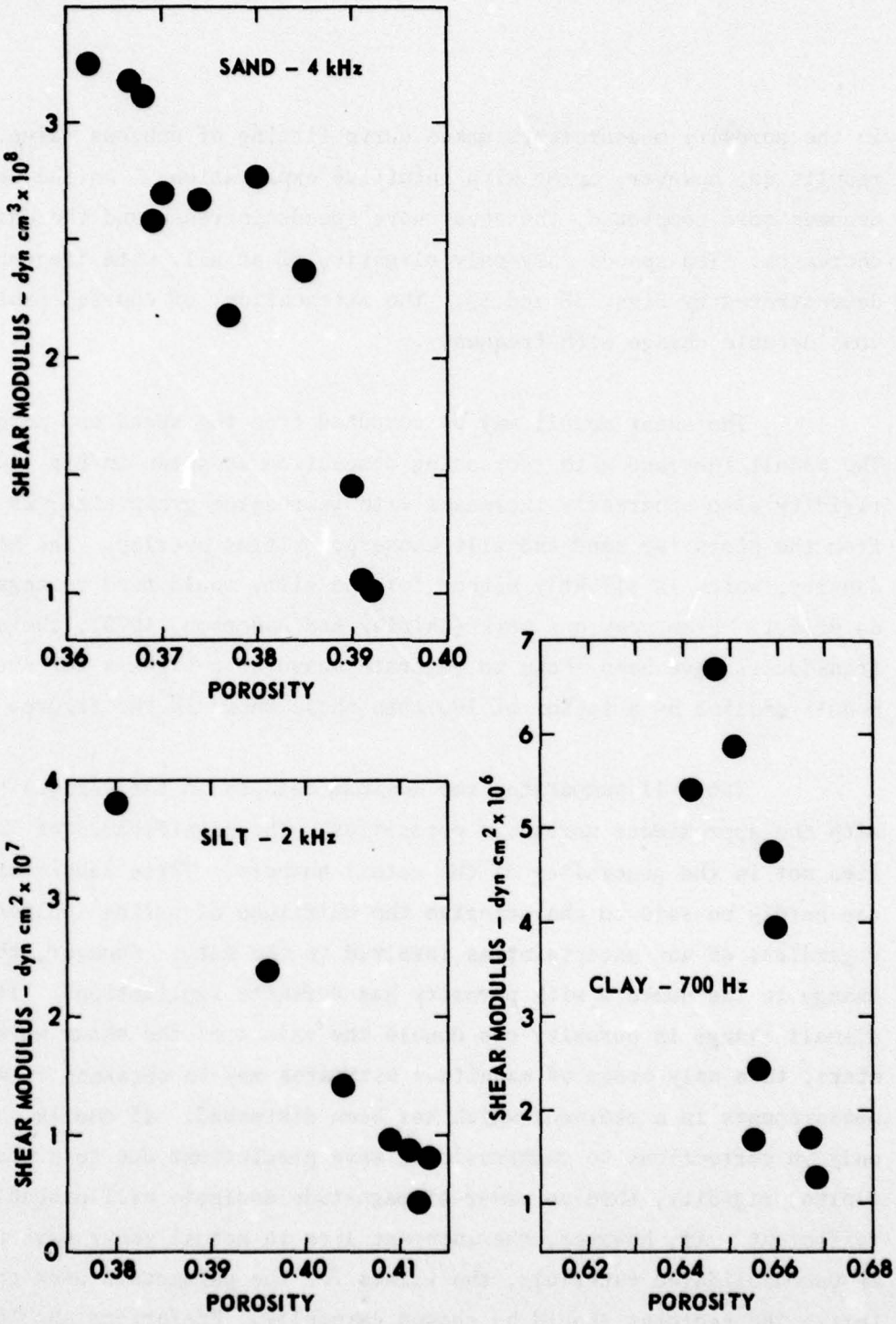

FIGURE 40
SHEAR MODULUS versus POROSITY

ARL:UT
AS-78-206
DWB - GA
1 - 23 - 78

TABLE II

VARIATION OF ACOUSTIC PARAMETERS WITH CHANGE IN POROSITY

SEDIMENT	COMPRESSIONAL WAVE		SHEAR WAVE			
Porosity (n)	Speed m/sec	Attenuation dB/m	Freq. kHz	Speed m/sec	Attenuation dB/m	Shear Modulus* dyn cm^2 x 10^6
SAND						
			4.0	127 - 73.0	180 - 310	330 - 110
.36 - .39	1700 ± 4%	9 - 24				
			7.0	128 - 75.1	340 - 550	330 - 110
SILT			0.8	32.5 - 13.0	100 - 460	22 - 3.4
.37 - .41	1800 ± 4%	110 - 190	2.0	34.5 - 14.3	140 - 710	25 - 4.1
			5.0	36.7 -	190 -	28 -
CLAY			0.7	20.5 - 10.6	170 - 470	6.5 - 1.7
.62 - .67	1500 ± 4%	10 - 210	0.8	19.8 - 10.5	240 - 520	6.1 - 1.6
			1.0	19.5 - 10.4	400 - 650	5.9 - 1.6

*$\mu = c_s^2 \rho$; $\rho = \eta \rho_\omega + (1-n) \rho_{sed}$; ρ_{sand} = 2.60 g/cc, ρ_{silt} = 2.72 g/cc, ρ_{clay} = 2.52 g/cc.

given to in situ rather than shipboard or laboratory measurements, especially since the effects of pressure are still undetermined.

Since the quantitative interpretation of the data obtained during compaction is hampered by the inaccuracy of the porosity measurements, it is natural to plot the shear wave speed versus attenuation. Figures 41, 42, and 43 show the results for the three sediment types at different frequencies. The attenuation appears to vary exponentially with the speed, or equivalently, the log of the attenuation is linear with respect to speed, as plotted in the figures.

The above dependency suggests the possibility of predicting shear wave attenuation given only the shear wave speed and the parameters of a curve established for a particular sediment type. Note that the dependence of attenuation on porosity is inherit in the value of the speed and thus porosity need not be specified. The curves of Figs. 41 through 43 give a slightly different set of parameters, i.e., slope and intercept, for each frequency. If this frequency dependence can be characterized, then the predictive value would increase. The change with frequency of the slope of the speed versus attenuation curves is shown in Fig. 44. A linear fit is again reasonable so that a second slope and an intercept replace the one frequency dependent slope of Figs. 42 and 43. Similar results are obtained for the frequency variation of the speed versus attenuation intercept. Ideally then, four constants would allow the shear wave attenuation for a given sediment to be estimated from the shear wave speed and the frequency. However, data found in the literature (Hamilton, 1976) is too sparse to test such an hypothesis, and the data upon which it is based are open to question.

The data points of Fig. 44 are not directly measured quantities, but rather values taken from least squares fit having definite uncertainties.

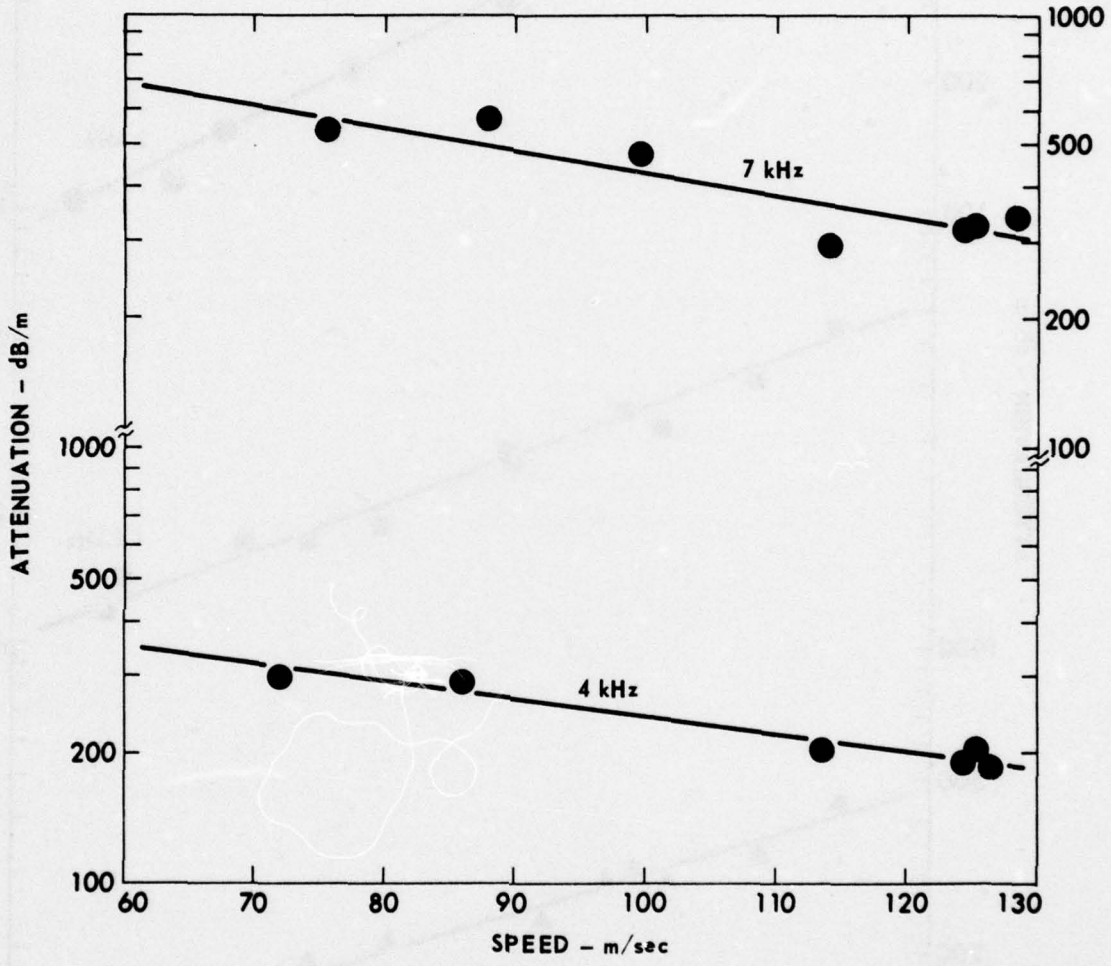

FIGURE 41
SHEAR WAVE SPEED versus ATTENUATION - SAND

ARL:UT
AS-78-207
GWB-GA
1-23-78

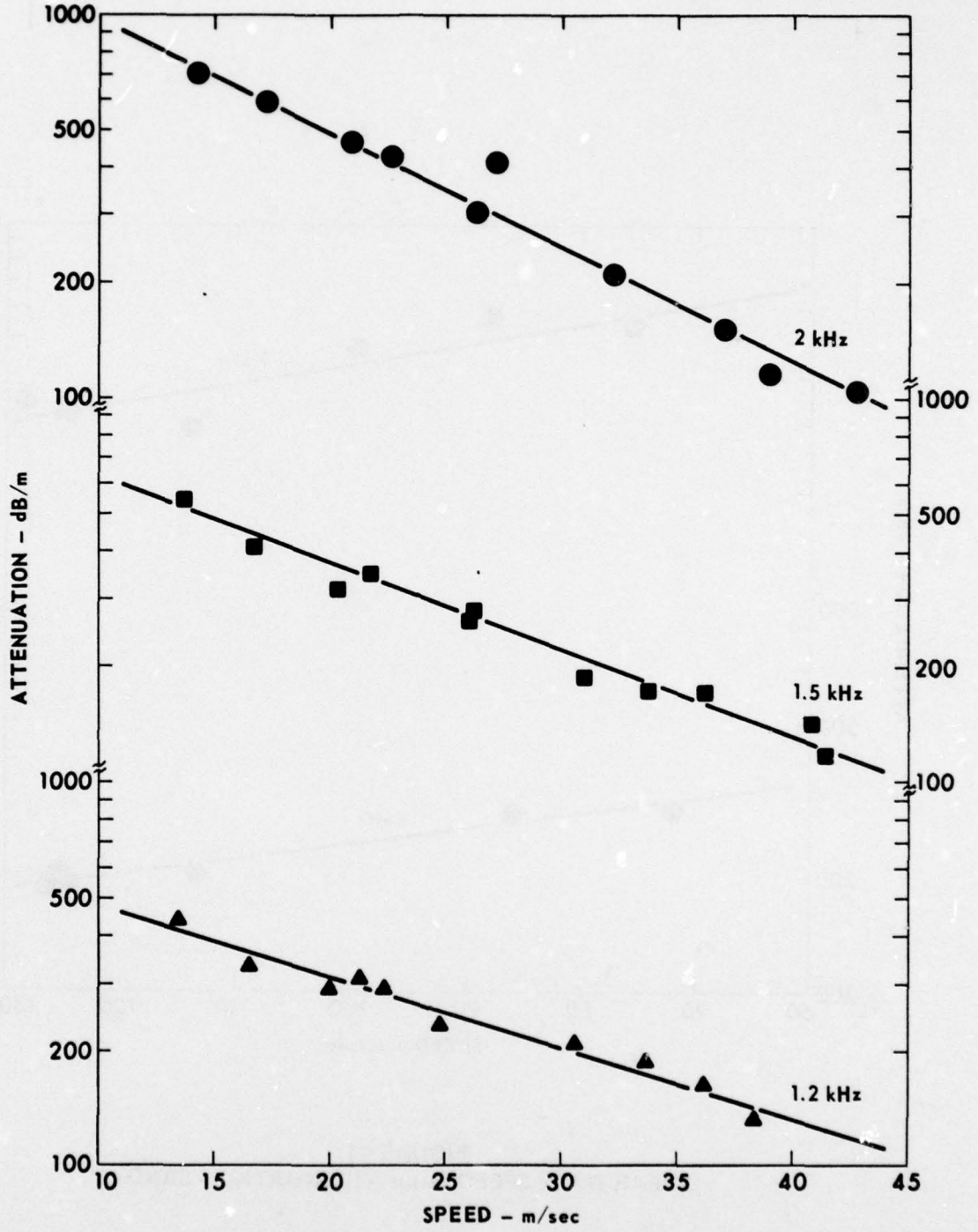

FIGURE 42
SHEAR WAVE SPEED versus ATTENUATION - SILT

ARL:UT
AS-78-208
DWB - GA
1-23-78

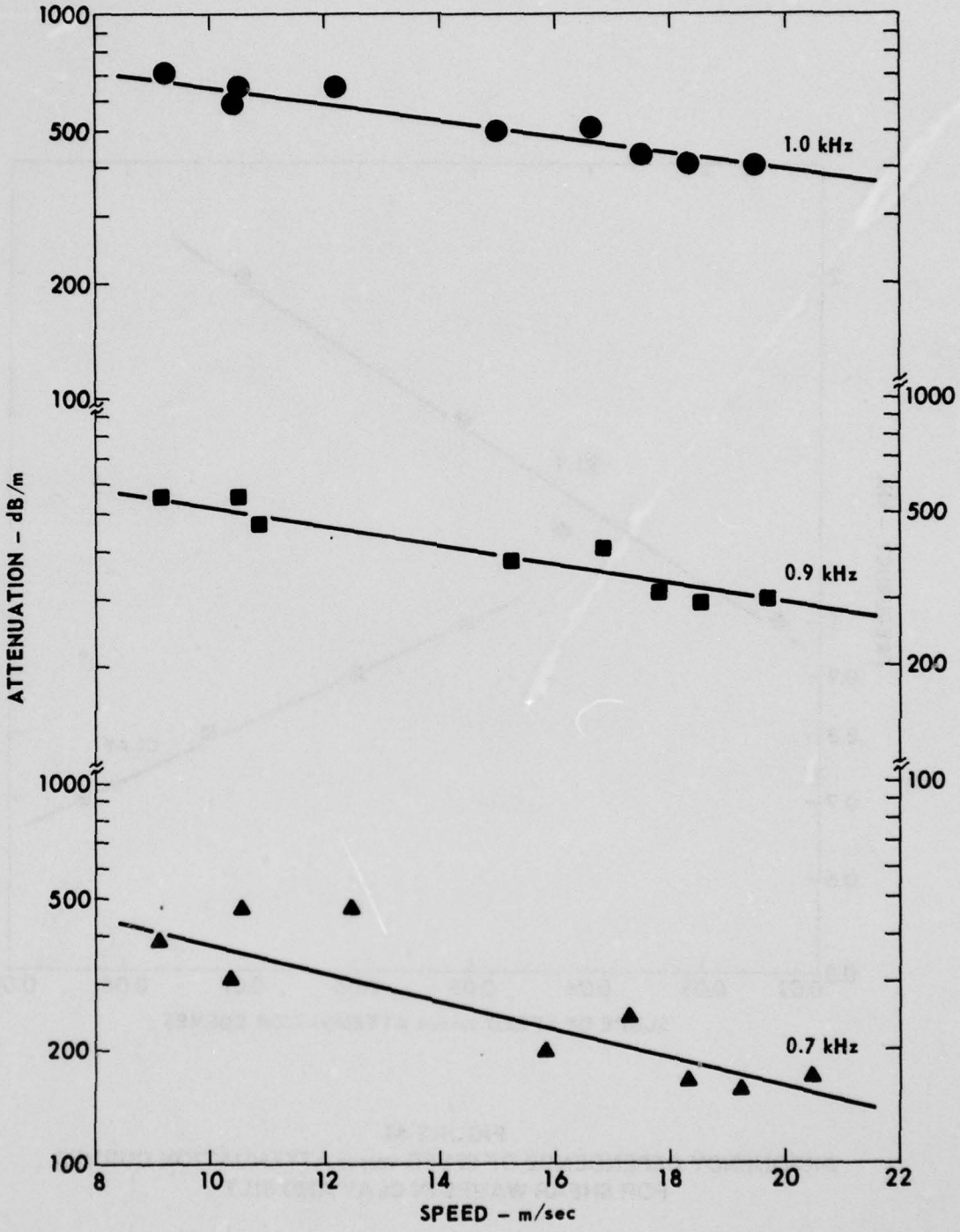

FIGURE 43
SHEAR WAVE SPEED versus ATTENUATION - CLAY

ARL:UT
AS-78-209
DWB-GA
1-23-78

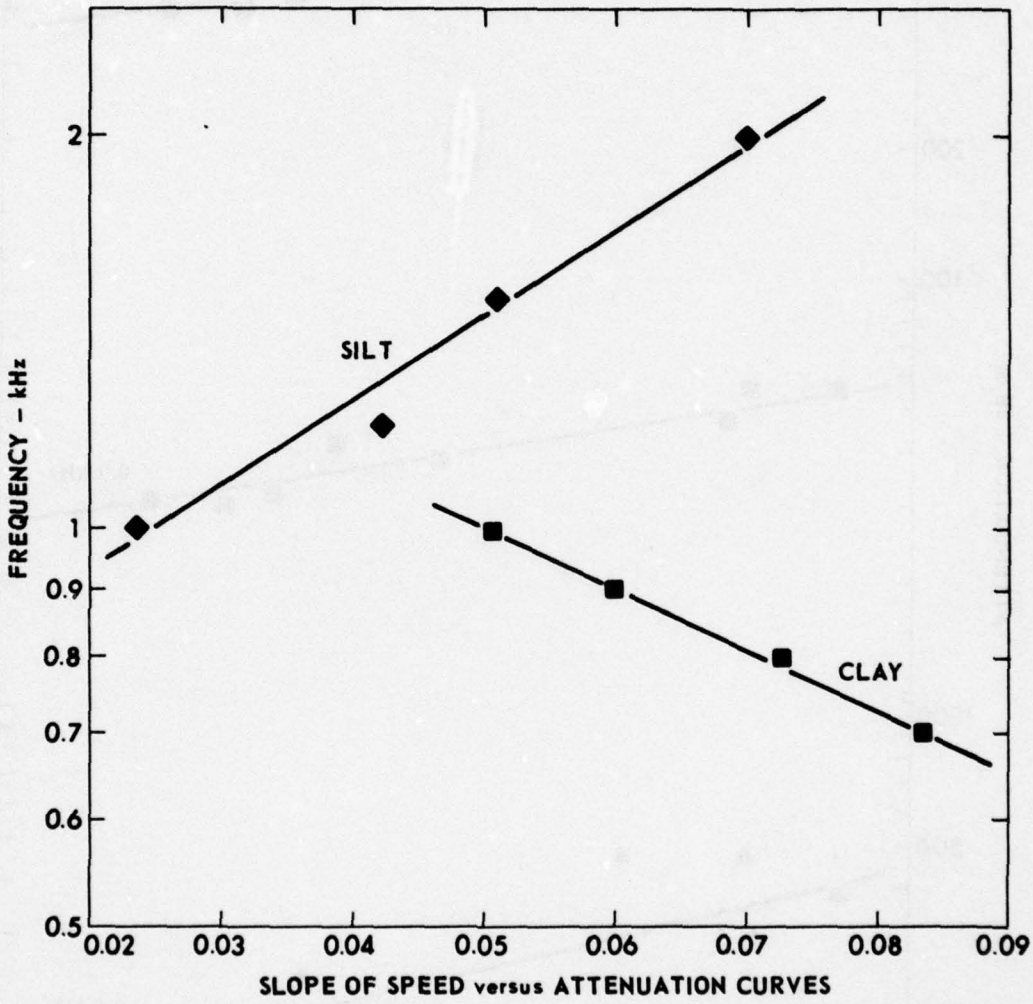

FIGURE 44
FREQUENCY DEPENDENCE OF SPEED versus ATTENUATION CURVES FOR SHEAR WAVES IN CLAY AND SILT

ARL:UT
AS-78-210
DWB-GA
1-23-78

The log plots give a better visual alignment than is indicated by the statistics. Thus, the small change in slope plotted in Fig. 44 may not be significant. It is not understood why the silt and clay reverse slopes. Also hidden in the data is the dispersion given in Fig. 29. Although only those frequencies for the silt giving a relatively constant speed were considered in Figs. 42 and 44, the data are still somewhat compromised if dispersion is rejected offhand. The relationship between speed and attenuation with variations in porosity thus awaits confirmation. There is unfortunately no adequate theory that predicts the effect of packing on attenuation. The common device of assigning attenuation to the imaginary part of a complex modulus gives no indication of the physical process involved, but depends entirely on empirical results to characterize changes due to variations of the physical parameters.

G. Conclusions

The preceding discussion shows that accurate shear wave measurements in unconsolidated sediments may be made with relative ease using single bender elements as both source and receiver. Routine shear wave measurements may now be made to compliment the large volume of compressional wave data in the literature. With both sets of data, the acoustic response of marine sediments can be better defined, including the viscoelastic properties, than has heretofore been commonly possible. The results indicate, however, that the amount of disturbance during measurement is critical. This suggests two broad objectives: first, the continued development of in situ shear wave capabilities and, second, the accumulation of sufficient laboratory data, including measurements under pressure, to be able to characterize the effect changes in any one parameter will have on the others.

The results reported here are of an exploratory rather than conclusive nature. In general, the results behaved as expected. The indicated

frequency dependence of the shear wave speed and attenuation is perhaps questionable, and the porosity determinations are poor. However, it is expected that unequivocal measurements will soon be made. In fact variations in the length of the transducer elements may extend the frequency range applied to a single sediment sufficiently to test the validity of the various theoretical models of acoustic propagation in fluid saturated media.

Dispersion and a variation with frequency of the log decrement of attenuation are predicted for both compressional and shear waves by theoretical models (Stoll, 1977). Comparisons of these predictions with experimental data are inconclusive. It is difficult to make compressional wave measurements in a single sediment over a wide enough frequency band to detect the supposed small variations. Data on shear wave attenuation in fluid saturated media are meager. However, the techniques outlined in this report should give conclusive shear wave results.

Due to the large number of parameters involved, natural sediments are not ideal for an initial experimental check of theory. Uniformly sized and shaped glass spheres should allow better handling of such variables as grain size and porosity. Such an artificial sediment, along with the various improvements suggested in the report, is being investigated.

REFERENCES

T. Akal, 1972. "The Relationship Between the Physical Properties of Underwater Sediments that Affect Bottom Reflection," Marine Geology 13, 251.

A. L. Anderson, 1974. "Acoustics of Gas-Bearing Sediments," ARL-TR-74-19.

M. A. Biot, 1962. "Generalized Theory of Acoustic Propagation in Porous Dissipative Media," J. Acoust. Soc. Am. 34, 1254-1264.

E. L. Hamilton, 1970. "Sound Velocity and Related Properties of Marine Sediments in the North Pacific," J. Geophys. Res. 75, 4423.

E. L. Hamilton, 1971. "Elastic Properties of Marine Sediments," J. Geophys. Res. 76, No. 2, 579-604.

E. L. Hamilton, 1976. "Attenuation of Shear Waves in Marine Sediments," J. Acoust. Soc. Am. 60, No. 2, 334-338.

D. J. Shirley and A. L. Anderson, 1975a. "In situ Measurement of Marine Sediment Acoustical Properties During Coring in Deep Water," IEEE Transactions on Geoscience Electronics GE-13, No. 4.

D. J. Shirley and A. L. Anderson, 1975b. "Acoustical and Engineering Properties of Sediments," ARL-TR-75-58.

D. J. Shirley, 1977a. "Laboratory and in situ Sediment Acoustics, ARL-TR-77-46.

D. J. Shirley, 1977b. "Method for Measuring in situ Impedance of Marine Sediments," J. Acoust. Soc. Am. 62, 1028-1032.

R. D. Stoll, 1977. "Acoustic Waves in Ocean Sediments," Geophysics 42, No. 4, 715-725.

BIBLIOGRAPHY

ONR CODE 480 PROGRAM DOCUMENTATION

"Status Report No. 1 under Texas A&M Research Foundation P.O. No. RF-11743 and ONR Contract N00014-70-A-0166-0005," 1 January - 1 July 1971, (7 July 1971).

"Final Report under Contract N00014-70-A-0166-0005," Applied Research Laboratories Technical Report (ARL-TR-72-6), 17 January 1972.

Anderson, A. L., and L. D. Hampton, "In situ Measurement of Sediment Acoustic Properties During Coring," paper presented at the ONR Symposium on Physical and Engineering Properties of Deep-Sea Sediments, Airlie House, Airlie, Virginia, 24-27 April 1973.

Anderson, A. L., and L. D. Hampton, "Measurement of in situ Acoustic Properties During Sediment Coring," paper presented at the ONR Symposium on the Physics of Sound in Marine Sediments, Lakeway Inn, Austin, Texas, 8-10 May 1973.

Anderson, A. L., "Acoustics of Gas-Bearing Sediments," Applied Research Laboratories Technical Report (ARL-TR-74-19), May 1974.

Anderson, A. L., and L. D. Hampton, "A Method for Measuring in situ Acoustic Properties During Sediment Coring," In Physics of Sound in Marine Sediments, Edited by Loyd D. Hampton (Plenum Press) 1974.

Anderson, A. L., and L. D. Hampton, "In situ Measurements of Sediment Acoustic Properties During Coring," In Deep-Sea Sediments, Physical and Mechanical Properties, Edited by A. L. Inderbitzen (Plenum Press) 1974.

Anderson, A. L., and L. D. Hampton, "Use of Tubes for Measurement of Acoustical Properties of Materials," paper presented at the 89th Meeting of The Acoustical Society of America, Austin, Texas, April 1975.

Hampton, L. D., "ARL Experience with Acoustics and Gas in Sediments," presented at Symposium on Natural Gases in Marine Sediments and Their Mode of Distribution, The University of California Lake Arrowhead Conference Center, Lake Arrowhead, California, 28-30 November 1972.

Hampton, L. D., and A. L. Anderson, "Acoustics and Gas in Sediments: Applied Research Laboratories (ARL) Experience," in Natural Gases in Marine Sediments, Marine Science Vol. III, Edited by Isaac R. Kaplan (Plenum Press) 1974.

Shirley, D. J.,and L. D. Hampton, "Acoustic Velocity Profilometer for Sediment Cores," Ocean '72, Record of the International Conference on Engineering in the Ocean Environment held in Newport, Rhode Island, 13-15 September 1972.

Shirley, D. J., and L. D. Hampton, "Determination of Sound Speed in Cored Sediments," Applied Research Laboratories Technical Report (ARL-TR-72-44), 20 December 1972.

Shirley, D. J., A. L. Anderson, and L. D. Hampton, "In situ Measurement of Sediment Sound Speed During Coring," Applied Research Laboratories Technical Report (ARL-TR-73-1), 14 March 1973.

Shirley, D. J., A. L. Anderson, and L. D. Hampton, "Measurement of in situ Sound Speed During Sediment Coring," Ocean '73, Record of the International Conference on Engineering in the Ocean Environment held in Seattle, Washington, 25-28 September 1973.

Shirley, D. J., and L. D. Hampton, "Acoustic Velocimeter for Ocean Bottoms Coring Apparatus," ARL Invention Disclosure, 9 November 1973.

Shirley, D. J., "Interim Technical Description of the ARL Compressional Wave in situ Core Profilometer," Applied Research Laboratories Technical Memorandum (ARL-TM-74-9), 21 March 1974.

Shirley, D. J., "Calibration Manual for ARL Profilometer," Informal Memorandum, July 1974.

Shirley, D. J., and A. L. Anderson, "Compressional Wave Profilometer For Deep Water Measurements," Applied Research Laboratories Technical Report (ARL-TR-74-51), 6 December 1974.

Shirley, D. J., and A. L. Anderson, "Studies of Sediment Shear Waves, Acoustical Impedance, and Engineering Properties," Applied Research Laboratories Technical Report (ARL-TR-75-23), 7 May 1975.

Shirley, D. J. "Fine Structure of the Sound Speed Profile in Ocean Bottom Sediments," paper presented at the 89th Meeting of The Acoustical Society of America held in Austin, Texas, 7-11 April 1975.

Shirley, D. J., "Transducer for Generation and Detection of Shear Waves," ARL Invention Disclosure, 18 August 1975.

Shirley, D. J., and A. L. Anderson, "Acoustical and Engineering Properties of Sediments," Applied Research Laboratories Technical Report (ARL-TR-75-58), 29 October 1975.

Shirley, D. J., and A. L. Anderson, "In situ Measurement of Marine Sediment Acoustical Properties During Coring in Deep Water," IEEE Transactions on Geoscience Electronics, Vol. GE-13, No. 4, October 1975.

Shirley, D. J., and A. L. Anderson, "Experimental Investigation of Shear Waves in Laboratory Sediments," paper presented at the 90th Meeting of the Acoustical Society of America held in San Francisco, California, 3-7 November 1975.

Shirley, D. J., "Determination of The Acoustic Properties of Deep Ocean Sediments from in situ Profiles," paper presented at the 92nd Meeting of The Acoustical Society of America held in San Diego, California, 15-19 November 1976.

Shirley, D. J., and A. L. Anderson, "Shear Waves in Unconsolidated Sediments," paper presented at the 92nd Meeting of The Acoustical Society of America held in San Diego, California, 15-19 November 1976.

Shirley, D. J., "Acoustic Impedance Measuring Device For Marine Sediments," paper presented at the 93rd Meeting of The Acoustical Society of America held in University Park, Pennsylvania, 6-10 June 1977.

Shirley, D. J., "Method For Measuring in situ Acoustic Impedance of Marine Sediments," J. Acoust. Soc. Am. 62, 1028, October 1977.

Shirley, D. J., and L. D. Hampton, "Shear Wave Measurements in Laboratory Sediments," J. Acoust. Soc. Am. 63, 607, February 1978.

Shirley, D. J., "Laboratory and in situ Sediment Acoustics," Applied Research Laboratories Technical Report (ARL-TR-77-46), 23 August 1977.

Shirley, D. J., "An Improved Shear Wave Transducer," J. Acoust. Soc. Am. 62, 1643, May 1978.

14 August 1978

DISTRIBUTION LIST FOR
ARL-TR-78-36
UNDER CONTRACT N00014-76-C-0117
1 January - 31 December 1977

Copy No.

Commanding Officer
Naval Ocean Research and Development Activity
NSTL Station, MS 39529
1 Attn: R. R. Goodman (Code 110)
2 R. D. Gaul (Code 600)
3 A. L. Anderson (Code 320)
4 Samuel Marshall (Code 340)
5 Herbert Eppert (Code 360)
6 G. J. Ranes (Code 500)
7 J. Paquin (Code 600)
8 K. V. Mackenzie (Code 340)
9 James Matthews (Code 362)
10 W. H. Geddes

Commanding Officer
Naval Electronic Systems Command
Department of the Navy
Washington, DC 20630
11 Attn: J. Sinsky (Code 320)
12 W. Kamminga (Code 320)
13 Jesse Reeves (Code PME 124-34)

14 Commander
Attn: A. P. Franceschetti
Naval Sea Systems Command
Department of the Navy
Washington, DC 20362

Commanding Officer
Office of Naval Research
Arlington, VA 22217
15 Attn: J. B. Hersey (Code 102-OS)
16 Al Sykes
17 Thomas Pyle (Code 430)
18 Hugo Bezdek (Code 460)
19 M. Odegard

20 Hawaii Institute of Geophysics
Attn: Dr. G. Sutton
The University of Hawaii
2525 Correa Road
Honolulu, HI 96822

Distribution List for ARL-TR-78-36, Contract N00014-76-C-0117 (Cont'd)

Copy No.

Commander
Naval Ocean Systems Center
Department of the Navy
San Diego, CA 92132

21 Attn: M. A. Pedersen (Code 307)
22 R. R. Gardner (Code 40)
23 Edwin L. Hamilton
24 Homer P. Bucker (Code 409)
25 G. Mohnkern
26 John Northrop

Director
Naval Research Laboratory
Department of the Navy
Washington, DC 20375

27 Attn: (Code 2627)
28 O. Diachok
29 Library (Code 2620)
30 Library (Code 2000)

31 Chief of Naval Operations
Attn: R. S. Winokur CNO (OP-95E1)
Department of the Navy
Washington, DC 20350

32 Commander
Attn: C. L. Bartberger
Naval Air Development Center
Department of the Navy
Warminster, PA 18974

33 Commander
Attn: P. Herstein
New London Laboratory
Naval Underwater Systems Center
Department of the Navy
New London, CT 06320

34 The Scripps Institution of Oceanography
Attn: Peter Lonsdale
The University of California/San Diego
San Diego, CA 92152

Copy No.

Commanding Officer
Naval Coastal Systems Laboratory
Panama City, FL 32401
35 Attn: E. G. McLeroy, Jr.
36 Bill Tolbert

37 Superintendent
Attn: H. Medwin
Naval Postgraduate School
Monterey, CA 93940

Woods Hole Oceanographic Institution
Woods Hole, MA 02543
38 Attn: Dr. Charles Hollister
39 Dr. Alan Driscoll
40 Dr. Earl Hayes

41 Department of Geological Oceanography
Attn: Dr. William R. Bryant
Texas A&M University
College Station, TX 77840

42 Underwater Systems, Inc.
Attn: Marvin S. Weinstein
3121 Georgia Avenue
Silver Spring, MD 20910

Geophysics Laboratory
Marine Science Institute
The University of Texas
700 The Strand
Galveston, TX 77550
43 Attn: J. Worzel
44 E. W. Beherns

45 TRACOR, Inc.
Attn: R. J. Urick
1601 Research Boulevard
Rockville, MD 20850

46 The Catholic University of America
Attn: H. M. Uberall
6220 Michigan Avenue, NE
Washington, DC 20017

Copy No.

	Lamont-Doherty Geological Observatory Palisades, NY 10964
47	Attn: G. Bryan
48	W. J. Ludwig
49	B. Tucholke
50	Robert D. Stoll
51	Department of Civil and Ocean Engineering Attn: Dr. Armand J. Silva The University of Rhode Island Kingston, RI 02881
52 - 61	Commanding Officer and Director Defense Documentation Center Defense Services Administration Cameron Station, Building 5 5010 Duke Street Alexandria, VA 22314
	University College of North Wales Marine Science Laboratories Menai Bridge Anglesey, North Wales
62	Attn: D. Taylor Smith
63	Peter Schultheiss
64	Director Attn: T. Akal SACLANT ASW Research Centre LeSpezia, Italy
65	The University of Auckland Attn: Alick Kibblewhite Physics Department Auckland, New Zealand
66	Defense Research Establishment Pacific CF Dockyard Victoria, B. C., Canada
67	Defense Research Establishment Atlantic Grove Street Dartmouth, N. S., Canada

Copy No.

68 Department of Civil Engineering
Attn: K. Stokoe
The University of Texas at Austin
Austin, TX 78712

69 The University of Texas Marine Science Institute
Attn: Dr. C. A. Burke
P. O. Box 7999
University Station
Austin, TX 78712

70 Office of Naval Research
Resident Representative
Room 582, Federal Building
Austin, TX 78701

71 Environmental Sciences Division, ARL:UT

72 Garland R. Barnard, ARL:UT

73 David T. Blackstock, ARL:UT

74 Glen E. Ellis, ARL:UT

75 Karl C. Focke, ARL:UT

76 Harlan G. Frey, ARL:UT

77 Loyd D. Hampton, ARL:UT

78 Kenneth E. Hawker, ARL:UT

79 C. W. Horton, ARL:UT

80 Chester M. McKinney, ARL:UT

81 Thomas G. Muir, ARL:UT

82 Donald J. Shirley, ARL:UT

83 Reuben H. Wallace, ARL:UT

84 Charles L. Wood, ARL:UT

85 Library, ARL:UT

86 - 102 Reserve, ARL:UT